Swansea University
Prifysgol Abertawe

A Single Phase Standalone Residential Photovoltaic Energy Management System

Manesh Dilip Patel

Swansea University

Submitted to Swansea University in fulfilment of the requirements for the degree of Doctor of Philosophy

Department of Electrical and Electronic Engineering

Swansea University

April 2025

Abstract

A Single Phase Standalone Photovoltaic Energy Management System (SPSAPVEMS) is presented. This SPSAPVEMS is comprised of an interleaved battery charging sub-system, and an interleaved switched capacitor inverter sub-system and has been developed to effectively control the Photovoltaic (PV) array, battery, and load voltage in a standalone energy management system for residential applications in off-grid solutions. A detailed literature review is presented that summarises the current topologies of the various Energy Management System (EMS) subsystems and identifies areas for improvement as a focus point of this study. One of the core sub-systems of the SPSAPVEMS is the inverter, an interleaved switched capacitor single-phase inverter for a Standalone PV System with Battery Storage is proposed with a novel control strategy based on the combination of Perturb & Observation (P&O) Maximum Power Point Tracking (MPPT) by phase shifted unipolar sinusoidal Pulse Width Modulation (PWM) with an Route Mean Squared (RMS) feedback loop to modulate the reference signal. The proposed modified interleaved inverter in this configuration shows improved harmonic performance compared with other existing methods, the simulation of the proposed inverter system recorded a Total Harmonic Distortion (THD) of 1.81% for the in-phase output current and voltage. This can be attributed to the interleaving of the switched capacitors that reduces the output ripple of the circuit. A second sub-system of the SPSAPVEMS is the single-phase bidirectional Direct Current (DC)/DC battery charger with a combined P&O MPPT and current control strategy is described and compared with an analysis of the existing battery charging techniques published in the industry. The conclusion of this study found a faster response time and reduced component count compared to a typical MPPT controlled boost converter in parallel to a voltage-controlled battery charger or other multiport solutions. A MATLAB/Simulink based simulation circuit was developed and used to validate the performance of the SPSAPVEMS. The system has been designed to respond to varying weather and load conditions as the battery supplements power to the home load when the PV output is impacted by variable conditions. In practice, a residential PV system will be exposed to changeable irradiance and temperature. MATLAB/Simulink package has been used to simulate and analyse the system behaviour. The results conclude that after reaching steady state, the system is responsive to the variable conditions. The combined MPPT, Current Control and RMS feedback voltage control methodologies allow power flow to be distributed across the load with minimal losses from multiple conversions or a high volume of components.

Keywords: PV, Standalone PV, Single-Phase, Battery Charger, Bidirectional, Buck-Boost, P&O, MPPT, Interleaved, Switched Capacitor, H-Bridge Inverter, RMS Feedback, Phase-Shifted, PWM, Home Load

Declarations

This work has not previously been accepted in substance for any degree and is not being concurrently submitted in candidature for any degree.

Signed.....

16-03-2025

Date.....

This thesis is the result of my own investigations, except where otherwise stated. Other sources are acknowledged by footnotes giving explicit references. A bibliography is appended.

Signed.....

16-03-2025

Date.....

I hereby give consent for my thesis, if accepted, to be available for photocopying and for inter-library loan, and for the title and summary to be made available to outside organisations.

Signed.....

16-03-2025

Date.....

The University's ethical procedures have been followed and, where appropriate, that ethical approval has been granted.

Signed.....

16-03-2025

Date.....

Acknowledgments

I would like to thank my supervisor and tutor, Dr Zhongfu Zhou. His enthusiasm in the field of power electronic system design is inspiring and his dedication to his students have been a large contributing factor to the completion of this thesis. The insights, opportunities, support and advice are hugely appreciated, and I have been lucky for this guidance throughout my PhD studies.

A thankyou is also owed to the Department of Electrical and Electronic Engineering, in particular, David Moody for allowing me to use of the facilities and software in the college of engineering at Swansea University – more importantly I would like to thank David for being a good friend. He is dedicated to his job and his students, the commitment he has shown in supporting me during my time as both an undergraduate and postgraduate student cannot be quantified or truly described but it will never be forgotten.

The submission of this thesis marks the end of 25 continuous years of schooling and studying, the seemingly never-ending journey is nearly over and there are some important family members who deserve an equal share in the achievement of this completed journey. Firstly, to my wife for always believing in me and supporting me with all the late nights and proof reading. You complete me, and I love you – I would never have made it this far without you, your strength and determination in spite of life's challenges reminds me every day of how lucky I am to have found you.

To my son, at the time of writing this, you have just learnt to crawl, you may not know it now but when I eventually make you read this, you should know that you have inspired me every day, watching you enter this world with your smiles and laughter makes me a proud dad.

I would like to thank my mama, twin, brother and sister for always being there for me, listening to my complaints, providing laughter, support and good memories on my academic journey. And finally, to dad, for pushing me to be better than I thought I could be, encouraging me to pursue my PhD, your unwavering emotional and mental support over these years has truly set an example to me about the type of father I hope to be.

Table of Contents

Table of Figures

Table of Tables

1 Introduction

1.1 Overview of PV Systems

Energy management systems are integrated solutions that allow the facilitation for the optimisation, monitoring, and control of solar energy generation, ensuring that the photovoltaic (PV) cells along with their associated components operate at their peak efficiency by managing the flow of energy. The current energy crisis, caused by global warming and an ever-increasing demand for energy, means that it is becoming inherently more pivotal in today's society to develop and improve sustainable energy management systems. The utilization of solar power as a renewable energy source is increasing due to the necessity of seeking alternative forms of renewable energy to fossil fuels. By optimizing PV cell energy captures and facilitating real-time monitoring, these energy management systems play a critical role in contributing to sustainability goals.

A stand-alone PV system that is not grid-tied requires a battery to ensure the system can support the home load when the solar panels are not generating electricity (at night). The envisaged use-case for the proposed stand-alone single-phase PV EMS would be to provide renewable energy to rural geographies where a grid connection is not available, or the local grid is not capable of adequately serving the load requirements.

Demand for electricity in recent years has substantially increased and is forecast to increase in the future. With the recent development of Plug-In Hybrid Electric Vehicles (PHEV) and political 'net-zero' policies, the number of PHEVs on the road is increasing year on year, this will substantially increase the load demand of national grids. Increased digital transformation and the advancement of Artificial Intelligence (AI) are driving an increased demand for datacentres which also put a large strain on local grid capacities. With the Climate Change Committee (CCC) advising that the UK is required to reduce their emissions by 78% by 2035 relative to 1990, a 63% reduction from 2019 [1] it positions the UK of a world leading commitment, placing the UK on its path to Net Zero by 2050 at the latest, a trajectory that is consistent with the Paris Agreement, the need to improve PV cell output has never been highlighted more on a global platform. Previous analysis suggests the UK has the potential to deploy capacity to generate 130-540 TWh (145-65 GW) of solar power [2]. Solar generates mostly during the summer months when the solar radiance is at its greatest, and therefore it is commonly felt that solar generation is less suitable to meet seasonal patterns of demand, however improvements across the overall solar energy management system could help to improve the efficacy of solar as a renewable energy solution in periods of lower solar radiance.

1.2 Renewable Energy

As of April 2024, 40.6% of the UK energy mix came from renewable energy sources, with wind accounting for 29.7%, biomass for 5.2%, solar for 4.5% and hydro for 1.2%, with 31.1% of the energy mix coming from fossil fuels [3]. Over the last 10 years, the percentage of the UKs energy that has been accounted for by renewable sources has increased significantly from 10.7% in 2014 to 39.5% in 2023, with fossil fuels decreasing from 58.1% to 32.2% [3].

Following the Climate Change Act 2008, the UK committed itself to reducing the number of greenhouse gases to net zero by 2050. To achieve this target, the UK government set the target of decarbonising the electricity system by 2035. The British Energy Security Strategy published a paper in April 2022 [4] highlighting that in order to achieve this target, solar energy capacity needed to increase from 14GW to 70GW by 2035 and wind from 11GW to 50GW by 2030. For renewables to play their part, it is vital that there is an increase in capacity, backed up by battery storage.

With 173,000 terawatts (TW) of energy hitting the earth every second, producing enough energy to power the world 10,000 times over, solar power is the most abundant source of energy on the planet. Between 2.5 and 8 kW can typically be produced via a domestic solar installation with an efficiency of around 20%, with a single solar-powered home slashing CO2 emissions by 100 tonnes in 30 years [4]. With only 5% of the global energy demand currently being met by solar and with a 4 time increase in the forecasted growth of the global solar capacity by 2030 [4] utilising this resource in a fashion that is accessible and efficient is a key move in achieving the UKs net zero goals by 2050.

1.3 Growth of Solar Energy

The concept of solar technology has been around since 1839 following the discovery of the photovoltaic effect by Edmond Becquerel, however the phenomenon was not widely recognised until 1905 following the first of four papers published by Albert Einstein in Annalen de Physik *"On a heuristic viewpoint concerning the production and transformation of light"* as part of his annus mirabilis papers. Today, there are over 1.09 million domestic systems in use today, with the number set to drastically increase over the next few years, with the International Energy Agency (IEA) estimating that the global solar capacity with quadruple by 2030, with their estimate of a total 3000 GW PV capacity worldwide, which will contribute 11% of the global electricity supply [5].

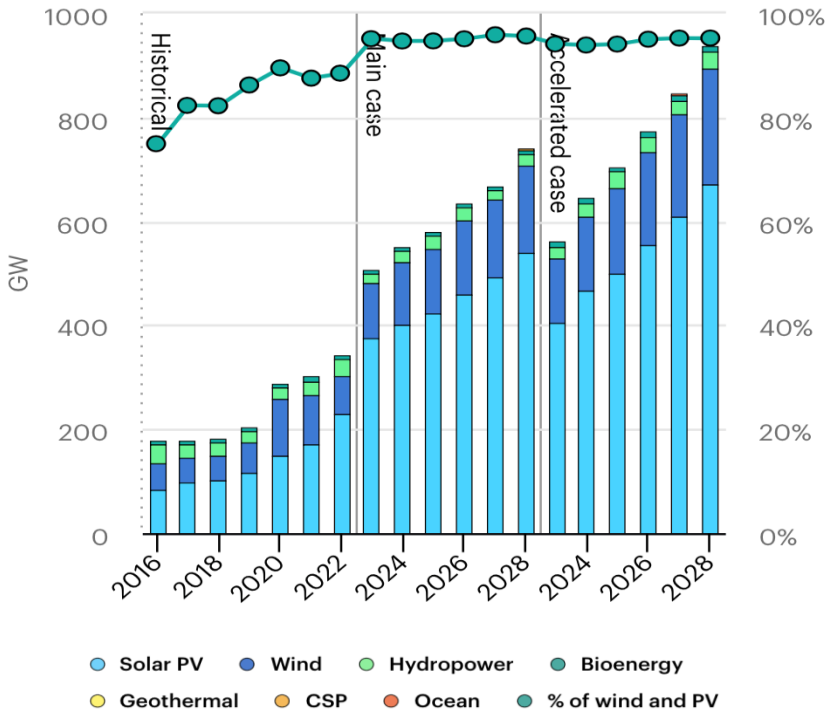

Figure 1.1 - Elements of a Grid Connected System : Renewable electricity capacity for 2016 through to 2028 [5]

As can be seen from Figure 1.1, Solar PV demonstrated the largest generation growth of all renewable technologies in 2022, surpassing wind for the first time on record, with the generation growth rate matching the level envisaged from 2023 to 2030 in the Net Zero Emissions by 2050 scenario [5]. The tracking status of solar PV has since been upgraded in 2023 from *"more effort needed"* to *"on track"* [5].

1.4 Energy Production

On average 4 million exajoules (1 TW = 1.0×10^{-6} EJ = 1×10^{18} J) of solar power reaches the Earth every year with 5×10^{4} EJ estimated to be harvested [5]. Solar energy is not readily utilised across the globe due to a variety of factors, including diurnal variation, latitude, climate, and geographic variation, all of which contribute towards the intensity of the solar influx that passes through the atmosphere. The annual solar irradiance across the globe varies from 60W/m^{-2} to 250W/m^{-2} [5]. To reach the annual solar PV generation level of 8300 TWh in 2030 in alignment with Net Zero Scenario, up from the current 1300 TWh, will require an annual average generation growth of around 26% through 2023 to 2030, similar to the high rate seen in 2022, however maintaining this growth across the market will require continuous efforts [5].

1.5 Solar Management Systems

Solar management systems, a type of energy management system specifically designed for solar panels, work by analysing various data points, such as sunlight intensity and temperature, allowing the system to make real-time adjustments to the system to maximize the PV cell outputs and increase overall efficiency of the system. An array of components is included within the solar management system and include the solar panels, inverters, batteries, and monitoring systems.

Solar management systems are an important aspect of modern-day infrastructure due to their innate ability to produce renewable energy, reduce electricity costs and reduce the environmental burden. They are vital to optimise the overall performance of the PV cells, ensuring that the energy consumption meets the energy demands.

1.6 Solar Energy Technology Classifications

Solar energy technology can be divided into two categories, namely passive solar technology, and active solar technology. Passive solar technology accumulates the solar energy without transferring thermal or light energy into any other forms, e.g., collection, storage, and distribution. Active solar technology collects the solar radiation and applies it to mechanical and electrical devices for the conversion of solar energy to heat and generate power. Active solar technologies can be further classified by either photovoltaic technology, concentrated solar power and solar thermal technologies.

The technology of interest for this Ph.D. focuses on photovoltaic technology, whereby the photons are directly converted into electricity using semiconductor materials such as silicon and selenium.

1.7 Types of Solar Systems

A grid connected system is connected to the local electricity grid which allows for excess energy generated by the PV cells to be fed back into the local grid. These systems often do not have battery storage as the system can pull energy to and from the grid when solar production is inadequate. A standalone PV system is independent from the local electricity grid and relies on batteries to store the generated electricity. They are single phase systems rather than a three-phase system and are required to be supplied from the home load from the PV cell output directly.

1.7.1 Grid Connected Systems

Grid connected systems obtain power from the local electricity grid when there is not enough power generation via the solar irradiance. The system is able to feed the generated power back to the local electricity grid when more power is generated than can be utilised, named as “net metering.”

Grid connected systems need to be designed to be suitable for whichever countries grid it is set to be integrated with and must adhere to the countries set guidelines, such as the British Standard (BS) 7671:2018 regulations [6] for the UK Grid, before implementation is approved. A standard grid

connected system is the most popular system with their primary advantage being their ability to offset electricity costs by selling excess energy back to the local grid and being less complicated than standalone systems as they do not require a battery. Systems that do not require a battery are far cheaper due to the conditions needed for storage, their installation, and associated costs of recycling. Grid connected systems convert solar energy into AC power. Solar irradiation falls onto the PV cell which generates PV energy, known to be DC in nature, then using a DC-DC converter, the total PV DC voltage from the solar panel is raised to a higher DC level. The inverter within the PV system converts the DC voltage (either the DC voltage from the solar panels or the DC-DC converted output voltage) into AC voltage. As the AC voltage is integrated into the grid, the inverter converts the PV energy into AC power with a frequency that matches that of the local electricity grid. The quality requirements of the voltage and power are thus satisfied by the AC converter. A DC-DC converter is not an essential part of a grid connected system, however it ensures that the DC link voltage is large enough to feed the DC/AC inverter, approximately 500V, to ensure a root mean square (RMS) voltage of 339V is fed to the output of this system. For these systems to work practically, a close integration with the energy provider is required to ensure the amount of energy delivered back (or sold) to the grid or delivered (or bought) from the Grid is monitored. This can be done by use of a smart meter. The elements of a grid connected system can be seen in the illustrated system overview shown below in Figure 1.2.

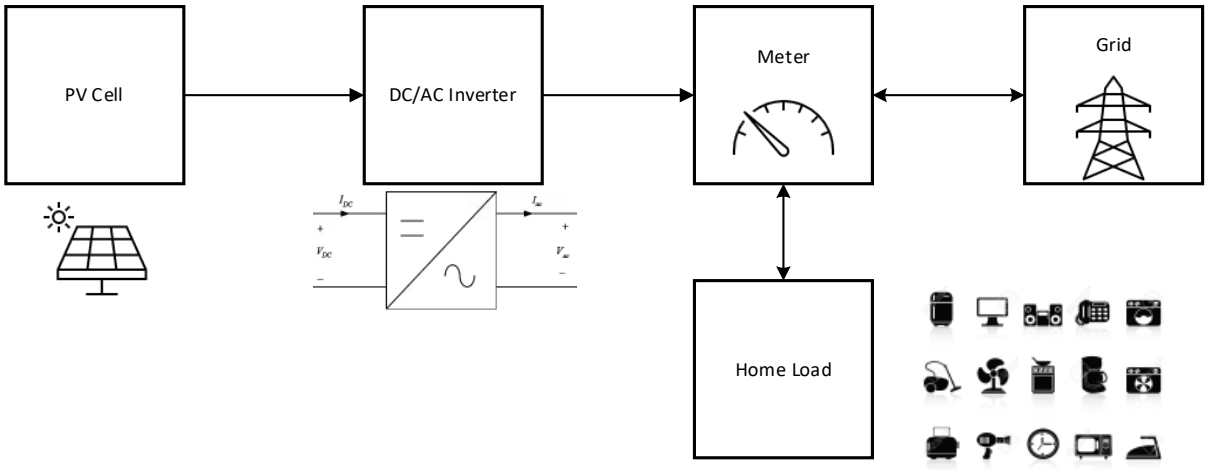

Figure 1.2 - Elements of a Grid Connected System

The energy produced by the PV system can be transferred to the grid via a DC-AC converter which is used as an MPPT controller and an inverter which converts the DC bus voltage to the AC grid voltage.

1.7.2 Standalone PV Systems

Standalone PV systems do not have a connection to the grid and its produced energy is normally matched with the energy requirements by the load and it is an economical superior where other sources

of energy are difficult to utilise. These systems are usually supported by energy storage systems, such as a battery, which can store any surplus energy produced and provide electricity when no sunlight is available. As these systems are not connected to the grid the home load is the last link of the system, as seen when comparing Figure 1.2 to Figure 1.3. This system must supply the necessary load requirements of the home load from the output for the PV cell under all conditions as there can be no additional supply from the grid. During the night, when the sun has set, there will be no output coming from the home load, for this reason, the battery is essential to feed the home load during this period. The battery is required to charge and discharge and therefore can be described as bidirectional. Traditionally, a stand-alone PV system is used for small loads that are far from a cities grid and therefore it is more cost effective to have these systems run from a standalone renewable resource than it is to install and commission a grid connection, a good example are electronic road signs in rural areas.

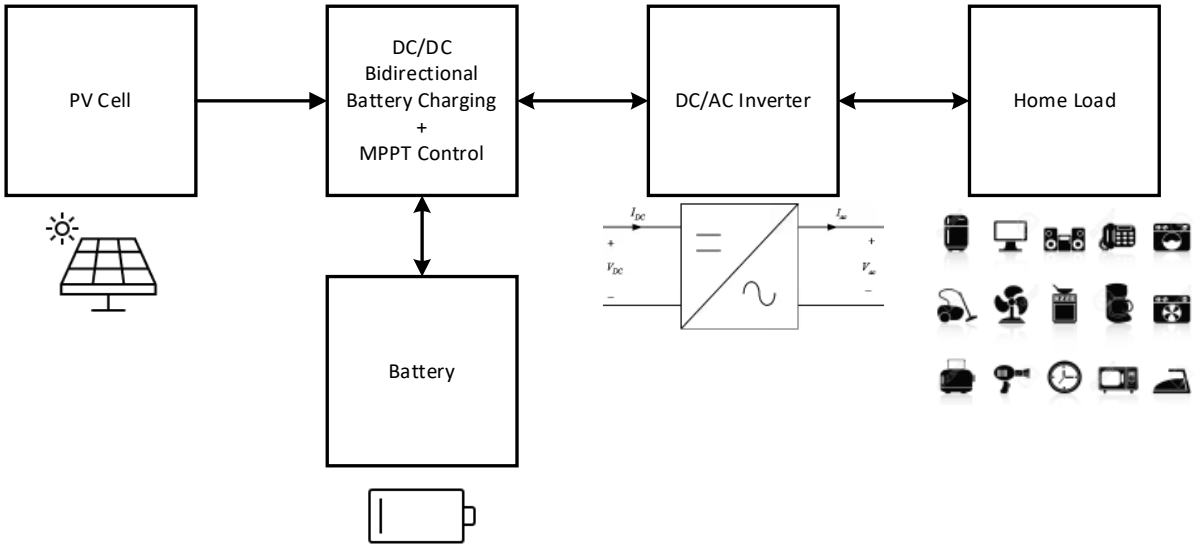

Figure 1.3 - Elements of a Standalone System

The home load is positioned across the output for the inverter circuit. There is a current measurement placed in series with the home load which allows the output signal I_{out} to be tracked, and a voltage measurement placed in parallel with the home load, which allows V_{out} to be tracked.

Standalone systems are being utilised for solar cars, remote houses, parking ticket machines, solar pump systems and traffic lights. The use of stand-alone systems primarily focuses on electricity delivery in areas where there is none or limited access to the grid or where the cost of delivering electricity to remote areas is extremely high.

PV systems have numerous disadvantages including their high manufacturing costs, low working efficiency especially under varying conditions (e.g., irradiance, temperature, non-linearity characteristics produced by the output power and current of PV panels) and their low conversion efficiency.

1.8 Research Objectives

The aim of this research is to investigate the Photovoltaic (PV) energy management systems (EMSs), specifically for residential applications. For these types of systems, they are typically single-phase as opposed to the three-phase for more industrial or commercial applications. A more specific focus of this research focused on stand-alone PV systems, i.e., a system that is not grid-tied.

The objectives of this project are to investigate where improvements can be made to existing standalone PV EMS to provide simpler, high performance and cost-effective alternatives. To understand how improvements can be made to PV EMSs the following research objectives were outlined:

1. Conduct a detailed literature review on "Single-Phase Standalone PV Energy Management Systems" to understand the current and latest topologies, configurations, and control strategies currently utilised.
2. Divide the literature into the key EMS sub-systems/building blocks: Maximum Power Point Tracking (MPPT), DC-DC Battery Charging and DC-AC Inverter. Focus the review of two key areas for each sub-system: circuit design and circuit control strategy.
3. Design a modified/novel control system and circuit configuration for a PV EMS Battery charger.
4. Design a modified/novel control system and circuit configuration for a PV EMS DC-AC Inverter.
5. Validate the design of the proposed circuits/control strategies through simulation, collect and analyse the data using the MATLAB/Simulink software package. .

1.9 Research Contributions

This research has contributed to the development of power electronic energy management systems. There are two key areas described in this thesis where original contributions have been made to the industry:

- Based on existing published literature investigating inverter subsystems, this research proposes a modification to the existing interleaved switched capacitor DC-AC inverter control strategy to include a Root Mean Square (RMS) voltage control feedback loop. The standard control strategy is a based phase shifted unipolar sinusoidal pulse width modulation (PWM).
- A modification to the existing control methodology for a DC-DC battery charging circuit to include a combination of MPPT and reference charge current control to drive the Insulated Gate Bipolar Transistors (IGBTs) in the circuit configuration of a bidirectional buck-boost battery charging circuit.

- When the modified inverter and modified battery charging subsystems are combined into an overall PVEMS the resulting configuration is considered to be a novel contribution. There is no other published literature that contains the same combination of subsystems.

1.10 Publications

- Patel, M. and Zhou, Z. (2023) 'An interleaved switched capacitor single-phase inverter with a modified control strategy for a standalone PV system with battery storage', 2023 IEEE IAS Global Conference on Emerging Technologies (GlobConET) [Preprint]. doi:10.1109/globconet56651.2023.10149904.
- Patel, M., & Zhou, Z. (2023). An Interleaved Battery Charger Circuit for a Switched Capacitor Inverter-Based Standalone Single-Phase Photovoltaic Energy Management System. *Energies*, *16*(20), 7155. https://doi.org/10.3390/en16207155
- *"A Switched Capacitor-Based Single-Phase Inverter for a Standalone PV System with Battery Storage"* has been submitted to IEEE IAS Journal in January 2024.

1.11 Thesis Rationale and Research Objectives

In recent years, the IEA issued a statement highlighting that new infrastructure was needed to *"support the adoption of off-grid electrification systems".* Decentralised systems can help fill the energy access gap by delivering electricity at a level of access that is currently too expensive to be met through a grid connection, and in urban areas by providing back-up for an unreliable grid supply [3]. Under this pretence, it is pivotal that the working efficiency of PV energy management systems is improved and problems in practical applications of these management systems are addressed. Focusing on the improvement of off-grid energy management systems, the design and implementation of a more efficient and accurate MPPT, battery charger and inverter set-up is pivotal to drive change in this key area of renewable energies and is the focus of this PhD study.

Firstly, the thesis will focus on reviewing the current evidence base surrounding the existing topologies for MPPT, battery charging and inverters for standalone PV energy management systems. Secondly, the thesis describes and discusses novel/modified sub-system designs for battery charging and inversion. The thesis then moves on to describe how the proposed novel system performs under varying input conditions.

1.12 Thesis Outline

Chapter 2: Background & Literature Review – An overview of photovoltaics, a description of the fundamental characteristics and principles of energy management systems, along with their sub-systems. The rationale of the project is explained, and a list of the study objectives is detailed. Finally, an outline of the chapters in the thesis is provided. This chapter also outlines the current literature pertaining to PV energy management systems highlighting key issues and identifying gaps across the current evidence-base. The literature review includes research across all key sub-systems of the energy

management system including, MPPT, battery charging and inverting along with a review of combined standalone energy management systems.

Chapter 3: Proposed SPSAPVEMS Configuration and Performance Under Variable Irradiance and Temperature Conditions – The performance of the proposed PV EMS is tested against changing dependent variables including temperature, irradiance, and load conditions. The results of these tests are gathered and compared with expected performance for similar systems.

Chapter 4: SPSAPVEMS Battery Charger Subsystem – A summary of the literature review that focused on battery charging circuits and controls strategies is highlighted and the proposed interleaved bidirectional buck-boost DC-DC converter with combined MPPT and current control is explained and simulated. Simulation results for this proposed subsystem are gathered, analysed, and discussed.

Chapter 5: SPSAPVEMS Inverter Subsystem – This chapter describes the outcomes of the literature review that focused on inversion sub-system circuits and control strategies. The design of an interleaved switched capacitor DC-AC inverter with a modified phase shifted unipolar pulse width modulation (PWM) with root mean square (RMS) feedback control strategy is then theorised. The results of the simulation are discussed in detail to compare how the harmonic performance of the inverter in this PV EMS compares with other inverters.

Chapter 6: Conclusions and Recommendations – In the final chapter, the achievements of the thesis are summarised and the recommendation for future work is outlined.

2 Literature Review

2.1 Introduction and Rationale

Solar management systems are projected to have a leading role in the current energy transition to tackle the negative impacts of global warming arisen from the overuse of fossil fuel-based energy generation. PV technology is a clean way of generating electricity. The global growth of PV technologies has increased by a compound annual growth rate of 34% between 2010 and 2020, evidencing the continuously evolving field of solar energy generation.

The output power for PV cells depends on a number of factors including the solar irradiance, temperature and the load impedance, whereby the solar irradiance and temperature are dynamic factors, and the load impedance depends upon the application where a DC-DC converter is used to improve the overall performance of the PV cell.

One of the problems faced by these energy management systems is the inability to coherently regulate and stabilise the output of the PV module, resulting in a loss of efficiency of the PV module. The most commonly used mechanism to circumvent this issue is to use an algorithm for the maximum power point tracking (MPPT) within the PV module, which computes the operating point of the PV cell. To improve the overall performance of the battery charging system this algorithm needs to be optimised. Currently, there are multiple algorithms for MPPT in use, with many novel approaches being developed [7].

2.2 Photovoltaics Characteristics & Mathematical Modelling

A Photovoltaic (PV) cell can be used as part of a renewable energy initiative targeted and harnessing solar energy. The PV cell utilises a property of semiconductor materials that allows it to interact with incoming photons from the sun. A photon can be described "*as a single unit of light, a very small piece of matter that is the basic unit of electromagnetic energy, and that travels in waves and carries light and other forms of radiation"* [8].

A semiconducting material can be described as a material that conducts electricity under certain conditions. They are not considered as insulating or conducting materials therefore present the ideal characteristics to control the electric current generated by the PV cell. An example of a semiconducting material is Silicon. Silicon has 4 valent electrons which form strong covalent bonds with other Silicon atoms. This creates a lattice that is not positively or negatively charged. For Silicon to be used as a semiconducting material it must be doped with n or p type dopants. An n-type semiconductor material has an excess of free electrons (negatively charged) whereas a p-type semiconducting material will have an excess of free holes (positively charged). This is known as the photovoltaic effect and is shown in Equation (2.1) below where E is the energy of the photon, h is Planck's constant (6.626×10^{-34} Js), c is the speed of light (3×10^{8} m/s) and λ is the wavelength of the photon.

$$E = \frac{hc}{\lambda} \tag{2.1}$$

The photovoltaic material embedded within the PV cell allows for the generation of voltage or current when it is exposed to solar light, the semiconductors within the PV cell are n-type and p-type and the points at which the semiconductors are joined, a p-n junction is created, an electric field is then formed and electrons will move from the n-side to the positive p-side and holes will move from the p-side to the negative n-side [9].

When light collides with the PV cell the photons energise the electrons of the semiconductive material and causes the electron to move to a higher state known as the conduction band. The electrons in the conduction band move through the material and it is this movement that generates the electric current in the PV cell. The electric current generated is DC, for this to be used in a home, the DC will need to be converted to AC.

There are two types of PV cells utilised widely across the market:

1. Crystalline Silicon: this method is more popular due to its efficiency benefits, there are two types of crystalline silicon used:
    a. Polycrystalline
    b. Monocrystalline
2. Thin Film: this method is newer, the PV cells that use the thin film method are (as described) thinner, this method is becoming increasingly more popular. There are a few types of thin film materials:
    a. Silicon
    b. CdTe (Cadmium Telluride)
    c. CIGS (Copper Indium Gallium Selenide)

The most common thin film material is silicon; they are much more flexible and durable as a technology, making their installation and commissioning much easier. The typical shelf life of PV cells that form a PV panel is between 20 to 25 years, with this being improved year on year as innovative PV materials are becoming progressively more efficient.

The relationship between MPP (displayed as the product of $V_{pv\text{-}max}$ and $I_{pv\text{-}max}$) and the product of I_{sc} and V_{oc} is known as the fill factor (FF below). This gives an indication of the quality of the p-n junction, higher values are more desirable.

$$V_{oc} = V_d = \frac{nKT}{q} \ln\left(\frac{I_{ph}}{I_{sc}} + 1\right), \tag{2.2}$$

$$I_{sc} = \frac{I_{ph}}{1 + \frac{R_s}{R_{sh}}} \tag{2.3}$$

$$FF = \frac{V_{pv-max} * I_{pv-max}}{I_{sc} * V_{oc}} \tag{2.4}$$

2.2.1 PV Cell Equivalent Circuit

Solar cells can be wired in series and parallel to boost voltage and current, respectively. The equivalent circuit shown in Figure 2.1 shows the current source equivalent circuit where I_{ph} can be considered as the Photon current. I_d is the diode current shown in parallel to the Photon current. R_s and R_{sh} the series and shunt resistance of the solar cell. However, the values of R_s and R_{sh} can be considered negligible for an equivalent circuit [10].

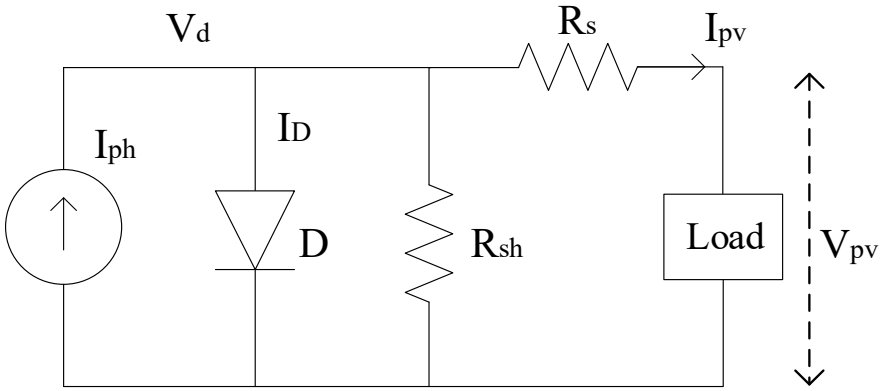

Figure 2.1 - PV Equivalent Circuit

This means that for a simple PV cell the theoretical equations for I_{pv}, I_{ph} & I_D (2.5) can apply [10]:

$$I_{pv} = I_{ph} - I_D \, , \tag{2.5}$$

$$\text{Where: } I_{ph} = \left(I_{sc} + C_t\left(T_c - T_{ref}\right)\right)\frac{s}{S_{ref}} \, , \tag{2.6}$$

$$\text{And: } I_D = I_o\left[\left(e^{\frac{V_d}{nV_t}}\right) - 1\right] \tag{2.7}$$

When N_s and N_p are considered I_{pv} can be rewritten as follows in (2.9) [10] :

$$I_{pv} = N_p I_{ph} - N_p I_D \, , \tag{2.8}$$

$$I_D = I_o\left[\left(e^{\frac{V_d}{nN_sV_t}}\right) - 1\right] \tag{2.9}$$

When the Schottky expression is considered for temperature variation, I_{ph} and I_D can be rewritten as (2.12) follows [10]:

$$V_T = \frac{KT_C}{q}, \tag{2.10}$$

$$I_D = I_o\left[\left(e^{\frac{qV_d}{nkN_ST_C}}\right) - 1\right] \tag{2.11}$$

$$I_{ph} = \left(I_{sc} + C_t\left(T_c - T_{ref}\right)\right)\frac{s}{S_{ref}}, \tag{2.12}$$

2.2.2 PV Cell Measurement Circuit

Figure 2.2 shows the PV cell and measurement topology deployed to monitor the PV cell in this energy management system. The circuit diagram shows: the input parameters (temperature & irradiance), the current measurement block connected in series to give I_{pv}, a voltage measurement block connected in parallel to give V_{pv}. There is also a display block connected across the voltage measurement to ease the troubleshooting of the circuit. The output of Figure 2.2 feeds the rest of the energy management system.

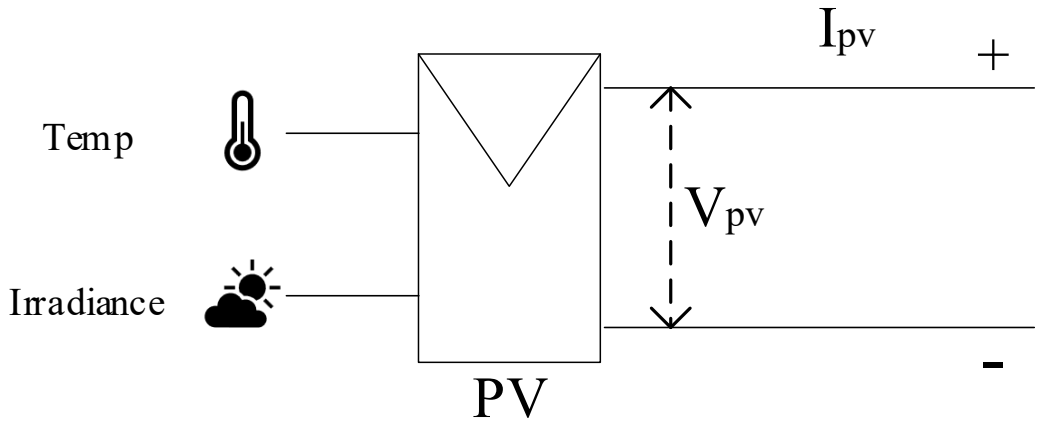

Figure 2.2 - PV Cell Circuit & Measurement

This thesis goes into detail regarding each of the system elements and the parameters/settings for components. This thesis also analyses relevant literature for each circuit element as well as general literature for standalone PV systems.

2.3 Maximum Power Point Tracking

Maximum Power Point Tracking (MPPT) is used within a PV system to ensure that the maximum power is utilised for the energy management system despite variable conditions. If the PV cell experiences partial shading or a change in temperature, an MPPT circuit will ensure that the output power P_{pv} will be as high as possible for the DC link of the system.

Graphically when analysing a PV cell output I-V curve shown in Figure 2.3 below, the bend of the curve is the theoretical Maximum Power Point (MPP). Theoretically when implemented a PV panel will rarely be at the peak power capability [11].

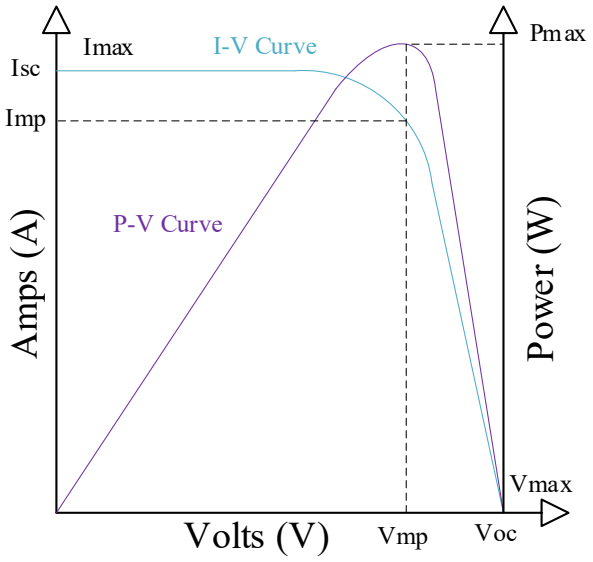

Figure 2.3 - IV Curve for PV Cell Output

Taking Ohms law (2.13):

$$V = I * R \tag{2.13}$$

a formula for Power can be derived (2.14):

$$P = V * I \tag{2.14}$$

This is the basic principle used for measuring the voltage and current and therefore calculating and tracking the MPP.

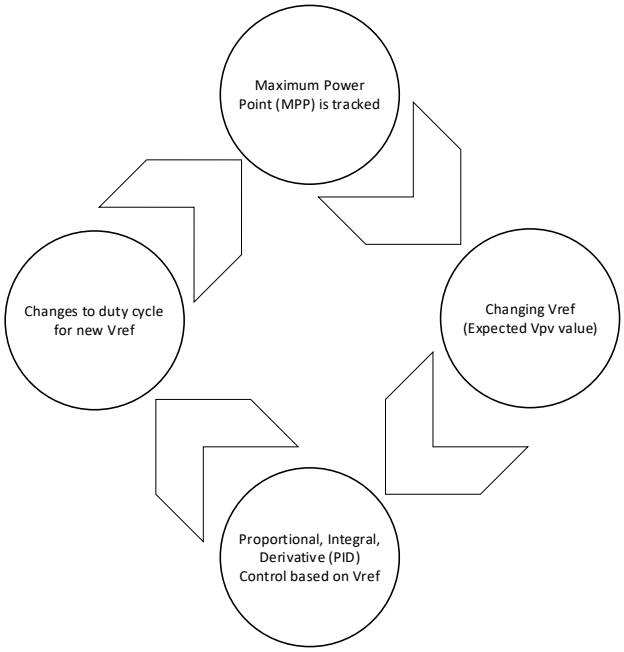

Figure 2.4 - Cycle Maximum Power Point Tracking Steps

There are many different methods for MPPT with each having their advantages and disadvantages. A summary of each method is described below. MPPT can be used to improve the efficiency of the PV energy management system. A typical domestic solar panel can convert between 30 and 40% of the incident solar irradiation into electrical energy. Multiple methods exist for MPPT algorithms and multiple topologies and control strategies for PV inverters and battery chargers.

MPPT is an algorithm which is implemented within PV systems that continuously adjust the impedance seen by the solar array to keep the system operating at, or close to, the peak power point of the PV panel under varying conditions, including solar irradiance, temperature, and load [12].

2.3.1 Perturb and Observation

The controller in the P&O method makes small adjustments to the voltage and takes current and voltage measurements to give the power. When the power increases the controller adjusts further until an increase in power is no longer detected. The output scope of the MPPT controller is similar to the V_{pv} graph but it shows more steps and is more square; this method and its nature can result in large oscillations for the output power [11].

P&O algorithms perturb the operating voltage to ensure maximum power. P&O algorithms are widely applied to practical applications due to their simplicity and easy implementations and are often applied to stand-alone systems.

The efficiency of this method can be improved by ensuring the predictive steps used to take the measurements are refined and accurate. The P&O is the most used method for MPPT as it is easy to implement within an energy management system.

With varying weather conditions, the MPP can change continuously. P&O takes it as a change in MPP due to its perturbation rather than that of irradiance and has been known to calculate the MPP in the wrong direction under rapid changes in irradiance. This issue can be resolved by using incremental conductance algorithms as it is able to take samples of the voltage and current to calculate the MPP, however, instead of an increased efficiency of the system, the complexity of the algorithm is high when compared with the P&O algorithm and as such the cost implications are noticeable [11].

2.3.2 Incremental Conductance

Incremental conductance algorithms compare the incremental conductance to the instantaneous conductance in a PV system, and depending upon the results, it can increase or decrease the voltage until the MPP is reached and then keeps the voltage constant. These algorithms are also widely utilised due to their accurate tracking [11].

Incremental conductance is a computational method that can track changes much quicker than the P&O method and does not produce as much oscillation on the output power. It works by predicting the effect of voltage change.

The incremental conductance MPPT method tracks $\frac{\Delta I}{\Delta V}$ to figure out if this is positive or negative (increasing or decreasing) in the first instance, this will then assume the change in power with respect to voltage $\frac{\Delta P}{\Delta V}$. If $-\frac{I}{V} = \frac{\Delta I}{\Delta V}$ the output voltage is the MPP voltage [11].

- The method assumes that at MPP $\frac{\Delta P}{\Delta V} = 0$, this means that MPP is achieved when the incremental conductance is equal to the negative of the instantaneous conductance.
- When the voltage is smaller than V_{mpp} , $\frac{\Delta P}{\Delta V} > 0$, $\frac{\Delta I}{\Delta V} > -\frac{I}{V}$
- When the voltage is larger than V_{mpp} , $\frac{\Delta P}{\Delta V} < 0$, $\frac{\Delta I}{\Delta V} < -\frac{I}{V}$

Therefore, the MPP tracker works by equating ΔI or ΔV to the PV curve shown which gives the actual current and voltage values [11].

The P&O and I&C methods are more complex by nature and require more calculation as they do not rely on reference data for comparison. They also provide a true MPP due to the measuring that is done as part of the method.

The I&C method can determine the MPP without oscillations around MPP whereas the P&O method does oscillate. P&O is more adaptable under varying conditions (temperature and irradiance) and due to the amount of calculation required for the I&C method, the P&O method will dictate a lower sampling frequency for the energy management system [11].

2.4 Batteries and Battery Chargers

2.4.1 Batteries

Batteries release stored electricity over time in the form of DC power. As current flows through the battery a chemical reaction starts. Inside each battery are a number of cells, with each cell containing two electrodes. Electrodes are electrical terminals, with one electrode being positive, and the other electrode being negative. A chemical in liquid form separates the two electrodes and is referred to as an electrolyte. These reactions cause electrons to flow around the circuit that the battery is feeding, however there is a limited supply of the electrolyte in the battery for these reactions to take place which means that the supply is limited. When the electrolyte is depleted, the chemical reaction stops which means the electrons will no longer flow around the feeding circuit. In a rechargeable battery, these reactions can run in the opposite direction which allows the electrolyte to return to its beginning state. A battery charger is required to ensure this takes place.

2.4.2 Battery Size

When designing a PV energy management system, the size of the battery must be suitable to supply the home load for the system in an event where V_{pv} is zero. For the longevity of the battery, the battery must not be totally or nearly totally discharged to support the home load when the PV panel is not generating any electricity. This value is approximately 25% or less of the battery value. The life expectancy of the battery must also be factored in, meaning that derating factors must be analysed when an appropriate battery is selected for the practical system.

2.4.3 Battery Charging

A principle of battery charging is converting from DC-DC. A PV system requires a DC boost such that the PV output is high enough to then be inverted to serve a home load ($240V_{ac}$). Prior to the inversion, another buck/boost converter is utilised to charge and discharge a battery, current must therefore be able to flow in both directions (bi-directional).

A battery experiences four optimal phases during a charging cycle, as seen in Figure 2.5 [11]. Stage one is known as the bulking stage which is a constant current mode. Stage one of the battery charging cycle sees the battery charge up to 80% of its full capacity. Stage two is the absorption phase which is a constant voltage mode. For a 12V battery in stage two of the cycle, the battery voltage is held at 14.5V and the battery current is reduced. During this time, the last 20% of the battery is charged. The battery voltage is held at 14.5V until the battery current reaches approximately 5% of its rated current value. Stage three is the float phase, which is again a constant voltage mode. During the float phase, when the battery reaches 5% of its rated current value, the battery voltage drops to 13.5V allowing the battery to maintain and hold its charge, without causing any damage. The last phase, stage four, is known as the equalisation phase, which is a low current and high voltage mode. By maintaining a low current and a high voltage, the electrolyte within the battery is protected, a process known as de-sulphation.

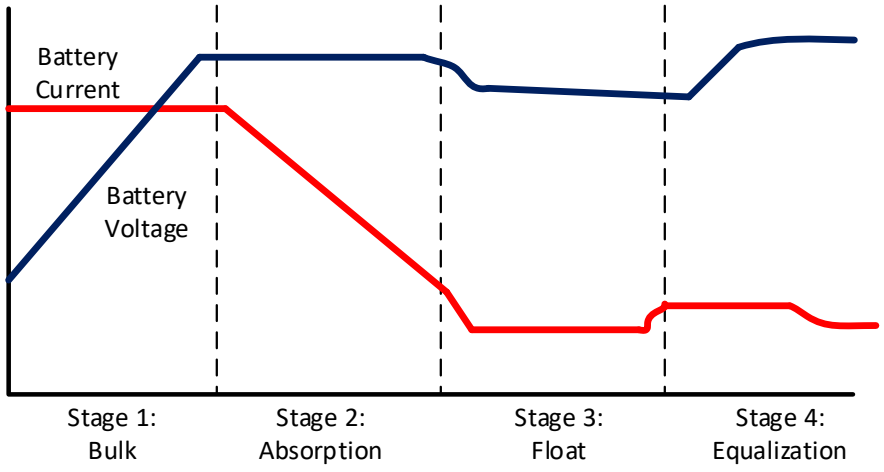

Figure 2.5 - Battery Charging Phased Cycle [11]

2.4.4 Battery Type

For this study, a basic lithium-ion (Li-Ion) battery is being modelled due to its many advantages, including being inherently safe due to their chemical composition, being 2 to 5 times more efficient at lower working temperatures and being safely operational up to 65 degrees Celsius, and their highly efficient charging capabilities. Li-Ion batteries are long lasting, require little maintenance, are light weight and over prolonged periods of time show better discharge characteristics than many other battery types. However, Li-Ion batteries are known to suffer from being over charged and they are by nature difficult to manufacture. A nominal battery voltage on the market would be 12Volts. For this energy management system, the DC Battery voltage is being set to 48V which is the equivalent of 3 x 12Volt batteries connected in series.

2.4.5 Bidirectional DC/DC

The topology of the battery charging circuit in energy management system is described as a bidirectional buck/boost DC-DC Converter and is shown in Figure 2.6.

This topology operates in Boost (Battery discharging mode) or Buck (Battery charging mode) modes. Boost mode is where the G2 gate pulse is high and the IGBT is switched on. During this mode, the G1 can exist in either one of two states, namely state 1 whereby G2 is high and G1 is low, demonstrating that the DC-DC converter is in a short circuit state and the inductor L1 is charged by the battery voltage, or state 2 whereby both G1 and G2 are low, showing that the DC-DC converter is in an open circuit state, with the inductor voltage operating in series with the DC link voltage meaning that capacitor C1 is charged allowing the output voltage to be boosted up [14].

In comparison, Buck mode is where the G1 gate pulse is high and the IGBT is switched on, and instead of G1 existing in two states, G2 can exist in two states. State 1 is where G1 is high and G2 is low meaning the battery will be charging the capacitor C1 and inductor L1 and state 2 is where both G1 and G2 are low meaning that the inductor will be discharged across the freewheeling diode and the voltage across the battery will step down [14].

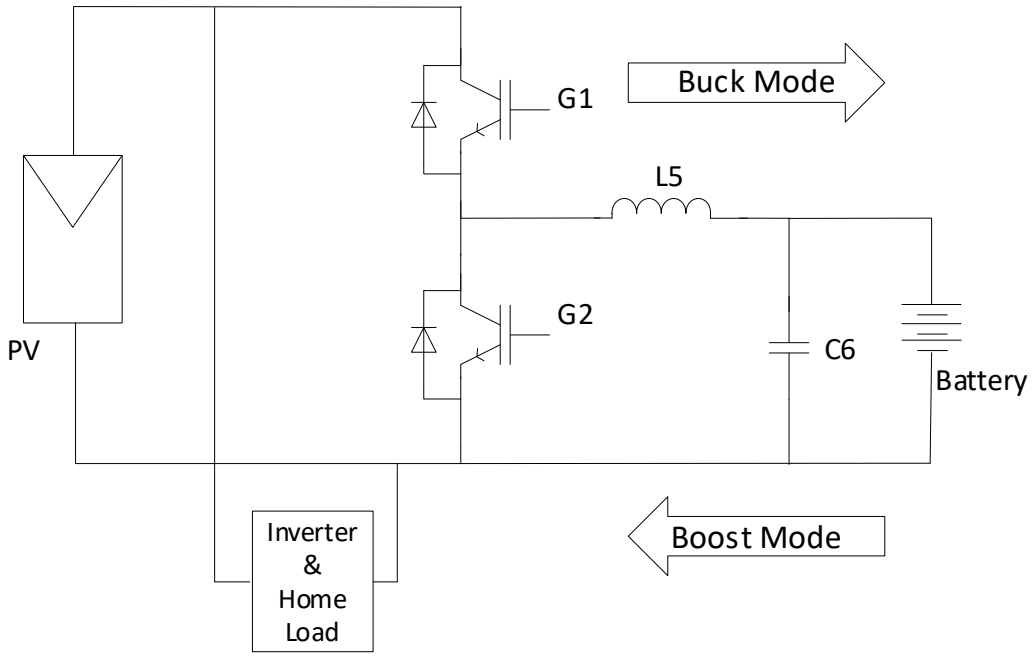

Figure 2.6 - Bidirectional Buck Boost DC/DC Converter Topology

2.5 DC-AC Inverters

The DC-AC inverter aspect of the PV system is used to convert the current produced from a DC (produced by the PV Cell) to AC which is useable by most nominal home loads. The inverter must output and maintain a stable sinusoidal signal in steady state, which is achieved by the control circuit and PWM generator which ensures the IGBT switches are driven with the intention of producing a stable sinusoidal signal > 339V.

For the nominated load for which this PV system will be required to supply, it is important to analyse the current requirements of the system such that the appropriate voltage or current control can be designed for the DC-AC inverter, this will ensure better performance and output characteristics for the system. A voltage control is far simpler and cheaper to deploy than a more complicated and expensive current control method.

2.5.1 Inverter

By nature, it is a complicated process to convert current from DC to AC, with the process being to convert a square wave to a sine wave. To do this, an arrangement of IGBTs operating as switches in pairs is required. There is also a requirement for a control process called PWM to take place. In a practical system, a filter will also be required to refine the sine wave and remove all unwanted frequencies and harmonics.

The standard approach to DC-AC inversion is to utilise a H-bridge inverter, this allows for the conversion of the DC power generated by the PV array (and stored in the battery) into AC power for use in a home load. The objective of the AC signal is to generate a stable $240V_{rms}$ sinusoidal waveform that has a Total Harmonic Distortion (THD) of lower than 5% to meet the IEEE 519 [15] standard for

residential usage. There are many properties that are expected from standalone inverters including a sinusoidal output voltage, a system disconnection when the DC link voltage drops, an output voltage and frequency that can be maintained within permissible values, must be highly efficient in light loads and have cables capable of withstanding large fluctuations in the input voltage [16]. The performance of an inverter is measured as harmonic distortion, multiple methods for reducing the harmonic distortion form part of the literature review.

2.5.2 H Bridge

A H-Bridge is a term used to describe a single-phase full bridge inverter. A simple H-bridge inverter can be seen in Figure 2.7. There are two pairs of IGBTs which behave as switches in this circuit. The switches are then operational as two pairs: S1 & S4 and S2 & S3. When signals are applied to the gates of these switches they are switched on; this means that when S1 & S4 are switched on, a positive DC supply is fed to the load, and when S2 & S3 are switched on, a negative DC supply is fed to the load, meanings that the signals that feed the gates of S1 & S4 are totally opposite to the signals that feed the gates of S2 & S3.

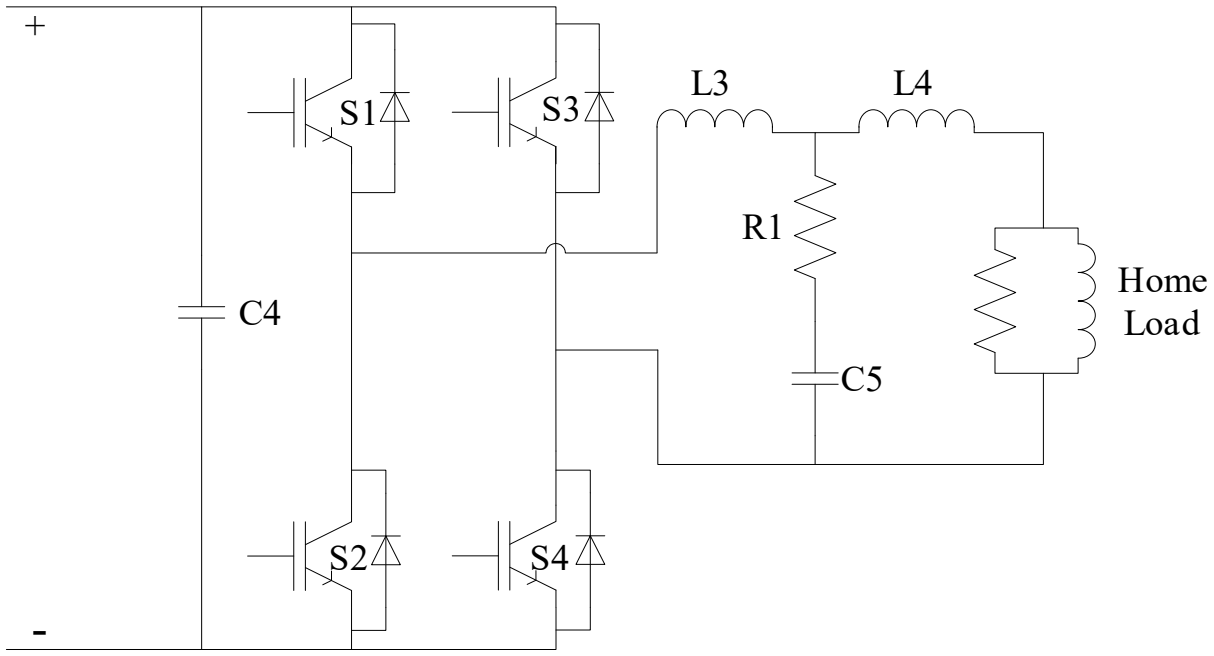

Figure 2.7 – H Bridge Inverter

2.5.3 Pulse Width Modulation

Pulse Width Modulation (PWM) is a form of modulation where the width of the peaks of the pulse varies based on a modulating input signal. PWM is a digital control strategy which means its state exists as either 1 or 0 in binary terms. This high or low state allows the PWM to be used for the control strategy for the IGBTs that make up the H bridge inverter for this energy management system. The output of a PWM generator is a rectangular wave, the ratio between the on and off states of the PWM output signal is referred to as the duty cycle. The duty cycle is nominally expressed as a percentage.

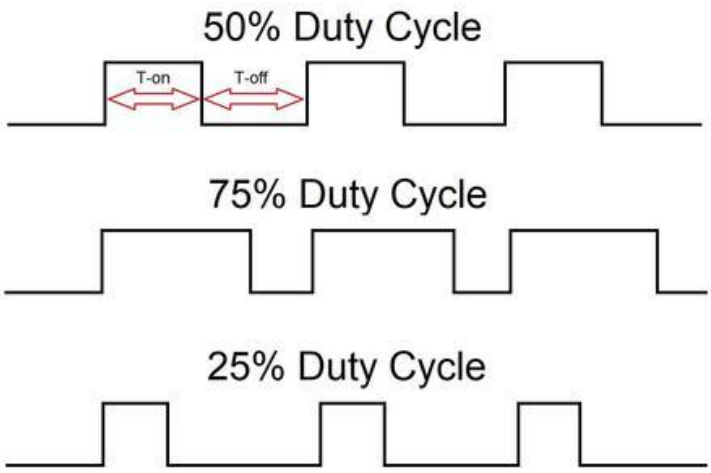

Figure 2.8 - Duty Cycle Measurement Signals

For inversion, Sinusoidal PWM is utilised, which involves the reference signal (as described in Figure 2.9) being V_{out}, which is the AC sine wave +/- 240V, and the carrier signal which is a high frequency triangular wave. The triangular wave must have the same amplitude as the DC link voltage V_{in} for the inverter.

The two signals are compared with a basic comparator and the switching state for the PWM generator follows the basic principle of a comparator. For Reference Signal > Carrier Signal the output of the comparator is high, 1 or “on”, for Reference Signal < Carrier Signal the output of the comparator is low, 0 or “off”.

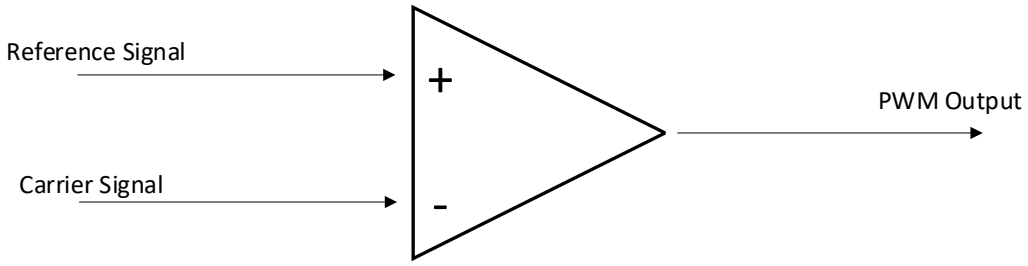

Figure 2.9 - PWM Fundamental Principle

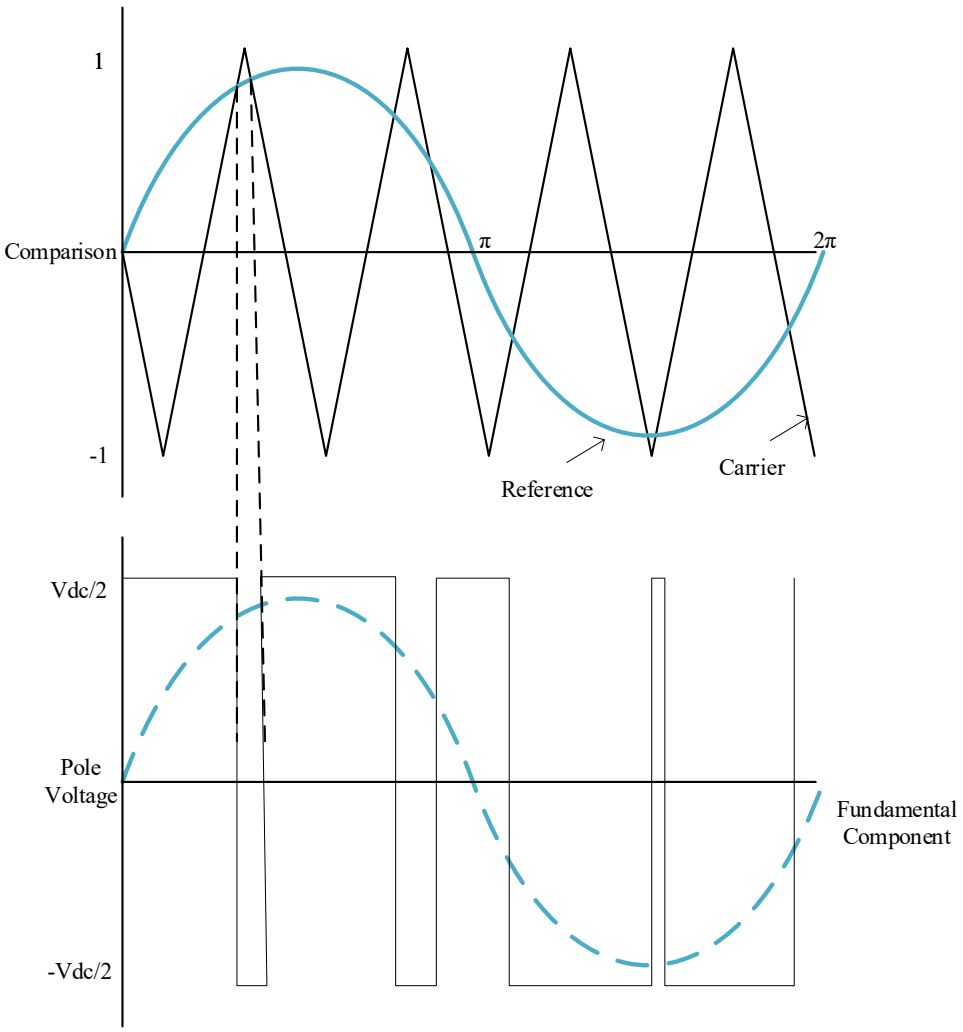

Figure 2.10 - PWM Indicative Signal

2.5.4 Filtering

The DC/AC inverter also utilises a critical Low Pass Filter (LPF) to reduce the noise of the output signal. The noise is usually generated by the PWM generator in the form of harmonics. The LPF will remove all the higher frequencies of a signal and allow the lower frequencies to pass through. The filter used in most PV systems can be described as a passive filter, which means that it is built from passive components such as resistors, capacitors, and inductors. Active components are components that include amplifying elements such as transistors [17].

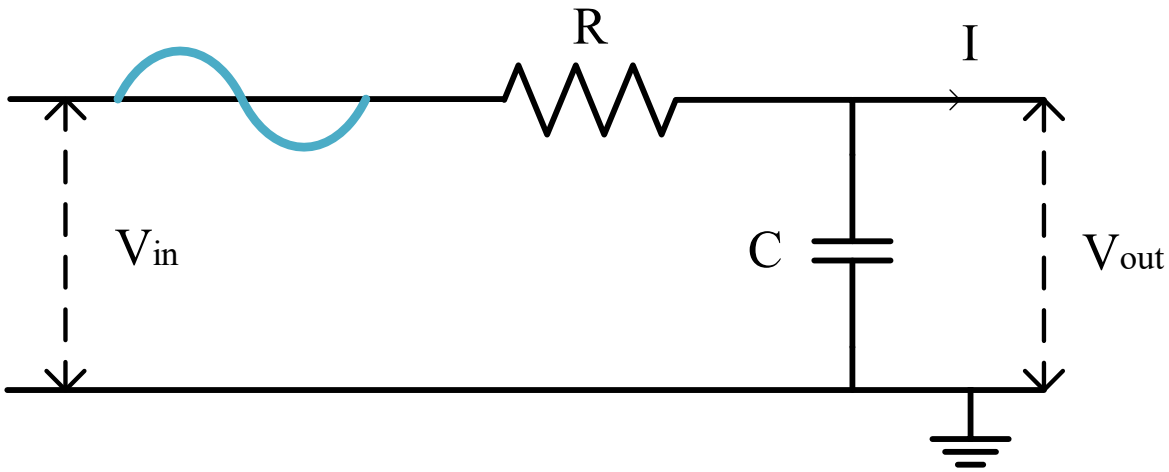

Figure 2.11 - Circuit for Low Pass Filter

Based on the circuit in Figure 2.11, the following equations show how the design for this filter will be calculated.

$$V_{out} = V_{in} \frac{X_C}{Z+X_C} \tag{2.15}$$

$$X_c = \frac{1}{2\,\pi\,f\,C} \tag{2.16}$$

$$Z = \sqrt{R^2 + {X_c}^2} \tag{2.17}$$

When equations (2.17) and (2.18) are substituted within equation (2.19) the following equation can be derived:

$$V_{out} = V_{in} \frac{X_c}{\sqrt{R^2 + {X_c}^2}} \tag{2.18}$$

$$V_{out} = V_{in} \frac{X_c}{Z} \tag{2.19}$$

The gain of the filter can be described as:

$$Gain\ in\ dB = 20 \log \frac{V_{out}}{V_{in}} \tag{2.20}$$

2.6 Approach to Gathering Literature

2.6.1 Rationale

The objective of this review is to provide a comprehensive assessment of the existing and novel PV technologies with updated information on MPPT, battery charger and inverter uses, including the various types and topologies, and their observed efficiencies. The various advantages and disadvantages to each will be discussed. Given the volume of variables associated with standalone PV systems to accurately investigate the systems it is necessary to investigate whole systems (which contain multiple sub-systems) as well as the individual sub-systems separately. A typical PV system should contain MPPT, Battery Charing and Inversion, however, a volume of published literature contains a boost converter sub system or modified control circuits for the various subsystems. From reviewing the current evidence-base, it is apparent that many of the review papers addressed these aspects individually and therefore this review has three sub-group analyses to ensure comparable conclusions could be drawn. Currently available PV technologies possess less than 23% conversion efficiencies [18], which highlights the need for further improvements to current technologies.

The literature review includes all available MPPT methods that have been conducted as a sub-system of a stand-alone PV energy management system and does not include any grid connected, micro-grid or hybrid wind energy MPPT sub-systems, in keeping with the pre-defined inclusion and exclusion criteria (appendix 1.2) outlined prior to conducting the review. The highlighted exclusion criteria were implemented to ensure that all investigated topologies were easily comparable.

2.6.2 PV EMS Literature Search Strategy

The databases IEEE Xplore, Scopus and Web of Science were used to systematically search for experimental and simulation studies of existing topologies for MPPT, battery charging and inverters for standalone PV energy management systems. Searches were conducted from 2018 to 2024 (latest build) ensuring only the most recent papers were included across the review.

Keyword searches and MeSH search terms were used to identify papers of interest. These terms were related to standalone systems (e.g., “stand-alone”, “non-grid connected”, etc.,), photovoltaic (e.g., “PV”, “photovoltaic cells”, “solar” etc.,) and management systems (e.g., “solar management systems”, “energy management systems” etc.,). The language was restricted to that of English language only, due to translational services within the University being unavailable. All duplicate records were removed from the compilation of results. The full search strategies for all databases can be seen in Appendix 1.2. The search strategies were approved by the Library Services team prior to use across the databases.

Table 2.1 – Databases and Articles

Database	Article Type
IEEE Xplore	Research Articles Review Articles Conference Papers
Scopus	Research Articles Review Articles Conference Papers
Web of Science	Research Articles Review Articles Conference Papers

2.6.3 Literature Eligibility Criteria

The databases were searched for all papers describing either practical experimental studies or simulated experimental studies focusing on standalone photovoltaic energy management systems, MPPT, inverters and battery charging. Studies were included if they discussed MPPT, battery charging, inverters in either a combined or individual manner. Studies were also included if they discussed single-phase systems whereas three-phase systems were excluded.

Inclusion criteria included 1) standalone systems, 2) photovoltaic systems, 3) inclusion of either MPPT, battery charging, or inverters or discussed all three in a combined manner, and 4) single-phase systems. Studies were excluded from the review if they discussed 1) grid systems, 2) hybrid solar and wind systems, 3) microgrid systems, 4) single-use case configurations, 5) three-phase systems, 6) micro-controllers and/or integrated controllers and 7) fuzzy logic controllers. Full exclusion criteria can be found in Appendix.

2.6.4 Extracting Data from Literature

To identify studies for inclusion, EndNote reference management system was used to conduct title and abstract screening against the pre-defined eligibility criteria. Full-text papers were then retrieved and screened using the pre-defined inclusion and exclusion criteria. Reference lists were manually screened for additional eligibility studies. The results of this review have been narratively synthesised and no statistical analysis pertaining to the relevance of the included study's findings have been conducted.

2.6.5 Study Identification and Selection

The literature searching of databases yielded 1,161 eligible studies for inclusion that were independently screened against the pre-defined eligibility criteria. After initial screening based upon

full title and abstracts, 200 papers were identified as being eligible for inclusion, with a further 71 papers being found through citation searches. Following full text retrieval and analysis,

2.6.6 Study Characteristics

In total, 94 papers that were published between 2018 and 2024 were included within the review as they met the pre-defined inclusion criteria. Out of the 94 papers, 35 studies discussed maximum power point tracking algorithms and topologies, 18 discussed battery chargers and their relative efficiencies, and 26 discussed inverters. Varying study designs were included such as experimental, simulation and review articles. The majority of studies were conducted across India and China, partly due to their wide-ranging collaboration network, with their main knowledge transfer emphasis being in areas such as engineering.

2.7 PV EMS Literature Review Findings

2.7.1 Baseline Findings

Three studies combined two out of the three basic sub-systems of an energy management system (EMS). Amara et al., proposed a basic two stage converter EMS which combined all the basic elements and circuit fundamentals, including H-bridge inverter, simplified P&O MPPT, in the absence of a battery charger whereby the basic sub-systems were shown to provide a suitable but not perfect performance characteristics providing scope for improvement through the modification of these basic sub-systems [19]. Nagarjun et al. proposed a modification of a three-port converter that combines the boost and battery charging elements of traditional DC-DC converters [20], with their proposed topology utilising a reduced switch count in comparison to a traditional PV EMS. An entirely mathematic algorithm was suggested by Deshmukh et al., who proposed a control algorithm whereby the layout of the system aligns with conventional energy management sub-systems, however, no inverter sub-system was proposed [21]. The control system described by Deshmukh et al., may be suitable to use as a comparison.

Eight studies investigated the use of all three sub-systems within their papers. Haque, Das and Razzak proposed an EMS that includes all of the key sub systems (MPPT, Battery & Inverter), with their proposed flowchart showing the battery charging circuit in series with a boost converter that feeds an inverter, as opposed to the conventional arrangement whereby a battery is connected in parallel [22]. Barathi et al. also proposed an EMS that included all of the key sub-systems, but specifically targeted rural areas where a grid connected system would not be feasible [23]. The control system uses an embedded controller which requires a low voltage battery power to run. The topology shows a high frequency transformer that feeds a voltage double which serves the home load. Postovoit et al., have proposed a standalone EMS that uses a charge controller that feeds an inverter [24], but also contains a battery bank of two 12V batteries, however detailed circuit topology is not detailed but control system appears to be running on an embedded controlled based upon presented flow charts.

A decoupled control strategy that feeds a multilevel voltage source inverter (VSI) was proposed by Ruttala et al., [25]. The presented circuit has 3 levels that are replicated and feed the single-phase multilevel inverter. The battery charging circuits are controlled using PI block diagrams with the paper providing a detailed flowchart demonstrating how the multilevel inverter is controlled. Hivziefendic et al., also proposed a full EMS with all three sub-systems for a standalone PV EMS that contained a bidirectional DC-DC converter in parallel with a PWM controlled DC-AC inverter feeding a home load [26], typical of a standalone PV EMS. However, the topology also depicted a grid connection that was linked to the home load, but the paper did provide a comparison between P&O, INC and fuzzy logic based MPPT algorithms. Algahassab [27] and Betti et al., [28] both presented studies that used conventional sub-systems such as MPPT, bidirectional DC-DC conversion in parallel to DC-AC inversion for a home load. To test this circuit performance, the irradiance profile was varied and the system current, voltage and power output was recorded. The circuits contained an additional sub-system, called a boost DC-DC conversion, which falls outside the scope for this review due to the increased switching loss caused by the additional conversion stage which impacts the overall response of the circuit. With a further study by Singh and Gupta [29] presenting an almost identical study as Algahassab and Betti et al. but using a multi-level inverter.

Three papers proposed new and novel strategies and topologies to improve output performance and efficiency. Mane et al. proposed a novel control strategy for a combined energy management system, whereby instead of controlling the two converter stages individually it combines the control strategies for both converter stages. The study did not include an inverter however it could be easily adapted for an AC home load [30]. Dalala and Saadeh have also studied and proposed a new control strategy for a multistage PV system that includes a battery charger [31]. Another novel approach was proposed by Bodele and Kulkarni who suggested using multiple input converters to serve a standalone home load, with the converter combining MPPT and inverter key principles [32].

Due to the volume of different sub systems and variables of a standalone PV energy management system, one of the ways to assess the performance of the system is to evaluate its response to variable input conditions. Multiple studies examined factors related to varying input conditions ([33], [30], [20], [22], [23], [32], [24], [21], [25], [31], [26], [27]). One outcome that was determined was the optimisation of the proportional integral (PI) control strategy, whereby Eid et al., tested a standalone energy management system (EMS) under varying load and environmental conditions. The P&O MPPT controller was used which fed the boost converter, which in turn was feeding a bidirectional DC-DC battery charger and inverter with a single phase-home load [33].

2.7.2 SPSAPVEMS Sub-System Literature Analyses

2.7.2.1 Maximum Power Point Tracking

Throughout the literature, thirty-five papers discussed MPPT algorithms to maximise the energy production., with three studies discussing conventional methods, seventeen papers discussing modified methods and fourteen papers discussing novel approaches.

Table 2.2 – MPPT Articles by Type

Method	Reference
Conventional	[34], [35], [36]
Modified	[37], [38], [39], [40], [41], [42], [43], [44], [45], [46], [47], [48], [49], [50], [51], [52], [53], [54], [55]
Novel	[56], [57], [58], [59], [60], [61], [62], [63], [64], [65], [66], [67]

A study conducted by Ali et al., [35] summarized the findings of an in-depth review into all MPPT method variations that have been published between 2015-2024, as shown in Figure 2.12 below the study focused on summarising and comparing conventional methods such as P&O, INC, Hill Climb, Variable Inductance, Variable Step Size, Linear Current Control, Slide Control, Ripple Correlation, Steepest Descent, Constant Voltage, Constant Current, and Curve Fitting. The review categorised these methods under one of three headings, namely online (where readings and measurements are taken in the form of sensors), offline (that are pre-configured models, based on the PV panel characteristics; the system is configured and controlled to ensure that it reaches optimal conditions) and hybrid (where systems combine more than one method to effectively track the MPP under varying environmental conditions).

Ali et al. highlighted the strengths and weaknesses of the two most popular MPPT methods whereby, from the viewpoint of harmonic analysis, the INC method performs in a more superior manner to that of the P&O method, a finding that was also substantiated by Atri et al., [48]. Salah et al. also produced a very similar review of many conventional MPPT methods concluding that hybrid MPPT methods provide a faster and more accurate response compared with conventional systems for tracking MPP [36].

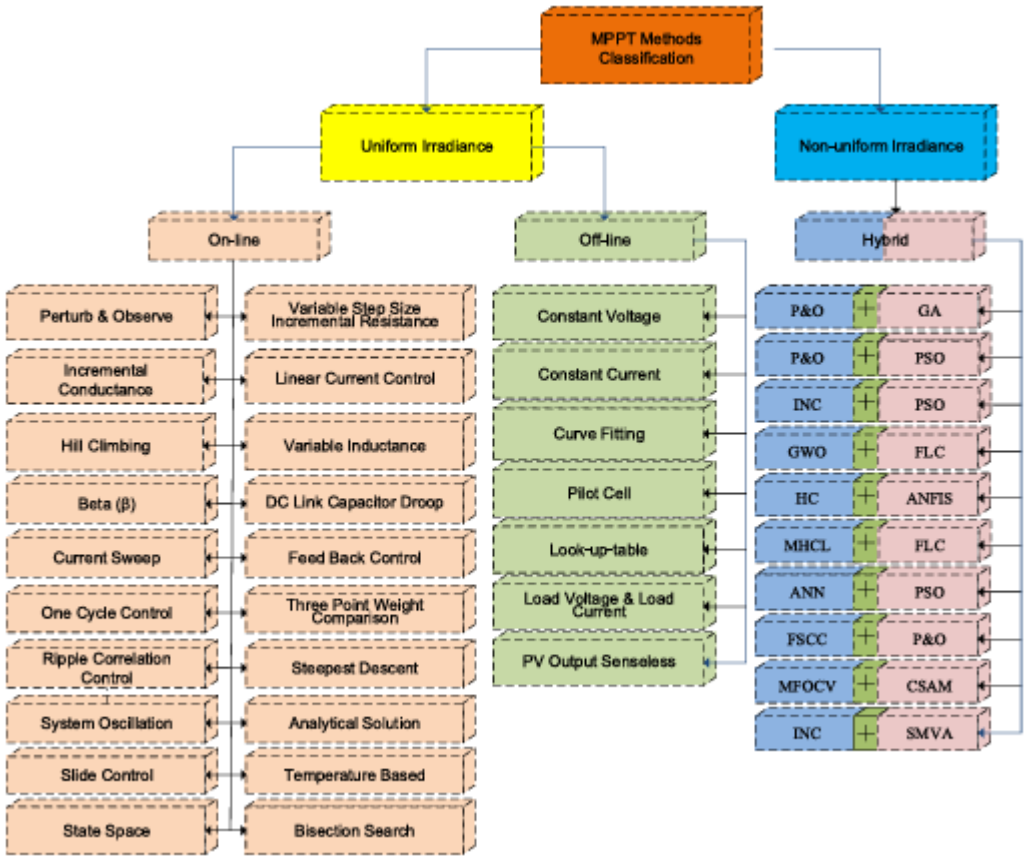

Figure 2.12 – Types of MPPT in a Flowchart *[35]*

Garg et al., [34] also compared conventional methods of MPPT including P&O, INC, FOCV & FOCC and discussed modified/hybrid MPPT methods and algorithms. The study investigated the pre-configuration, the ability of dynamic tracking, stability, complexity, and efficiency of the algorithms and also compared the MPPT methods for varying irradiance and temperature conditions.

Behera. P et al. presented a modified method of Direct Power P&O MPPT [68]. The objective of the proposed method is to combat the trade-off between a slow but accurate response caused by a small step-size selection for traditional P&O MPPT methods, which is achieved using two methods of control, firstly, directly controlling load power and secondly, by controlling the voltage to regulate the output voltage. A study by Sarika et al., described a varying step-size P&O MPPT method [39], with further studies by Agrawal et al., [51] and Abdrahim et al., [55] proposing similar methods. Karthika et al. conducted a simulation and practical study that verified their enhanced modified P&O and solar tracker method that improves the efficiency of MPPT for standalone PV systems [44]. The algorithm for this method of MPPT is shown on Figure 2.13 below. The solar tracker uses a system of LDR sensors and solar panels mounted on a bracket that is attached to a motor. When the LDR detects sunlight, the motor turns the brackets such that the solar panels are always pointing directly towards the sunlight. MPPT methods use the solar output power curves to track the maximum power point with this point only being found at the peak of the curve.

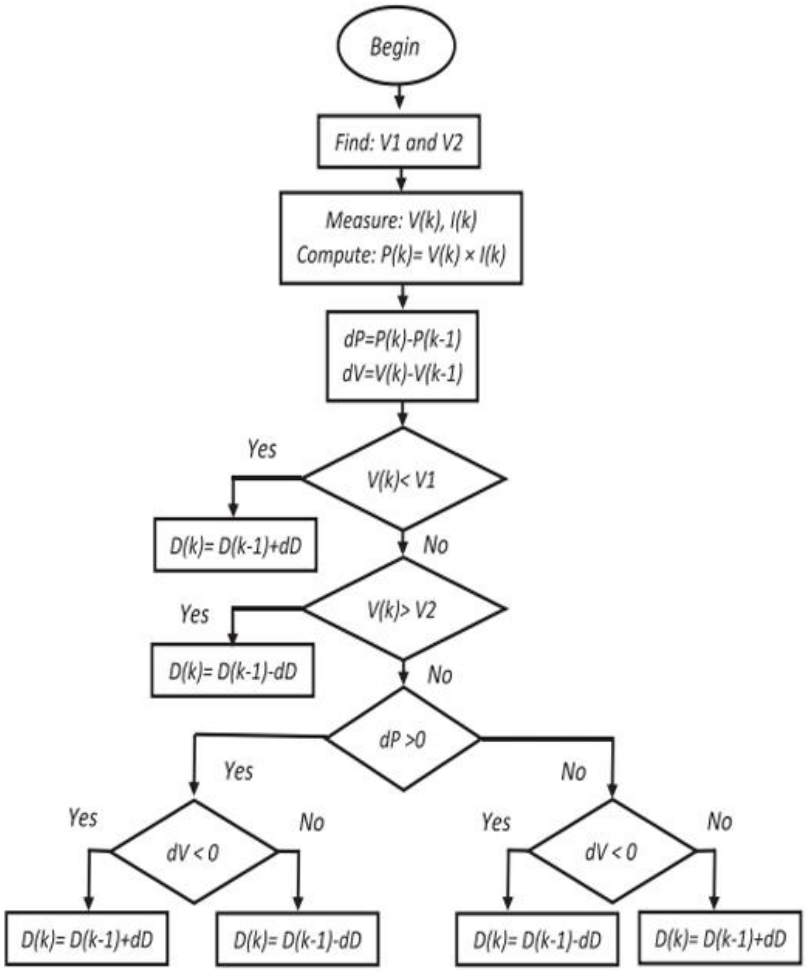

Figure 2.13 – Enhanced and Modified P&O Algorithm [44].

A number of papers discussed the amendment of the step-size of the MPPT algorithm including Swaminathan et al., [41], Behera. D et al., [38], Ali et al., [40], Rougab et al., [45], Anya et al., [46], Manuel et al., [47], Liu et al., [49], Chtita et al., [50], Adawi et al., [52], Al-Wesabi et al., [53], and Chaibi et al., [54]. The methods marginally improved the overall performance of the MPPT sub-system compared with their conventional method counterparts.

Several papers discussed novel approaches to MPPT algorithms and topologies. Faranda & Akkala proposed a novel approach to power point tracking using the conventional P&O MPPT method, however an additional stage has been added to the power point tracking flowchart that compares the load power with PV power, this is observed in Figure 2.14 [58]. If the load power is less than the PV power the system will then operate in RPPT mode. It is noted that on a P_{pv} curve, except for the MPP, there are always two possibilities for P_{pv}, either left of the MPP or right of the MPP. The method proposed by Faranda & Akkala seeks to understand which of the two points is being read and allows the system to regulate for varying loads. To do this a voltage step is applied to understand if there is an increase (left side power points) or decrease (right side power points).

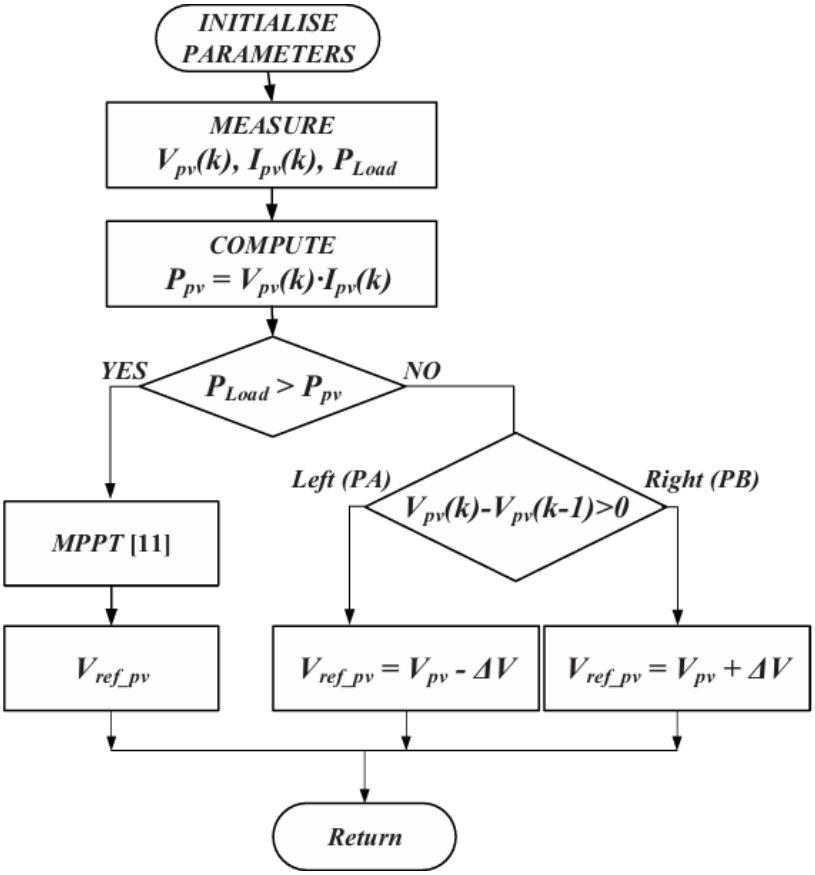

Figure 2.14 – Return Power Point Tracking Algorithm [58]

A number of novel approaches involve predictive control methodologies. Modified Predictive Model Controls designed by Ikaouassen, Moutaki and Raddaoui is an example of a modified MPPT method where the control circuit have been modified [56]. The proposed method contains two PV arrays connected to two boost converters. The boost converters in this topology are controlled independently with the objective of this approach being to maximise the efficiency of the system for all varying climate conditions, including weather changes and partial shading.

Ba et al. proposed a novel predictive control method with the principle of this method of MPPT allowing to compare the P_{pv} curve to determine the optimum duty cycle for the desired load voltage [59]. However, Chao et al., described a different type of MPPT controller namely that of an AI / learning based algorithm shown in Figure 2.15 [66]. These methodologies are complex by nature, however, the real-world applications of an AI based MPPT model will prove to be a key innovation attributed to the rise of AI and the development of quantum computing to perform these types of computations efficiently at scale.

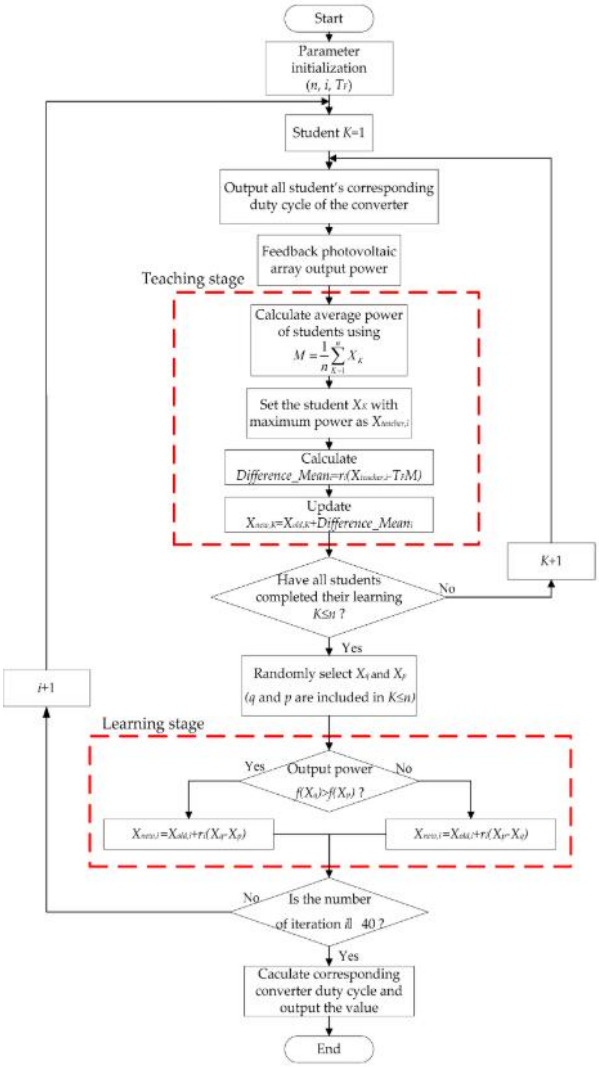

Figure 2.15 – Return Power Point Tracking Algorithm [66]

Sharma and Kumar propose a sliding mode (SM) controller based on Lyapunov stability theorem [61]. The SM approach is non-linear with the study comparing two types of SM controller, that of a conventional nature and a modified nature. The method shows traits of "chattering" meaning the system shows multiple oscillations before reaching steady state however, though the systems are more complex than traditional methods, they are accurate for realising MPPT. A further study conducted by Taissala et al., have optimised a nonlinear controller for MPPT resulting in *"increased convergence in steady and transient states"* [65].

A further novel approach was proposed by Rehman et al., who described an MPPT based on High Order Sliding Mode (HOSM) and twisting algorithms [60]. This method was compared with a standard P&O MPPT controlled with a PID controller for varying environmental conditions including temperature and irradiance. The two main functions of the method include determining the reference voltage and comparing the PV output voltage with the reference voltage, along with slowly reducing the error to 0.

In 2020, Huang et al., published an article that proposed an extremum seeking control method of MPPT [43]. The principle of the method was to observe, filter and adjust using closed loop feedback control, which was simulated in MATLAB and used an integrator, adjustable gain, and a high/low pass filter. The novel method was compared with three conventional MPPT algorithms (P&O, INC and FOCV).

Wibowo et al., propose another novel approach to MPPT that is compared to P&O and partial swarm methods [69]. A similar particle swarm-based methodology is also proposed in by Panda et al., [62], Obukov et al., [63] and Balaji and Fatima [64]. The solar panel power curves are divided into sectors, with the queen travelling to each sector. Scout bees will also travel to each sector and the probability of excitation is calculated for each sector. The final reading it takes is the MPP which is the area with the largest probability. Elbehairy et al., proposed an AI based algorithm with similar properties to the queen honey bee method (QHBM), however it is described as the "flower pollination" algorithm and is a method that is ultra-fast for finding MPPT but does require active electronic devices like all other learning-based AI algorithms, a visual flowchart for this algorithm is shown in Figure 2.16 [67].

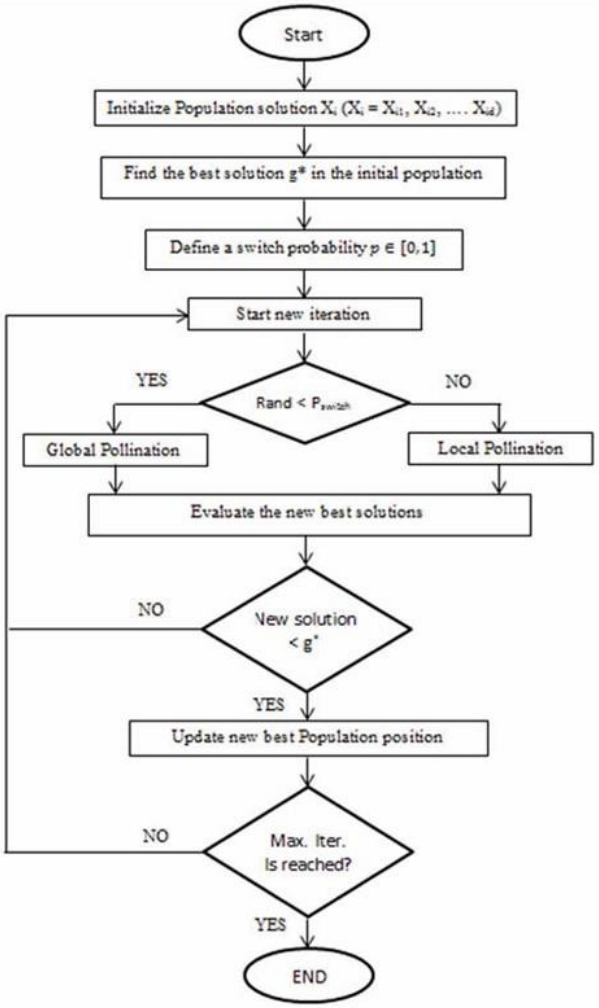

Figure 2.16 – AI Based MPPT Algorithm [67].

2.7.2.2 Battery Charging

As well as a battery, a super capacitor, ultra-capacitor, or hybrid battery can also be used to store the energy generated by a solar PV system. Saadeh et al., proposed adding additional energy storage elements in parallel and controlling them using separate bidirectional DC-DC converter [70], with the principle having the ability to charge multiple batteries. Whilst Sedaghati et al., [71] and Battula et al., [72] proposed a modified z-source dual input DC-DC converter with the principle of this method being to optimise the power loss by reducing the number of switches, the topology for this method is shown in Figure 2.17 below, which in theory improves the overall efficiency of the system.

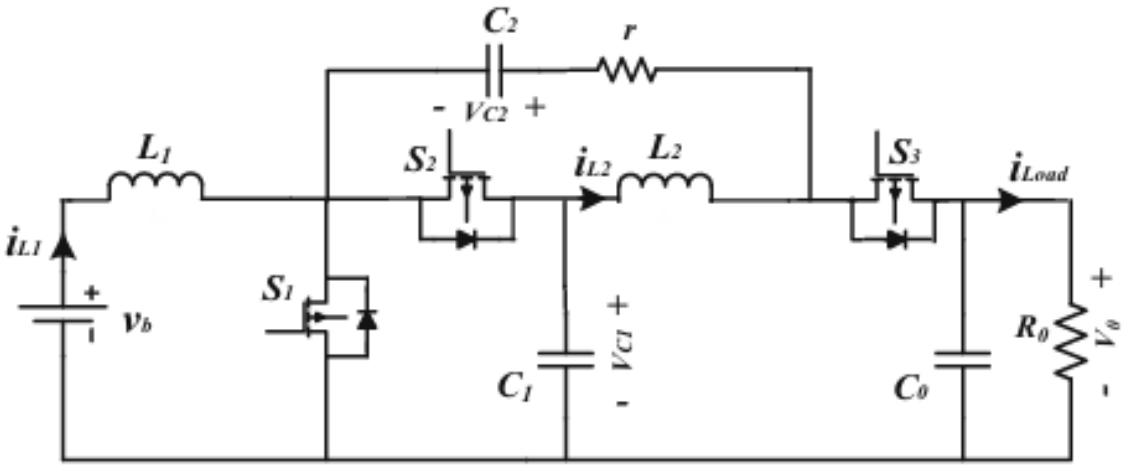

Figure 2.17 – Bidirectional Switched Quasi Z-source DC-DC Converter [72]

A control strategy has been developed by Bhule et al., for a bidirectional (buck-boost) converter, which is a single stage control targeting efficiency increases compared with conventional methods of battery charging control circuits [73]. The system uses has separate control methods for Buck/Boost and MPPT converters and each use PI controllers. The study considers a combination of current control and voltage control using reference current and voltage comparisons.

Bhattacharyya et al. proposed a bidirectional converter that is voltage controlled, whereby the power is automatically distributed between the load and the battery depending on the load power demand [74]. The topology of this system shows the battery and charger connected in parallel to the boost converter that is connected in series with the PV array and load. The control strategy for this system utilises a PI controller, with the study presenting both simulated and practical data. With Bhagiya and Patel outlining the concept of a dual loop passed PI controller (the topology for which is shown in Figure 2.18), a strategy that contains a PWM based feedback loop for inductor current within another feedback loop to control load voltage [75].

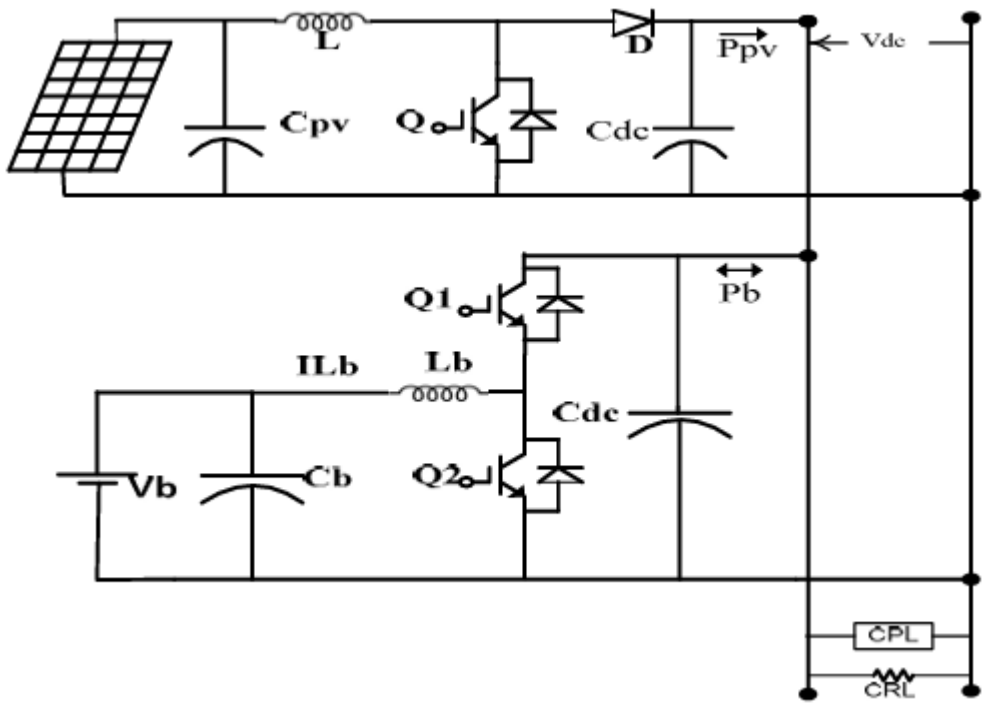

Figure 2.18 – Bidirectional DC-DC Converter [75].

Mahmud et al. proposed a non-linear control design for battery charging in a solar EMS [76]. The topology of the system is identical to a traditional bidirectional dc-dc converter, however in the control loop for this system, part of the control system is non linearised with a small part of the control system being linearised for stability purposes.

Pathak et al., describe an interleaved non isolated DC-DC converter that charges a battery as part of a solar EMS [77]. The PV panel feeds a boost converter that is controlled by an MPPT circuit (in this case a traditional P&O MPPT circuit). In parallel the non-isolated battery charger is controlled by a current and voltage PI feedback loop.

A dynamic power management strategy was proposed by Ananad et al., where the system uses a single stage and a single inductor [78]. The control scheme for this system is a time-based voltage mode control scheme. The dual active bridge methodology explained by Nalamati [79] splits the battery charging circuit into the sides, Low Voltage (Battery side) and High Voltage (PV/MPPT-Boost Side), connected by a high frequency transformer.

Sato et al. proposed a novel bidirectional PWM converter, and a phase shifted switch capacitor converter [80], whereby they compared the proposed methodology of a non-isolated multiport converter with phase shifted switch capacitor conversion with conventional approaches such as Ladder, Dickson, Series-Parallel and Fibonacci. Uno et al., also proposes a differential power processing capable system visually demonstrated in Figure 2.19 below [81], with this novel approach having a 1 to 1 ratio of PV

panel to DC/DC converter however, the DC-DC converters are connected in parallel to form a multiport converter.

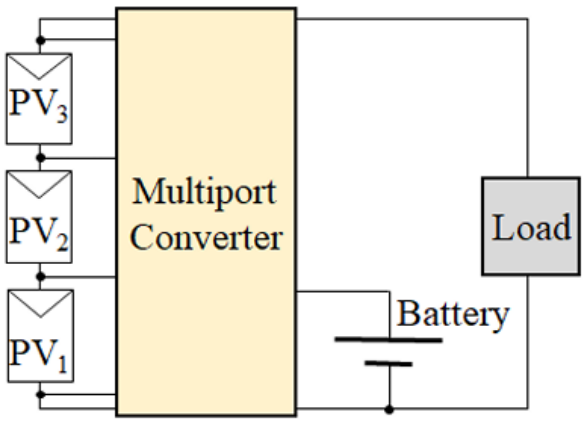

Figure 2.19 – Multiport Converter High Level Diagram [81]

2.7.2.3 DC-AC Inversion

A number of published literature uses an S-Packed U Cell Inverter (SPUC), an example of which in one proposed by Ouradi and Gadari in a standalone single phase photovoltaic topology that utilises a five level SPUC shown below in Figure 2.20 [82]. Inverters are commonly controlled using PWM switching, this methodology also uses two capacitors and 4 bidirectional switches. Aside from a SPUC inverter, other published literature also looked at cascaded inverter and multiport inverters, however, the most common topology type presenting in literature are types and variations of the multilevel inverter. The published literature attempts to mitigate the common drawbacks of multilevel topologies including large volume of switches, poor harmonic performance, slower response time, reduced overall converter efficiency.

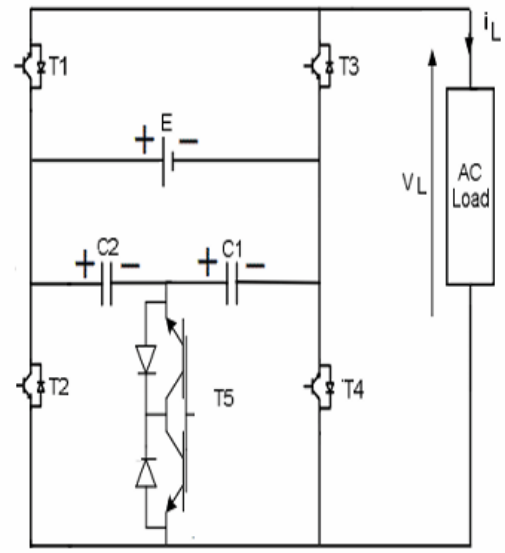

Figure 2.20 – Five Level SPUC Inverter [82].

Combining the bidirectional DC/DC converter stage with the DC/AC inverter stage is a popular method of developing a multiport inverter. These inverters are often multi-staged with the stages connected in parallel such as those proposed by Uno et al., [83] and Roy et al., [84]. The topology of a cascaded inverter involves splitting the PV input into two equally balanced inputs with two cross connected H bridge inverters as shown in studies presented by Boonmee et al., [85] and Yadav et al., [86]. Ankit et al. have conceptualised an interleaved inverter to reduce output ripple [87] with this concept being simulated and the results discussed. The topology is shown in Figure 2.21 below and can be used for as many interleaved converters as required as long as each of the gate pulses are offset. For example, for a 3-stage interleaved inverter, the gate pulses will be shifted by 120 degrees.

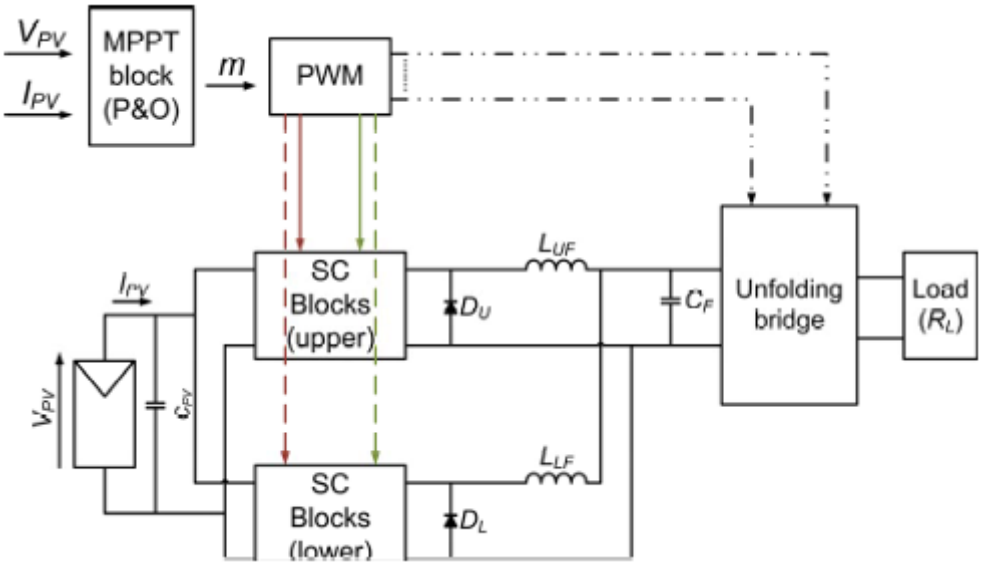

Figure 2.21 – Control Strategy of an Interleaved Switched Capacitor Inverter [87]

Behera. S et al. have published a study that compares multiple control techniques for a basic H bridge inverter. The methodologies are bipolar, bipolar phase shift, bipolar harmonic, unipolar, unipolar phase shift, and phase opposition PWM [88]. Further performance analysis is also carried on Bipolar vs Unipolar switching schemes by Behera. P et al., [68]. Convoluted control methodologies have been published in literature due to their novelty, however, in some cases, complexity of control often contributes to poor harmonic performance. Singh and Mishra have designed a control technique that can be used for a multiport inverter with this standalone mode inverter being controlled using a proportional resonant (PR) voltage controller [89].

2.8 PV EMS Findings

Across the literature many different configurations of sub-systems were presented. The studies that configured two out of the three basic sub-systems found that overall, the performance of the EMS was improved. Mane et al. determined that the combined control strategy for the MPPT, boost and battery charger improved the EMS efficiency and resulted in improved battery life [30], however the

study did not include an inverter sub-system, but the principle of combined control does provide some additional performance benefits. In the study presented by Nagarjun et al., it was found that their topologies were suited to specific functions (Figure 2.22 below), which is undesirable in a practical scenario and is aligned with a portion of published literature that proposes novel solutions have simulated improvements, however the real-world applications of these systems limit them from wide-spread utilisation in diverse geographies [90].

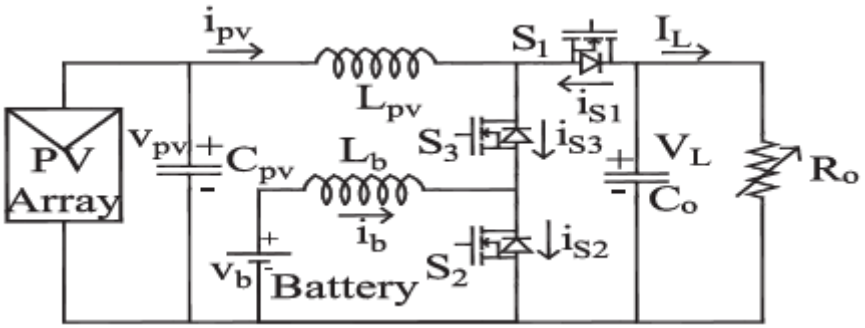

Figure 2.22 – Double Boost Input Output Converter [90].

Many studies included all three of the basic sub-system types, however their configurations and overall findings were highly similar. These studies opted to reduce the complexity of the circuits which resulted in improvements to the integration capability for the overall EMS circuit. The system proposed by Haque and Razzak shows a practical circuit that has been developed and tested to validate simulated information, from this data the inverter is shown to be 97% efficient [22], however, the inclusion of the boost stage introduces undesirable slower response of the overall system. It appears that the control circuit proposed by Bharathi et al., is run using an embedded controller and pule amplifier each requiring a 5V and 12V supply respectively [23]. Embedded controllers can be challenging and costly to both run and maintain and are therefore not desirable and unconventional. The study doesn't show how the battery is charged but instead focuses on the voltage doubler that occurs before the load is served.

Betti et al have investigated a fractional order PID control strategy for the control of a standalone EMS [28]. The control strategy utilised compared with other control schemes shows a better capacity to adapt to variable environmental conditions. Postovoit et al., have taken a practical exploration at the ability of a system to handle a typical large, medium, and small sized load throughout the day [24]. Whilst this system contains all the relevant PV energy management sub-systems, the data is purely practical and not comparable to simulated data commonly presented in other literature. Singh and Gupta have integrated their battery management technique with their cascaded H bridge multi-level inverter [29], this can be seen from the topology of this study denoted in Figure 2.23 below. The flowchart shown is similar in its topology to that presented by Ruttala et al., [25], however the control

strategy is not as complicated. The use of a sliding mode controller balances the power whenever the load changes.

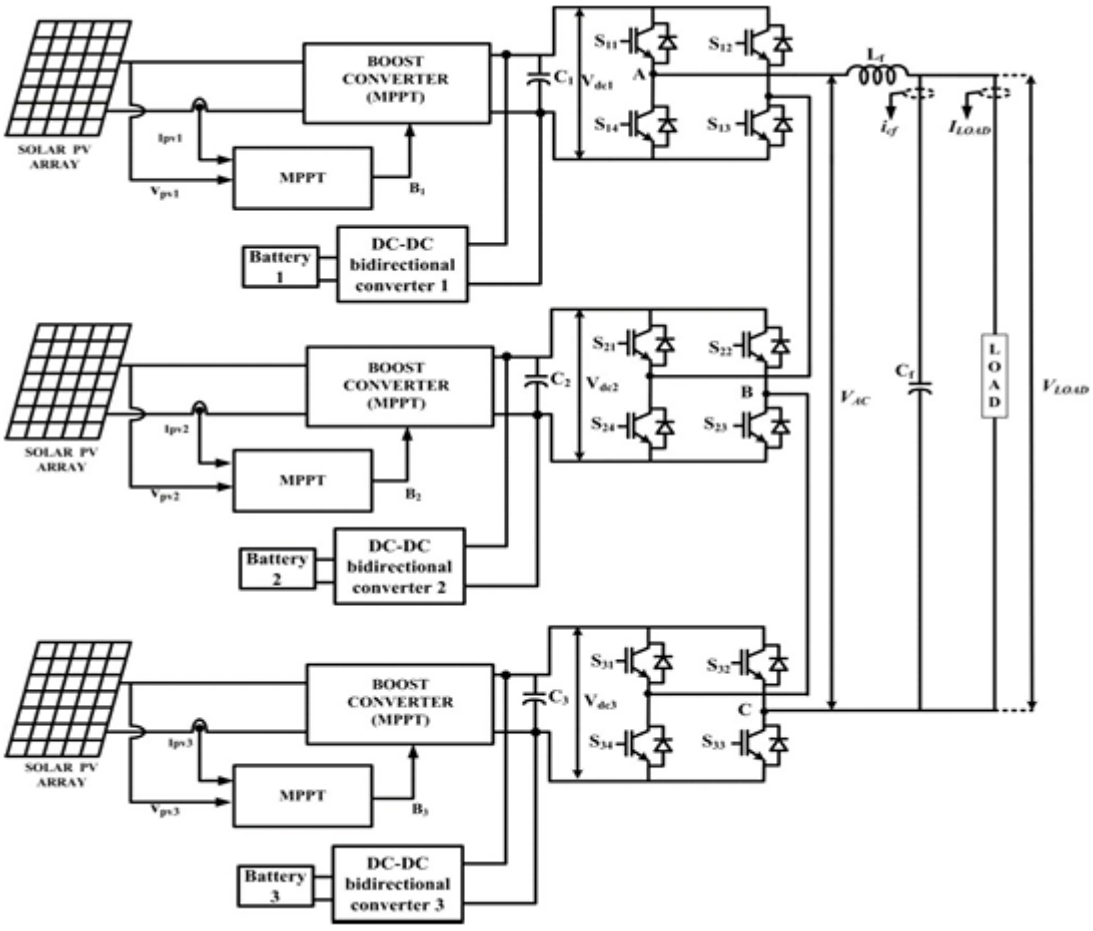

Figure 2.23 – Cascaded H Bridge Multi Level Inverter with battery storage [29].

Whilst the findings of these studies hold merit in terms of their ability to adapt to varying environmental conditions and increase the overall EMS efficiency, most of the studies retrieved contained an additional boost converter stage. The introduction of the boost converter increases the time for the inverter to reach steady state, dampening the overall response time of the EMS, which is undesirable for PV EMS, especially when considering environmental changes regularly impact the output of the PV array. Therefore, the response time of the circuit is critical to enable maximum efficiency for a standalone application.

The multiport converter presented by Bodele et al., in their novel approach is simpler than conventional methods and therefore has advantages such as the ability to shoot through protection and source side fault tolerance, however, a limitation of this paper is that it does not contain a battery or battery charging element and this could be explored further as a development [32]. The study by Eid et al. depicted in Figure 2.24 below, resulted in harmonic performances of under 1%, along with a further key finding highlighting that the battery capacity increases the performance of the circuit increases [33].

The system proposed by Dalala and Saadeh does not include a DC/AC inversion, and this presents a potential improvement such that the system can supply an AC home load. A three-loop cascaded controller proposed in this study could have additional benefits for an energy management system however in this study it is used to control a boost converter.

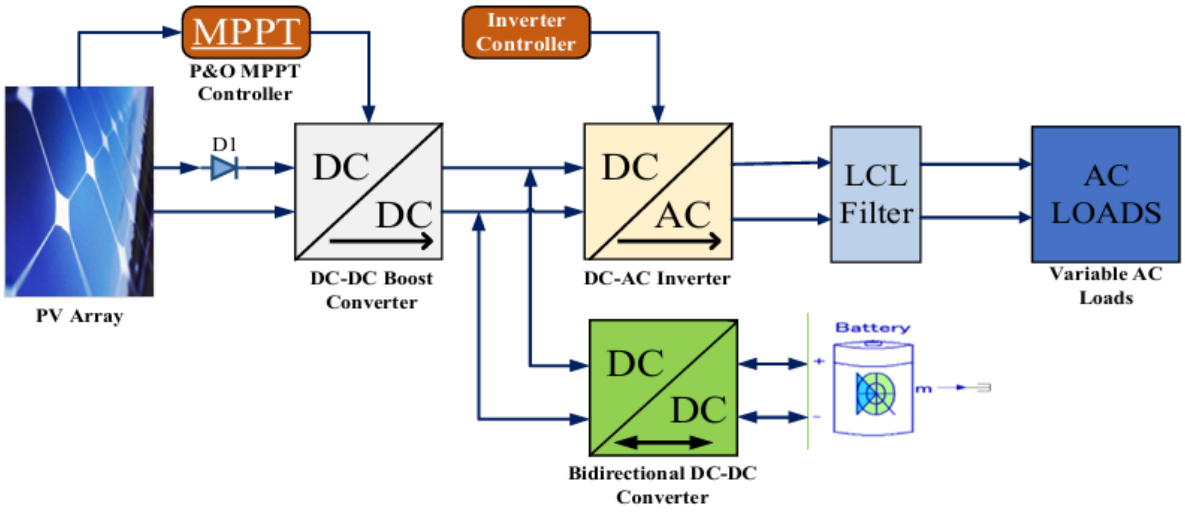

Figure 2.24 – Common Proposed PVEMS with additional DC-DC Boost Stage [33].

2.8.1 Maximum Power Point Tracking

There have been many different attempts to improve and optimize a standalone PV system through modifications to MPPT approaches. The key finding from analysing the existing literature shows that a hybrid model which involves a combination of two different MPPT elements is the most effective and gives a balance of performance when considering efficiency, response time and stability. Another important finding shows that non-hybrid model approaches do not totally give optimal or improved performance when compared to conventional methods. Novel approaches give a faster response and improved efficiency however they do not always give the most stable response. It can also be concluded that many novel approaches involve pre-configuration of the system to a known or expected dataset. Whilst in an ideal situation this is an ideal approach, in practical systems there is always data that are outliers and in the case of standalone PV systems, weather will always change, and therefore irradiance and temperature will also be changing frequently. Given that a standalone PV system will utilize a battery, there is less of a requirement for a rapid response time, more so the quality and the system's ability to adapt to variable conditions. It was determined that a hybrid MPPT system provides a faster and more accurate response for tracking the MPP compared to conventional systems such as P&O and INC, supported by conclusions of analysis conducted by Ali et al., [35] and Salah et al., [36] however, the hybrid MPPT systems introduces a level of complexity which can lead to installation and/or integration difficulties for embedded systems ultimately making them less desirable.

The direct power P&O method described by Behera et al., showed an efficiency of 95% [37]. The method was simulated using Simulink and validated with practical data, with the data providing

some assurance of the performance of the system, however, a traditional P&O MPPT method can also achieve a similar efficiency percentage of 92-96% in a simulated environment.

Amongst the studies, the most commonly utilised method was the P&O algorithm, which is widely used due to the algorithm's simplicity and ease of implementation. When analysing this method, it is demonstrated that the P&O algorithm has a commutation between the tracking speed and the number of oscillations due to the fixed step-size. The implementation of variable step-sizes and using alternative MPPT algorithms were navigated.

A variable step size P&O MPPT method is proposed in [39] where multiple step sizes are utilized by taking the derivative of Ppv and comparing instantaneous power with delayed power. The ratio of the derivative of Ppv / Vpv is compared to the system error. The conclusion of this study shows that the proposed method is substantially faster and more efficient than the conventional method. In the studies outlined by Agrawal et al., [51] and Abdrahim et al., [55] there are also modifications to P&O (Hill-climbing) MPPT whereby the step size is modified by an accelerating factor, this improves the speed of the response of the circuit and the 96% efficiency aligns with the standard P&O method the algorithm for an example of one these methods is shown in Figure 2.25 below.

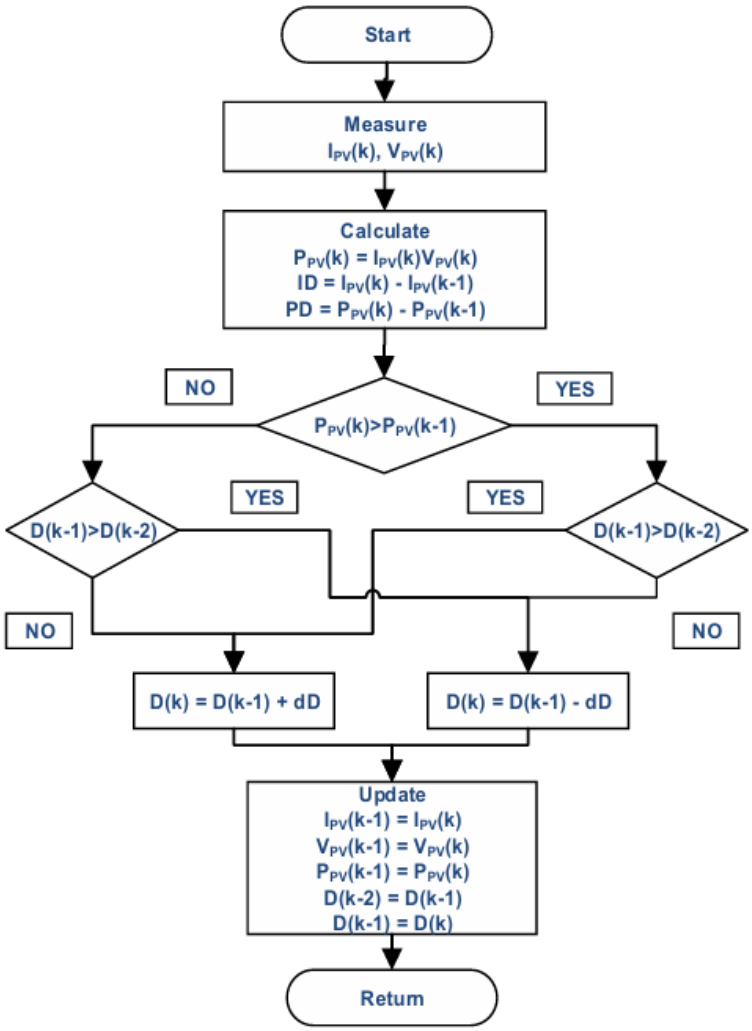

Figure 2.25 – Hill Climbing MPPT Algorithm (Modified P&O) [55]

Similarly, in the study by Swaminathan et al., the principle of variable step sizes is also explored via a different method [41]. Taking a standard Ppv curve, this curve is split into 4 zones and each zone shows similar trends for varying environmental conditions. This method shows minimal output oscillations and efficient reactions to varying environmental conditions. The circuit must be configured for known step changes in irradiance and temperature, thus alleviating the need for complex calculation during the MPPT cycle and therefore a faster response time to realize the MPP for the PV panel.

Variable Step Incremental Conductance has been implemented using an interleaved boost DC/DC converter rather than a conventional boost DC/DC converter by Behera D. et al., [38], however Chtita et al., [50] (shown in Figure 2.26 below) proposed an adapted algorithm for INC. Behera et al., was able to reduce the overall output ripple due to the addition of the interleaving topology, however both papers have successfully improved the traditional INC and PPT method by varying the algorithm step-size. The variable step method can be used across both P&O and INC MPPT methods with the objective focused on the speed of the response and the accuracy. This means that at different times, the

step size of the MPPT system is smaller, at this point, the speed of the response is reduced, hence the desire to not run a small step size for the whole process.

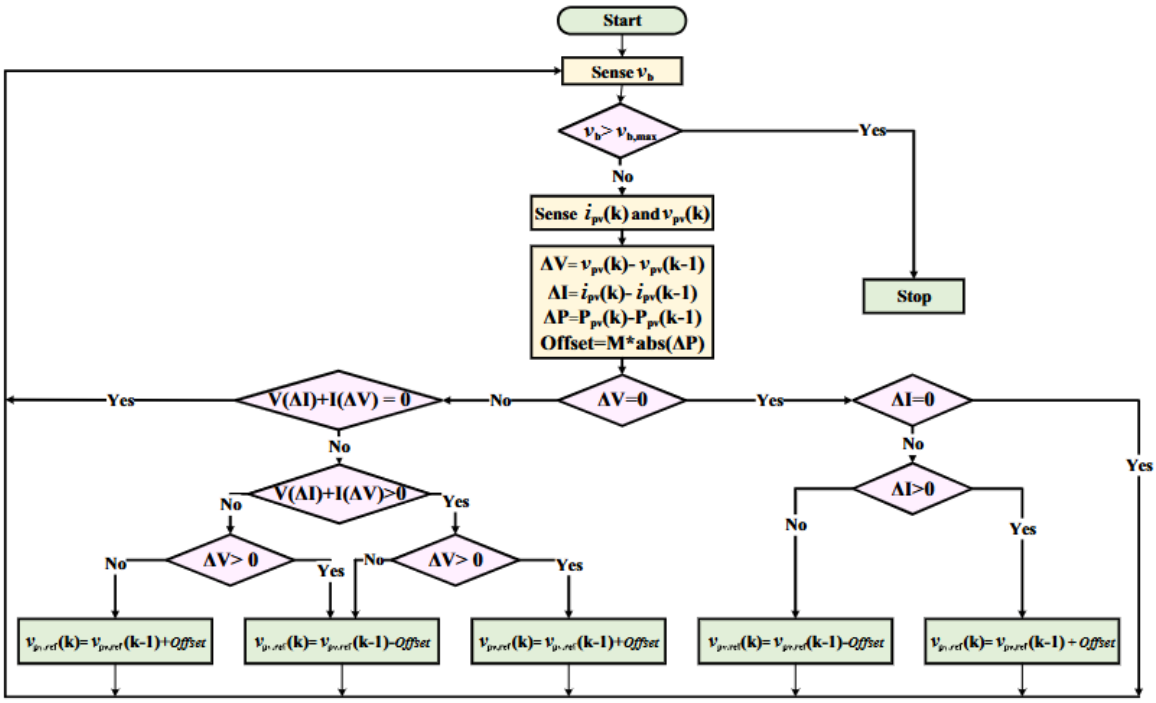

Figure 2.26 – Variable Step Incremental Conductance MPPT Algorithm (Modified INC) [50]

Another common P&O modification is the sliding-mode approach as proposed by Sharma et al., [61] and Ali et al., [40]. A sliding mode controller (SMC) nominally exhibits an unstable output known as “chattering”; this adaptation aims to limit and minimize the chattering as it reduces power quality and overall system efficiency. Whilst this method does improve the MPPT output characteristic compared with other sliding mode controllers, it still shows an unstable MPPT curve relative to other P&O variations. Similarly, Rougab et al., proposed a simple modification to conventional P&O using a PID regulator that is effective at efficiently reaching the MPPT for varying environmental conditions [45]. A number of studies proposed this method to modify the standard P&O approach ([61], [40], [49], [53], [54]).

Anya et al., [46] and Manuel et al., [47] proposed an adaptive method of P&O. In principle the approach improves the MPPT, however these applications are specifically configured for an EMS that has a boost converter stage and DC microgrid. The adaptive method demonstrated a reduced complexity and overall improved output signal when compared with the sliding mode controller model.

The use of a grey wolf optimisation (GWO) proposed by Chauhan et al., utilised a modified INC MPPT method shown in Figure 2.27 [57]. The method was simulated and suggested evidence that it reduced steady state oscillation compared to traditional INC MPPT, enabling the maximum power point to be found in a reduced amount of time.

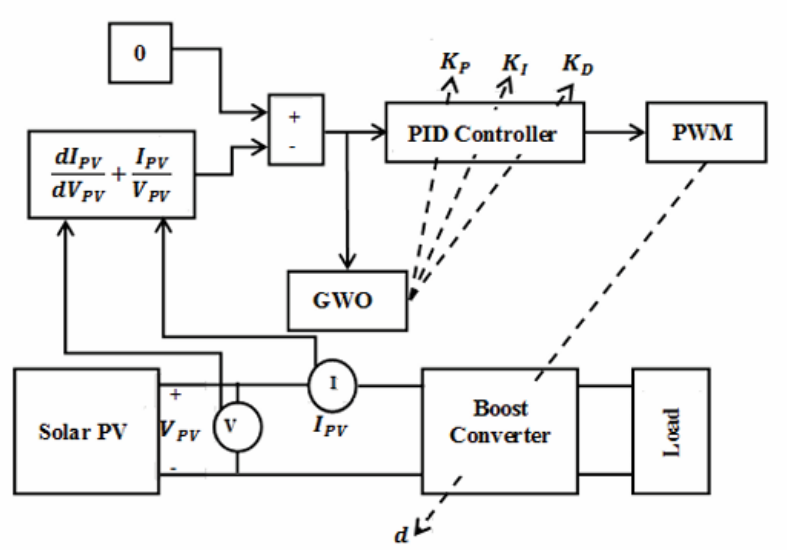

Figure 2.27 – Grey-Wolf Optimisation Schematic (Modified Incremental Conductance) [57]

Karthika et al. utilised a method that considers the area under the IV/PV curve to be split into three areas [44]. The focus of MPPT is only 20% of this area, 60% of the area is to the left and 20% is to the right. This method will only check the 20% where MPP should be found therefore increasing the speed of the response and the steady state oscillation. The method does not lend itself to being effective for varying environmental conditions without additional configuration as the MPP may not lay within this 20%.

Adawi et al. proposed a basic method of improving the MPPT whereby the method involves splitting the PV array such that it feeds multiple stages of MPPT (both double and quadruple) [52]. There are some advantages to this method for partial shading conditions provided the appropriate PV arrays are feeding the correct MPPT stages, however, this level of pre-configuration and volume of components required is not a practical solution for the proposed use case of easy-install and adaptable PV system.

From reviewing the reduction power point tracking novel MPPT method presented by Faranda & Akkala, it can be concluded that for power points that are to the right of the MPP, the response is unstable for power points that are to the left of MPP, compared with points to the right. Whilst it is effective in tracking the MPPT, the response is much slower, therefore resulting in a reduced overall efficiency when compared with conventional methods. Modified Predictive Control (MPC) methods as described by Ikaouassen, Moutaki and Raddaoui takes the standard P&O method but uses it to control two halves of the circuit independently, it is clear that the output power (across the same time frame) is higher and the response to environmental changes is faster. The drawback of some of the methods of predictive control (e.g. [59]) is that they require the environmental conditions to be precisely predetermined, this method would therefore require reconfiguration for varying environmental conditions.

The HOSM MPPT controller is suitable for varying conditions and errors however, there is a delayed response time of the MPPT algorithm compared with other methods of MPPT [60]. Whilst the extremum seeking control method as described by Huang et al., can perform under variable conditions as well as the incremental conductance method [43]. It does however require refinement to improve the response time and steady state oscillations.

The simulated data produced by Wibowo et al., [69] (and from Figure 2.28 below) Chen et al., [91] shows that the QHBM is highly efficient and tracks the MPP at a much higher efficiency than other methods (c.99%); this is proven via simulated and practical data, and it is also tested across varying irradiance conditions. The method does take slightly longer to reach steady state however the oscillations are limited.

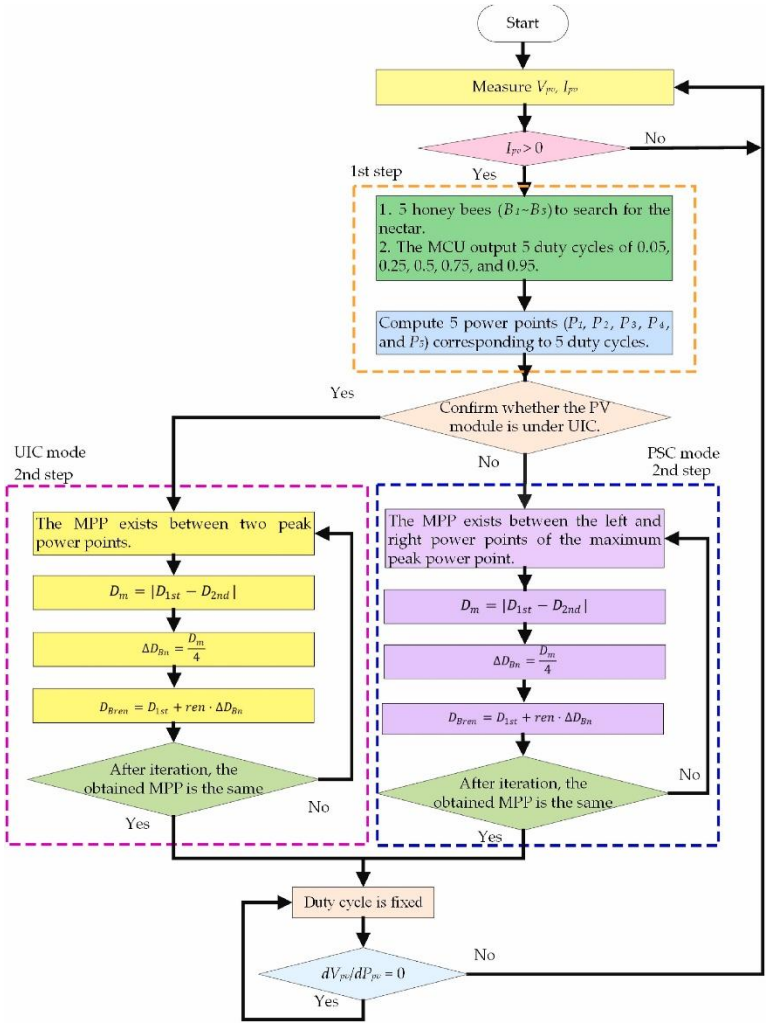

Figure 2.28 – Grey-Wolf Optimisation Schematic (Modified Incremental Conductance) [91]

2.8.2 Battery Charging

In alignment with much of the published literature in relation to battery charging, the literature focuses specifically on the battery charger in isolation and rarely shows overall EMS performance with

an integrated battery charger. An example is Bhandari et al., where a SEPIC/ZETA bidirectional converter is proposed with MPPT (P&O) whereby the DC load output is shown to react efficiently to changes in input conditions [92].

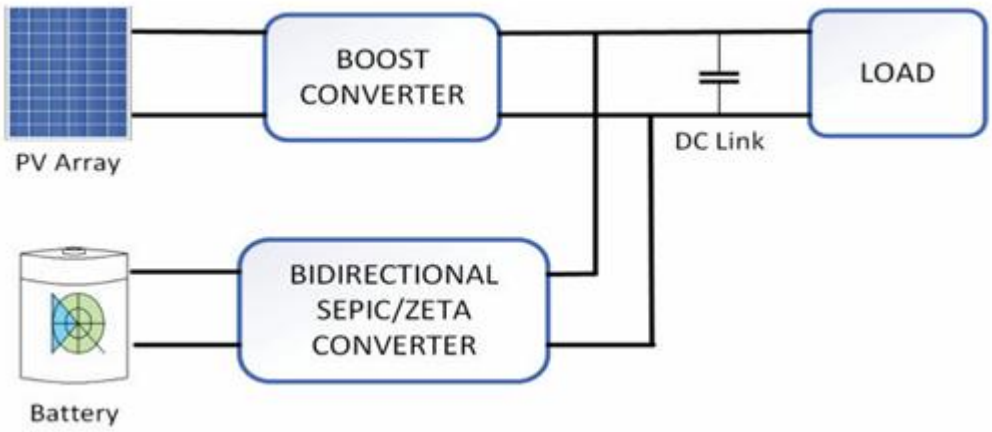

Figure 2.29 – Block Diagram for SEPIC/ZETA Bi-directional DC-DC Converter [92].

The idea of connecting batteries in series to reach 48V has been considered. Using separate converters for each battery could improve the efficiency of the system, however Saadeh et al., shows that charging these storage components in this topology improves the lifecycle and longevity of the components [70].

Rout et al. have proposed that a small efficiency improvement can be made that directly extends the longevity of a battery within a solar EMS [93]. The proposed improvement centres around the use of a super capacitor either directly in parallel with the battery (and the rest of the system) or in series with battery. In parallel its described as semi-active and in series it described as passive. The study also focused on rule based and filtration control, the rule-based controller proved to be considerably more efficient. The passive system proved to be simpler and easy to configure and install compared with the semi active system.

A proposed z-source dual input battery charger proposed by Sedaghati et al., could present some advantages for improved efficiency, however, this paper is limited as it doesn't present the control methodology for the overall circuit and there is no practical data to support the theorised approach [71]. Whilst Battula et al., utilised the quasi-Z-source converter which has a control loop that is configured specifically for a circuit that contains a boost converter serving only a DC load/battery [72].

Behera et al., proposed a novel control scheme for a DC-DC converter with their method involving the control of a time-sharing converter using a PI block in Simulink [94]. The results of this technique, as an improvement on a traditional bi-directional DC-DC converter, is validated through an improvement to the steady state response which was conducted in MATLAB. The combined boost and buck converter proposed by Bhule et al, shows the buck converter connected in parallel to the boost

converter [95]. As an isolated system that doesn't require an AC load, this topology has merits. The control method here uses two independent PI controllers, one for Boost and one for Buck. However, this battery charger has not been tested as part of a fully integrated EMS with a DC-AC inverter for a home load. Similarly to the combined multiport converter, Agarwal et al., proposes a three-port Luo converter that performs the same functions (battery charging, MPPT & DC load supply), which also utilised a PI controller for voltage control. The key differences between the two converters are the topology and layout of the system [42].

From Figure 2.30, Nagarjun et al. proposed a current controlled bidirectional converter; it is simple by design and there are a limited number of components in the topology compared with other methods. This is a combined converter (boost and battery charging), which has shown improved battery charging efficiency and has demonstrated that there is no current switching across the diode within the topology, which reduces the switching loss of the system [96].

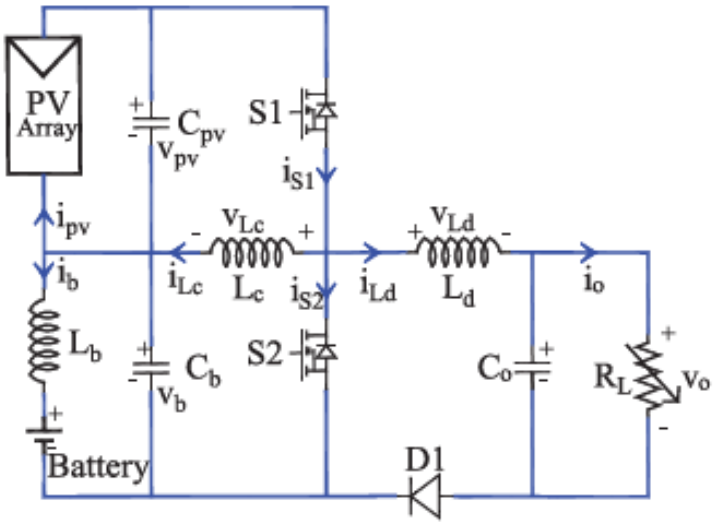

Figure 2.30 – A proposed bidirectional buck boost DC-DC converter [96].

Bhule et al., concluded that despite the utilisation of a single inductor the control strategy still allows segregation of charging and discharging modes, which is validated through simulations on Simulink [73]. Whilst the study described by Bhagiya and Patel doesn't compare with other methods or report specific data on efficiency, the concept of a dual loop control feedback does theorise improved efficiency for DC-DC conversion [75]. The proposed non-linear control proposed by Mahmud et al., does perform better than a traditional linear PI controller however the response time of the circuit may also be slower [76]. Whilst the nature of the control system design by Pathak et al., allows it to be responsive to changes in environmental conditions [77]. The control also allows the system to charge the battery when the load is exceeded. The paper shows successful attributes of combining multiple sub-systems of solar EMS'.

Figure 2.31 shows the topology of the system controlled by the dynamic power management strategy proposed by Anand et al., is unconventional and novel, with the study focusing on steady state performance at the load [78]. There is simulated and practical data that supports this study. The method is able to improve the efficiency by introducing an intermediate stage whereby the sub-system is neither charging or discharging and therefore the system can act like a buck boost converter. However, this system includes a boost converter with the control of the boost converter being tied in with the battery charging control strategy. For applications that did not utilise a boost converter, this control strategy would require re-design and re-integration.

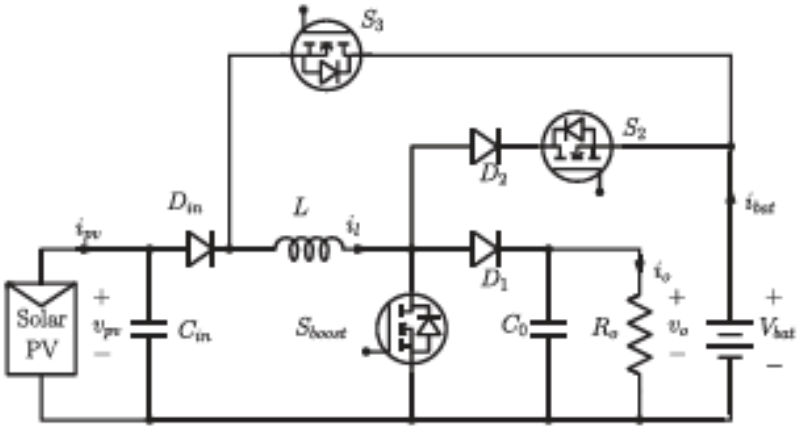

Figure 2.31 – Single Inductor Dual Input Dual Output DC-DC Converter Topology [78].

The study by Nalamati et al., denotes that an isolated Power Electronic Converter is more desirable for large power applications compared with non-isolated Power Electronic Converters such as the bi-directional DC/DC converter [79]. An extended phase shift control scheme in this application has proven (Simulated) to provide a better dynamic response. The proposed system utilises a three-phase inverter and high frequency transformer which are components that typically don't align with a standard single-phase EMS with substantially reduced load requirements.

The advantages of the proposed novel bidirectional PWM converter by Sato et al., is a reduction in switches and capacitors, leading to a faster and more stable output [80]. The load efficiency is limited to 95.7% due to the reduced number of capacitors utilised within the circuit. The study produces simulated and practical data to support the claim that this converter is smooth fast for all modes of operation. However, Uno et al., proposed a system controlled by a PWM and phase shift control circuit [81], with an overall efficiency of only 93.3% most likely due to the high number of switches, diodes and capacitors used across the circuit. An increased volume of components increases the overall cost of the system.

The majority of published literature with regards to PV energy management system battery charging circuits are focused on multiport bidirectional converters, there are some power control

strategies that have some merit. Some topologies described in published literature can serve as a basis for comparison [73], [80], as they utilise similar PV energy management subsystems, however, many of the novel approaches are not faster or more efficient than conventional methods some topologies/control strategies described propose designs that achieve a similar output with minimal overall improvements to the wider system. Due to the number of variables that can differ from system to system it is difficult to conclude which methods are both innovate by design but also have valid simulated data to improve the performance of an entire PV energy management system rather just the DC/DC battery charging circuit.

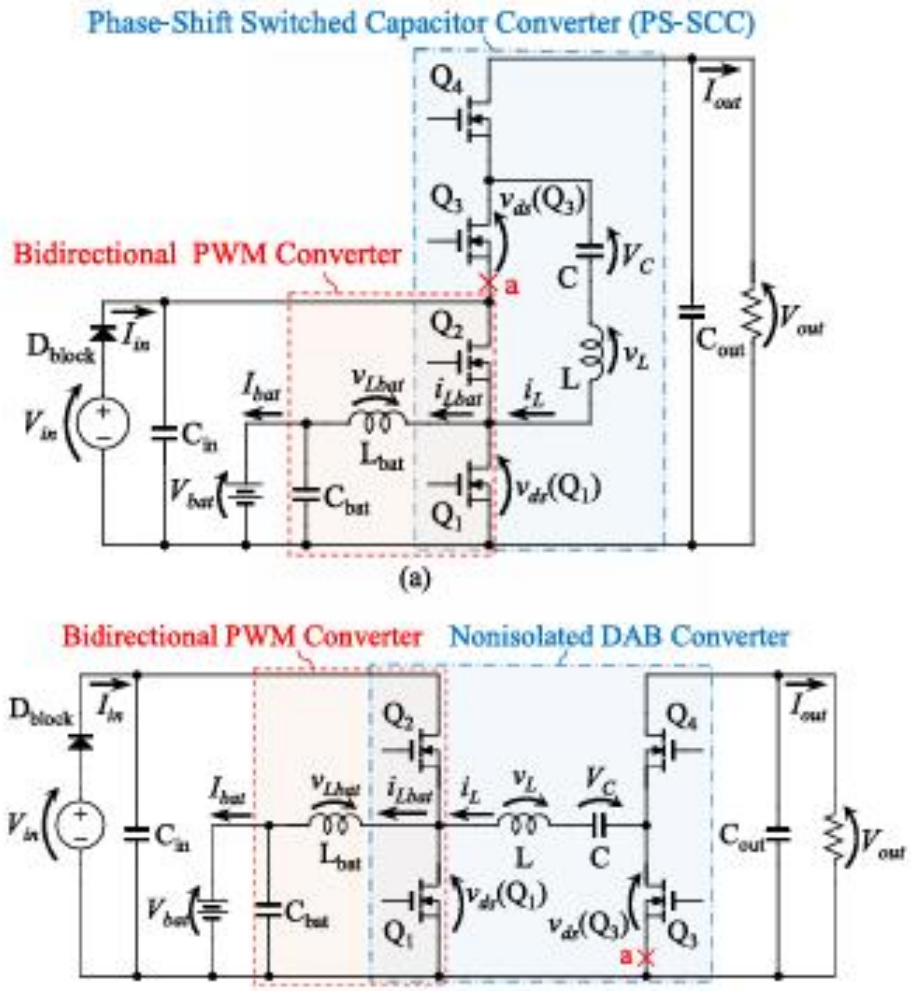

Figure 2.32 – Non-Isolated Multiport Converter with Phase Shift Switched Capacitor DC-DC Converter Topology [80]

2.8.3 DC-AC Inversion

The SPUC method proposed by El Ouradi and El Gadari reduces the standard number of components utilised in an inverter and produces a low THD [82]. The sinusoidal output characteristics of the current waveform is acceptable; however, the voltage waveform is not, resulting in a poor output quality which is undesirable for home loads that require an output below 5% THD to protect any devices or equipment run from the EMS power generated.

Iqbal et al. simulated a multilevel inversion topology (Figure 2.33) that considered a development upon a standard H bridge [97]. The results of this study concluded that the topology is highly reactive to variable conditions. Similarly to other multilevel inverters, the harmonic performance of this topology is not optimal. The simulation was reliant on a 0.02 step change for the P&O MPPT technique. This step size is a factor of ten smaller than the typical step size used for P&O MPPT which, in practice, will impact the response time of the circuit.

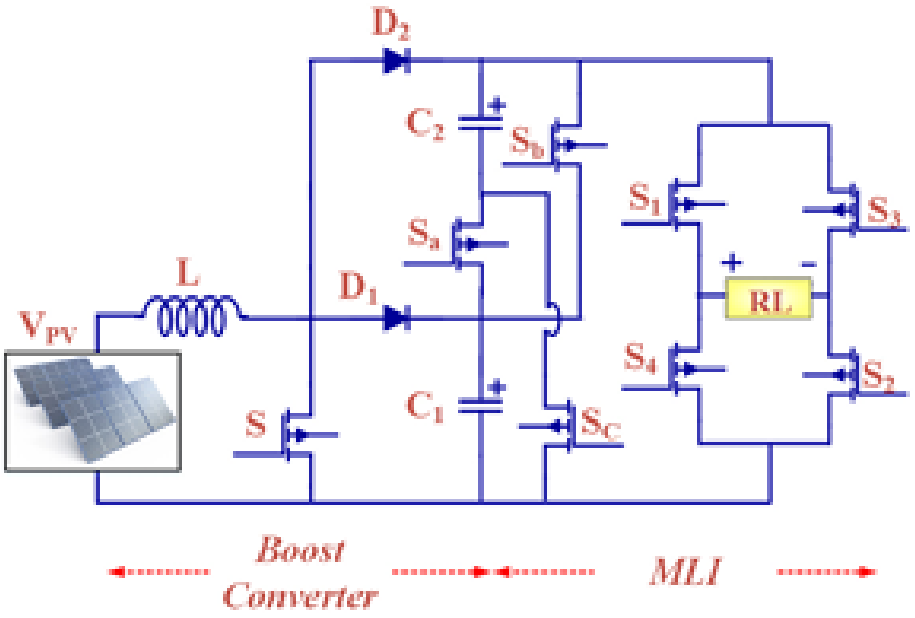

Figure 2.33 – Multilevel Inverter Topology with Boost Converter [97].

Other novel five level inverters have been proposed in multiple studies ([98], [99], [100], [101]). These systems position the switches to create the five levels, whilst the topology is unique, the output is highly undesirable due to its square nature. This is shown in both the simulated and practical data gathered and presented in the study. The above five level converter compares closely with the proposed topology investigated by Kumar et al., [102]. This single-phase inverter does not perform as well, with a THD performance of 14%, the output appears to not be as smooth as a sinusoidal 240V output required for a home load.

Aute and Naveed simulated a multilevel inverter that has good harmonic performance with the topology consisting of two H bridge inverters connected in parallel. This approach is similar to a multiport inverter, whereby the inverter has multiple inputs and outputs, along with a high number of switching components [103].

A 31-level multilevel inverter shown in Figure 2.34, has been proposed in a study conducted by Hamidi et al., [104]. The study concludes the topology presents a 97% efficient solution with a harmonic performance of less than 5%. This is due to the number of levels but also due to a capacitor compensator element of the circuit which helps to smooth the output of the inverter and removing spikes/noise caused by inductive loads. The drawback of this method is that it involves segregating the PV stages. Segregating PV stages is similar to a multiport method which can reduce the overall response time of the circuit.

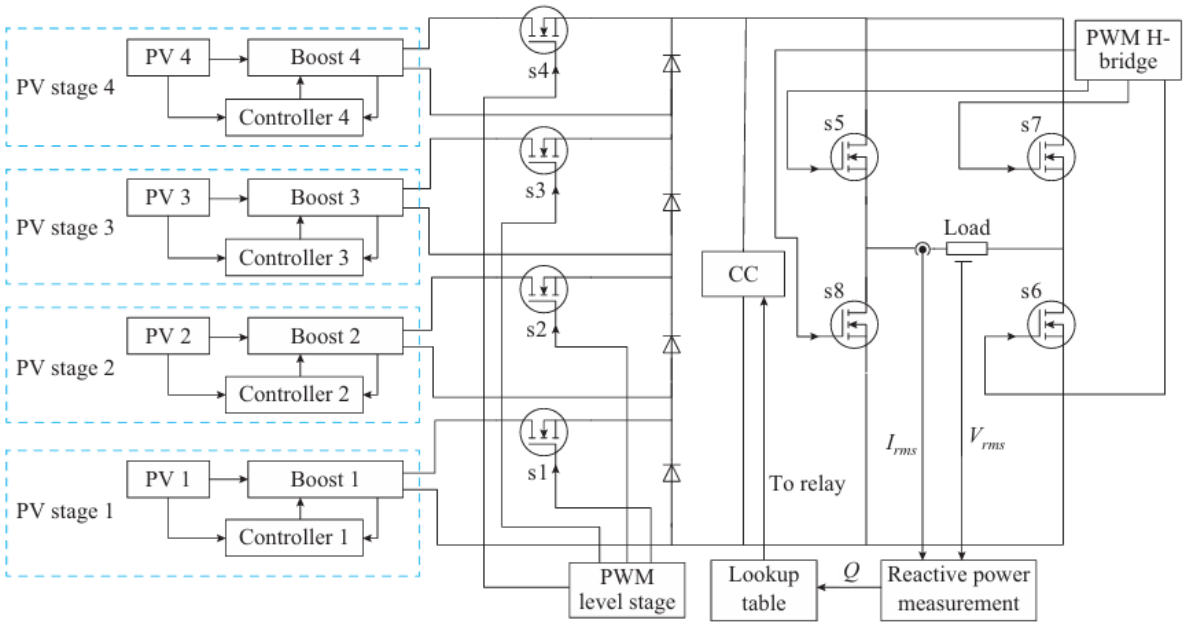

Figure 2.34 – A 31-level Multilevel Inverter Topology [104].

Sen proposes a novel multilevel inverter; there are seven stages and two topologies. One can handle reactive power and the other cannot. The converters are controlled using selective harmonic elimination [105]. The arrangement of the switches in this topology provides the reactive power handling capability which can be linked to managing the common issues caused by resistive/inductive loads. The main advantage of this study is linked with a reduction of switches and capacitors compared with conventional methods, resulting in an overall increased efficiency of the EMS.

Khasim et al. have published a study that focuses on reducing the switch count. The topology of the inverter uses a H bridge base to achieve a 21-level multilevel inverter [106]. There are 10 unidirectional switches utilised in this design; the efficiency of the system is 94% with a harmonic performance of 3.4%. As a multilevel inverter due to the number of levels the output voltage and current

waveforms are smoother by comparison to conventional multilevel inverters. There is a good trade-off between number of levels and system performance, however, a limitation of all multilevel topologies is the volume of components required to reach the required performance.

An 11-level cascaded H bridge inverter has been studied by Pratomo and Tjokro [107], this particular topology (as shown in Figure 2.35) is an asymmetrical design that achieves a THD of less than 4%. This is proven using practical data as well as simulated data. When reviewing the output voltage and current waveforms, there is evidence to suggest that the absence of filters and capacitor compensators is a factor that contributes to noisy output waveforms.

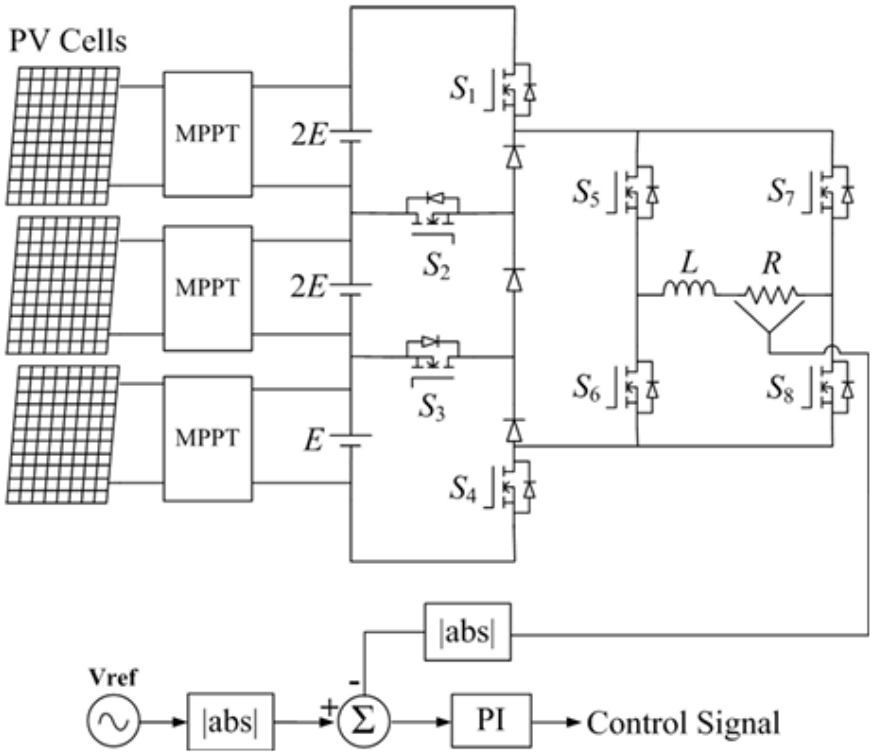

Figure 2.35 – An 11-level Multilevel Inverter Topology [104].

Kumar and Kumar have proposed a 9-level inverter which has a THD performance of 0.4%, the topology proposes that the inverter uses two inverse PV DC inputs [108]. This is good harmonic performance for a comparatively lower number of levels compared with most other published literature.

Bhukya et al. have proposed a multilevel inverter that is fed from a single input and multiple output, in this case 4 inputs [109]. The target of this study was to improve the harmonic performance of the system. This study proved both through simulation and practical data that the topology produces a harmonic performance of 2.2%.

Rout and Mishra have proposed a reduced switch 5-level inverter [110]. This topology is dual input with two parallel PV panels feeding two separate synchronous boost converters that feed the

inverter. The synchronous boost converter has suitable applications for this study and will be considered. The output of this study shows a very unstable and disrupted output voltage that has a harmonic performance of 26% which is not as effective as other novel MLIs studied in this review.

Uno and Sugiyama have combined an MPPT converter and bidirectional converter to form a multiport converter. The efficiency of this system is only 94% due to an increased number of switches and capacitors [83]. Roy et al., proposes another reliable multiport converter topology depicted in Figure 2.36, for a balanced load there are two H bridge converters one is connected to a home load and the other is a grid. The modular configuration is scalable for multiple H bridges. With an increased volume of components, this study shows a reduced output current ripple and improve harmonic performance compared with standard H bridge inverters [84].

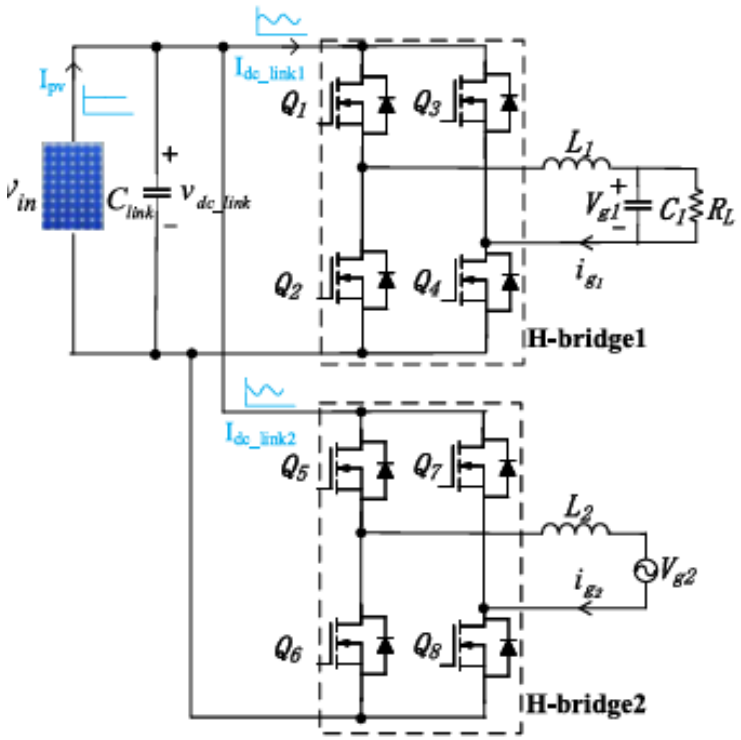

Figure 2.36 – Multiport Inverter Topology [84].

Yadav and Sambariya have studied a multilevel cascaded H-bridge inverter and investigated the harmonic performance of the circuits controlled by sinusoidal PWM [86]. A conclusion of this paper was that when input voltage is balanced the harmonic performance of the inverter is improved. A symmetrical inverter is preferred for this study compared with an asymmetrical inverter. The THD for this topology with an LC filter is 4.49%. Although the topology is complex by nature it is novel and does produce comparable harmonic performance to other conventional and modified methods of inversion.

Ankit et al., have shown an interleaved stage inverter whereby the reduced output ripple caused by the interleaving results in a THD for this circuit of 3.92% [87]. This concept can be used in line with any chosen inverter topology as the intention is to improve the converter performance and smooth the output voltage by phase shifting the gate pulses derived from the control circuit to allow legs of the circuit to be “on” and “off” interchangeably.

Behera et al., it can be concluded that for a constant DC source a unipolar phase shift PWM circuit had the best harmonic performance at 3.48% and the peak voltage was still above 240V however, this trend was mimicked for both constant and variable DC input source voltages [88]. Latif et al. have proposed a nonlinear control methodology based on Lyapunov stability theorem [111]. Whilst the proposed control methodology is novel, the THD is measured at 15% and the overall steady state oscillations of the output voltage waveform do not appear to be stable over time.

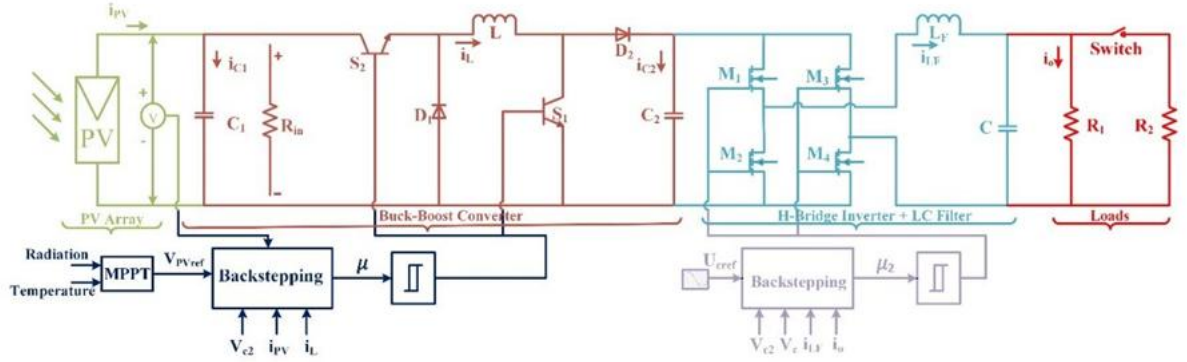

Figure 2.37 – Non-Linear Control for PV EMS H Bridge Inverter [111].

The topology proposed by Singh et al., in [89] is a control technique that can be used for a multiport inverter topology and has a harmonic performance of 0.7% and produces a highly stable sinusoidal output voltage as desired for a standalone home load. This method of control appears to be highly effective.

A standard H bridge has limitations with high switching losses, harmonics and the voltage stress are high, it is also less reactive to multiple voltage levels. Capacitor compensator and LC filters help to improve harmonic performance and interleaving the inverter helps to reduce the output ripple. For a multilevel inverter it can be concluded based on public literature that a 7 and above level inverter shows the desired smooth sinusoidal input required for a home load (less than 5% THD). Whilst the majority of publications focus on the multilevel or multiport solutions, there are some publications that look at additional concepts to improve the performance of the inverter; interleaving stages, unipolar phase shift control methods appear to improve the harmonic performance to greater effect compared with increase the number of levels in a multilevel inverter as the increase in components can introduce inefficiency and switching loss and delay the overall response of the system, in a PV energy management system,

efficient and fast response to variable input (environmental irradiance and temperature) conditions is highly desirable.

2.9 PV EMS Literature - Strengths and Limitations

As part of this literature review some key strengths were observed throughout; a wide range of relevant papers were factor into the review, considering relevancy by the use of a specific search criteria which included key words and removed publications that contained specific topics not relevant. Considering the volume of publications available and the recent developments and advancements in renewable energy management systems, only recent papers from the past 10 years were included as part of the review. The search also utilised multiple databases to ensure publications gathered were not from one specific source, there were 3 databases used to gather publications for this review. The review discussed EMSs as a whole looking at circuit configuration/control strategy for Single Phase Standalone PV Energy Management Systems (SPSAPVEMS) and performed analyses on three sub-system components; MPPT, Battery Charging (DC-DC Conversion) and Inverters (DC-AC Inversion). Due to multiple configurations and variables across published literature discussion in this review focussed on a number of performance output factors, steady state response, harmonic performance, efficiency, etc.

There were also some limitations of this review to note, firstly, due to the heterogeneity of the included studies, comparable conclusions were not able to be drawn looking at each paper, however, where possible, common themes across sub systems were explored to ensure relevant conclusions regarding published literature on the subject matter were summarised. Secondly, across the publications there were some papers that had a distinct lack of quantitative data: some papers did not quantitatively conclude or validate their performance which presented a challenge to compare and contrast the effectiveness of some of the methods. The final drawback centred around confirmation bias, it is easy to ignore inconsistencies in focus areas where conclusions are highly subjective, therefore, some papers were presenting their strategies/solutions as novel/improved on the basis that one out of three of the performance characteristics were improved rather than looking at all performance characteristics.

2.10 Gaps in Existing PV EMS Literature

The existing literature did not directly align with a proposed SPSAPVEMS in that common sub systems may have been mentioned but not detailed or control systems focused specifically on one sub system as opposed to the whole circuit. In cases that contained similar configurations, the few papers that did contain all three sub-systems either also contained an additional boost converter stage or the control strategy were proposed to be run on an embedded controller which requires an active low voltage source such as a battery which is undesirable for applications where power is limited or scarce. Such systems introduce complexity with maintenance/serviceability and can also be costly due to the components required to run the control system.

2.11 PV EMS Literature Review Conclusion

It can be concluded from this review that there have been many different attempts to improve and optimise a standalone PV system through modifications to MPPT approaches, battery charging an inverter. The key finding from analysing the existing literature shows that a hybrid model which involves a combination of two different MPPT elements are the most effective and give a balance of performance when considering efficiency, response time and stability. The conventional methods are not good enough singularly compared to the hybrid models. Non-hybrid model approaches do not totally give optimal or improved performance when compared to conventional methods. It is clear that novel approaches give a faster response and improved efficiency however they do not always give the most stable response.

It can also be concluded that many novel approaches involve pre-configuration of the system to a known or expected dataset. Whilst in an ideal situation this is an ideal approach, in practical systems there is always data that are outliers and in the case of standalone PV systems weather will always change and therefore irradiance and temperature will also be changing frequently. Given that a standalone PV system will utilise a battery there is less of a requirement for a rapid response time, more so the quality of the power and the system's ability to adapt to variable conditions. The approach for this study therefore disregards pre-configured systems that are modelled on known datasets as this will ensure that the system is adaptable for many different applications without the need for redesign or complex pre-configurations.

2.12 Chapter Summary

Chapter 3 summarised the process and findings of the literature review that was conducted over the first 2 years of the PhD. This looked at overall SPSAPVEMSs as a whole but also looked at each of the sub systems (MPPT, battery charging, inversion) separately. The full inclusion and exclusion criteria has been discussed, seen in Appendix, and the full search strategy has been listed in Appendix. The main findings of the review have been discussed. Chapter 4 of this report will discuss the experiments and simulations that were conducted for the DC-DC battery charging aspect of this PhD.

3 A Single-Phase Standalone Residential PV EMS Configuration & Performance for Variable Temperature and Irradiance

3.1 SPSAPVEMS Overall System

The proposed system utilises a conventional P&O MPPT that drives the switches in the bidirectional DC/DC interleaved battery charger, the battery charger is connected to the DC link that supply the dc voltage to the interleaved switched capacitor inverter in parallel. The inverter is controlled via phase shifted unipolar sinusoidal PWM with an RMS output voltage feedback loop to control the output voltage. The advantage of this system is that the system considers the combination of all the circuit elements compared with the literature described above that do not also contain a battery charging stage. The harmonic performance and efficiency of the proposed system is shown to be an improvement on existing method.

The aim of this section is to simulate the system performance for variable input conditions, such as, variable irradiance and temperature. The performance of the Single Phase Standalone Photovoltaic Energy Management System (SPSAPVEMS) for these variable input conditions is important to validate that the system is capable of supplying an off-grid residential home with a PV system that is fit for purpose to serve a variable home load. For this chapter, all sub systems shown in Figure 3.1 are observed

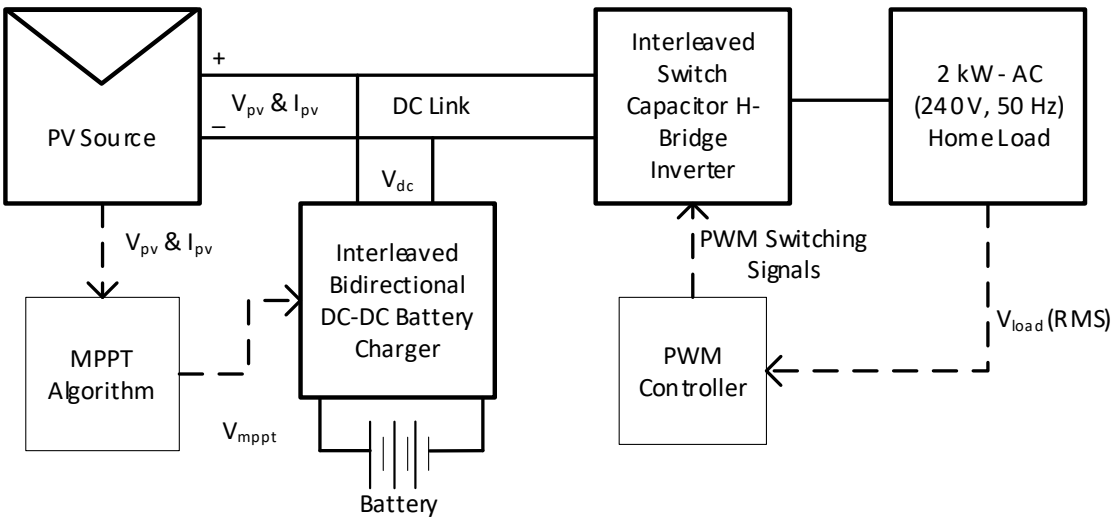

Figure 3.1 Chapter 5 Sub-systems of PV EMS

3.2 SPSAPVEMS Investigating Performance Under Variable Temperature and Irradiance – Simulation Strategy

Figure 3.2 shows the overall system configuration for the proposed SPSAPVEMS presented in this study. Each aspect of the circuit including the control strategies for each of the subsystems is included. The PV cell can be seen in Figure 3.2 (e) with the variable Irradiance and Temperature input parameters that are the focus of the investigation in this chapter, the PV cell is connected to the H bridge inverter and the Bidirectional Battery Charger in parallel such that load can be shared across both subsystem depending on power generated and the required load power from the home load.

Figure 3.2 (a) is the control strategy for the battery charging circuit and shows how V_{pv} and I_{pv} from the PV cell is used as input parameters for the control strategy as it passed through the P&O MPPT controller, the error from comparing V_{MPPT} and V_{pv} is then passed through a PI controller and compared with the reference current (found by taking P_{pv}, a product of I_{pv} and V_{pv}) and dividing it by the battery voltage. This reference current (I_{ref}) is compared with the Inductor currents I_{L5} and I_{L6}, which are the two interleaved stages of the battery charger, once this comparative signal is passed through another PI controller it is compared with a carrier signal, the output of this comparison and the inverse of this comparison creates the two signals per interleaving stage required to drive the gates of the IGBTs used in Figure 3.2 (e) for circuit operation once they have passed through the state of charge controller shown in Figure 3.2 (b). To ensure that the battery does not over charge or discharge a state of charge controller has been added to the proposed configuration and is shown in Figure 3.2 (b) based on comparing the state of the battery charge, to 99% and 0% as shown below, the use of AND gates takes the gate pulses generated in Figure 3.2 (a) which then feed the IGBTs used in Figure 3.2 (e).

Figure 3.2 (c) is the control strategy for the Inverter subsystem and is required for the operation of the IGBTs used for the switched capacitor interleaving circuit shown in Figure 3.2 (e) . This strategy compares the system output voltage from Figure 3.2 (e) to 240V, the output of comparison is passed through a PI controller and is then multiplied with a regular sine wave. This signal is then compared to 4 phase shifted carrier signals which then derives the 4 signals required to drive the IGBTs that drive the switched capacitor circuit. Figure 3.2 (d) shows the standard sinusoidal PWM arrangement where a reference sine wave is compared with a carrier signal, the output signal and the inverse of this output are the signals used to drive the IGBTs in the H-bridge arrangement.

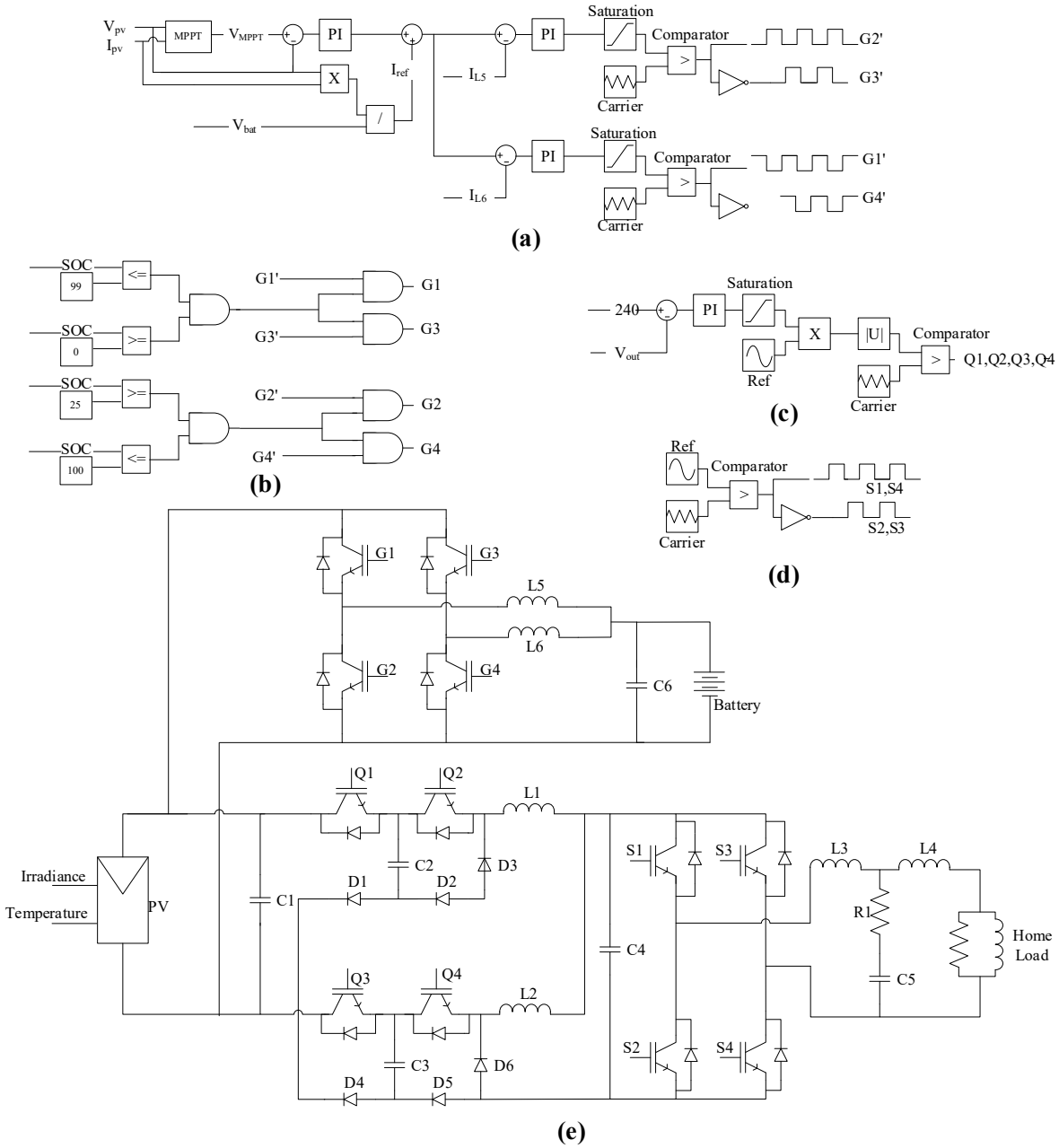

Figure 3.2 (a) Battery Charging Subsystem Control Strategy- MPPT/PI/Current Control/PWM (b) State of Charge Controller for Battery (c) Inverter Subsystem Control Strategy – RMS Feedback Phase Shifted Sinusoidal Pulse Width Modulation (d) Conventional H-Bridge Control Strategy – Sinusoidal PWM (e) Overall Proposed SPSAPVEMS Circuit

A signal builder with a dual signal output in MATLAB Simulink is the method used to simulate the two input conditions that are being varied for the purposes of this experiment. From Figure 3.3 the red Signal 1 is the irradiance profile that is varied from 1000 W/m^2 down to 500W/m^2 and back up again across a 3 second timescale, across the same timescale the temperature drops from 25 °C to 20°C

before it is increased up to 40°C and back down to 25°C. The two input conditions are varied independently such that for each condition clear conclusions on the circuit performance can be drawn.

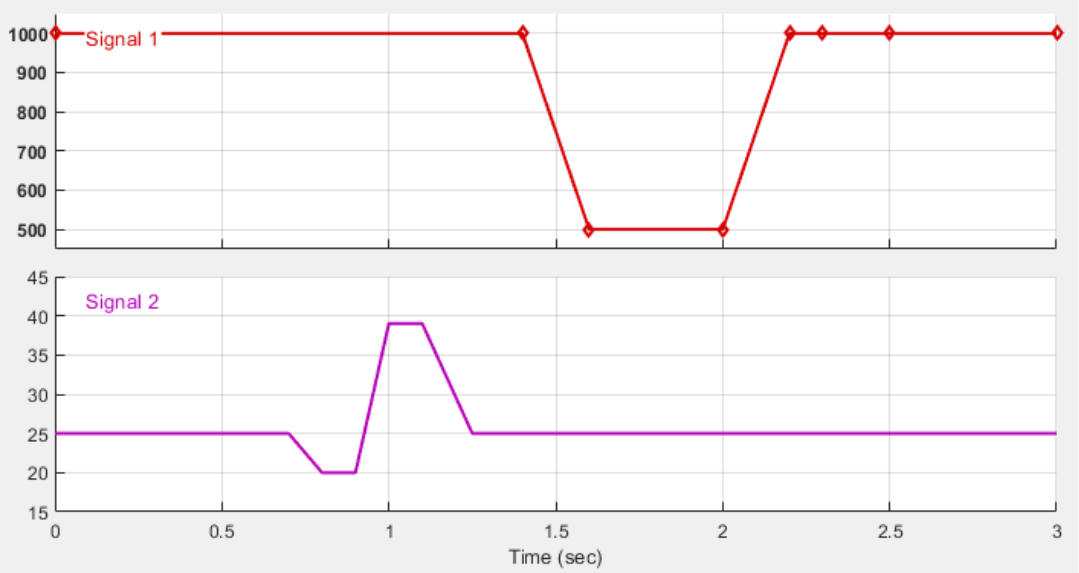

Figure 3.3 Variable Input Signal for Temperature and Irradiance

The values shown in Table 3.1 give the nominal values of a home load and allow this simulation to accurately represent a standard home load. A power of 2 kW was assigned to the home load which allowed the power regulation between the home load and the battery circuit to be observed.

Table 3.1 – Home Load Parameters

Parameter	**Value**
Nominal Voltage (Vrms)	240 V (339 V)
Nominal Frequency	50 Hz
Active Power	2 kW
Inductive Reactive Power QL	100 +var
Capacitive Reactive Power Qc	0 -var

3.3 Investigation into SPSAPVEMS Performance Under Variable Temperature and Irradiance - Results and Discussion

This section presents the results of this study, the charts are taken from a simulation on MATLAB using the Simulink package. The load parameters are outlined in Table 3.1, the output of the PV cell is shown in Figure 3.4. As can be seen from the chart, the circuit reaches its steady stage within 5.5 seconds. The output of the PV array charges the battery (controlled by MPPT to extract the maximum power from the PV array) and is connected in parallel to the inverter circuit.

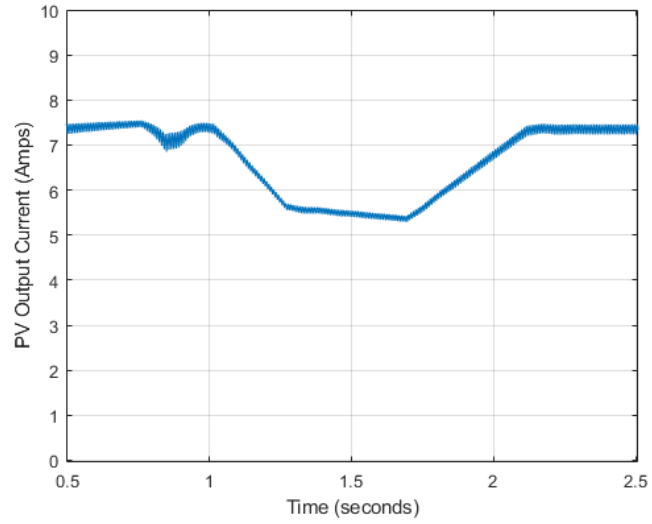

(a)

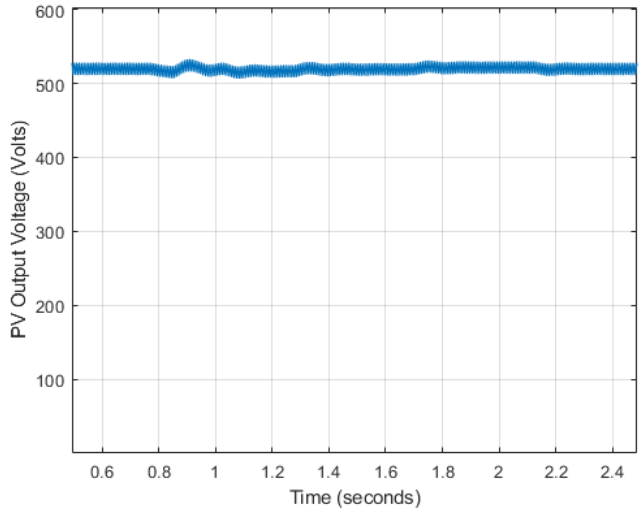

(b)

Figure 3.4 (a) PV Output Current and (b) PV Output Voltage

The waveforms shown in Figure 3.5 (a) depict the current across both inductors. The interleaving of the waveforms for L1 and L2 can be observed when the waveform is examined further, which is shown in Figure 3.5 (b) as the waveforms appear out of phase.

Based on the control of the switch pair (Q1 + Q2) described above, the switched capacitors charge and discharge therefore the current observed through the inductors L1 alternates from 0-12A. The same observation can be made for the other switch pair (Q3 + Q4) when observing the L2 current waveform, however as the arrangement is interleaved, the L2 current is out of phase with the L1 current waveform.

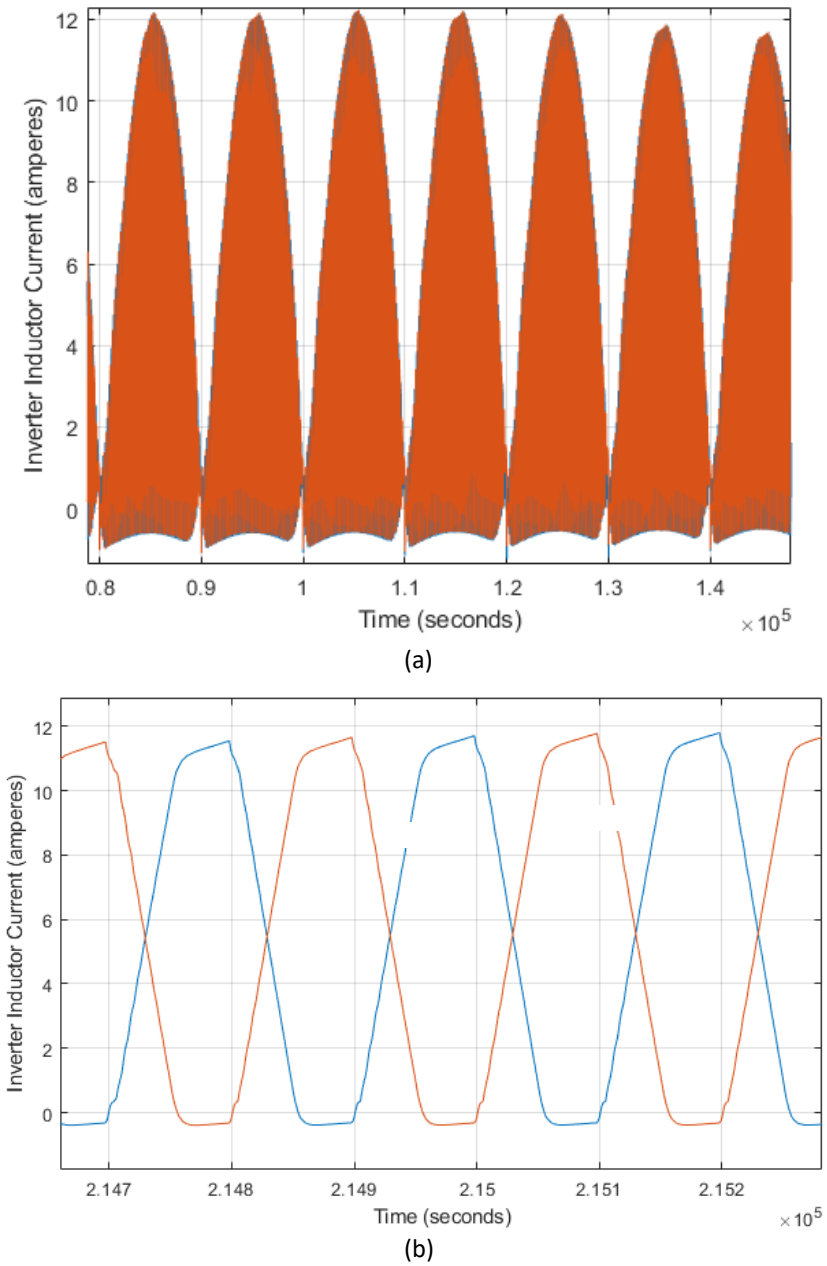

Figure 3.5 (a) Inductor Currents (Blue - L1 and Orange - L2) and (b) Inductor Currents Zoomed (Blue – L1 and Orange – L2)

The output of the switched capacitor circuit is shown in Figure 3.5 (a) whereby the current goes from 0A to 12A (as designed). From Figure 3.6, the H-bridge inverts this current to -12A to 12A. The overall objective of the system is to produce a sinusoidal AC output waveform at 240V with a frequency

of 50Hz to support a home load. Evidence of this system's overall output load is shown in Figure 3.6. and Figure 3.7. for current and voltage respectively, with these waveforms being sinusoidal as required. As expected, the output of the system shows a very small output ripple. Figure 3.8. is a combined chart of the output current and voltage.

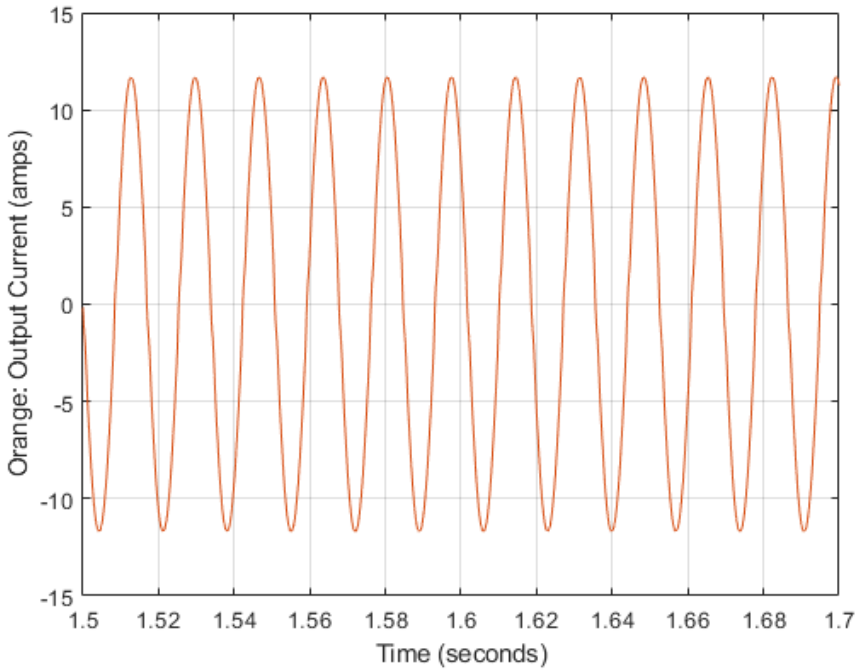

Figure 3.6 Inverter Output Current

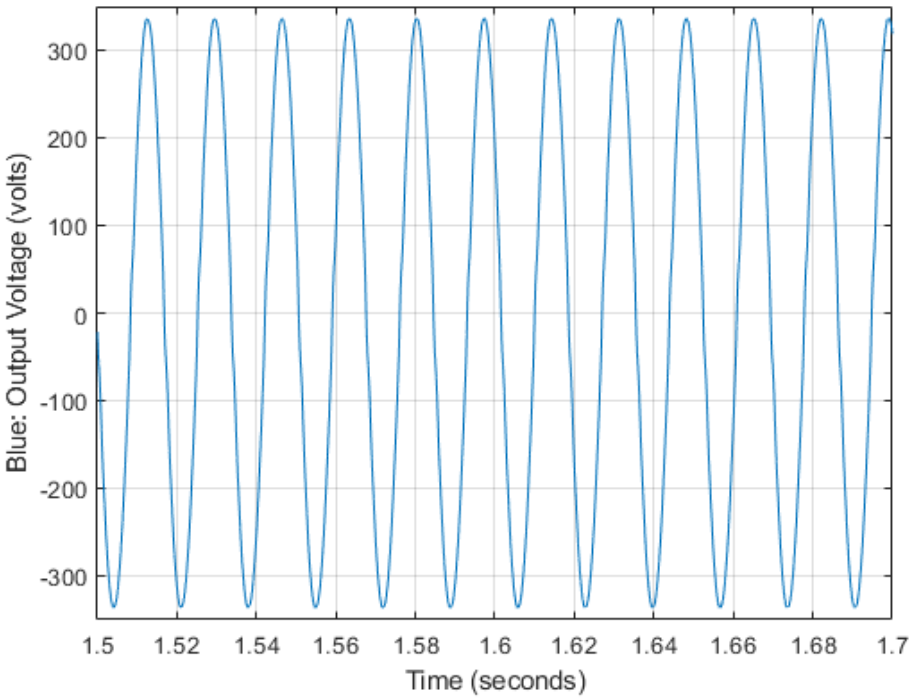

Figure 3.7 Inverter Output Voltage

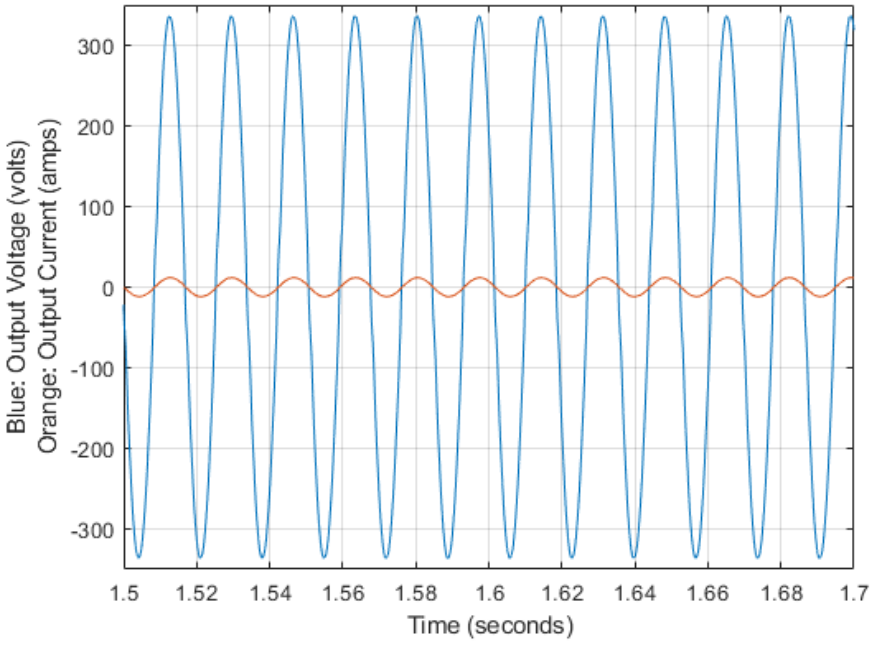

Figure 3.8 Load Voltage (orange) and Current (blue)

Harmonic analysis was undertaken from Simulink. The results from this analysis (considering a fundamental frequency of 50Hz) show that the THD for this circuit is 1.81%. Figure 3.9 shows how the irradiance and temperature profiles are varied with time for the duration of the simulation. The peak and optimal irradiance is approximately 1000 W/m^2. The optimal temperature is approximately 25°C. For the first half a second, whilst the circuit is reaching steady state, the irradiance stays at 1000 W/m^2 and the temperature at 25°C. The temperature then decreases to 20°C from 0.6 to 0.9 seconds, then the temperature sharply increases to 35°C at 1 second. There is then a decline in irradiance from 1000W/m^2 to 700W/m^2 by 2 seconds before it gradually increases up to 1000W/m^2 at 2.5 seconds. The purpose of this is to observe the behaviour of the circuit (PV Output Power, Battery Power and Load Power) in response to irradiance and temperature changes. Variable conditions are typical input characteristics for a real-life solar energy management system.

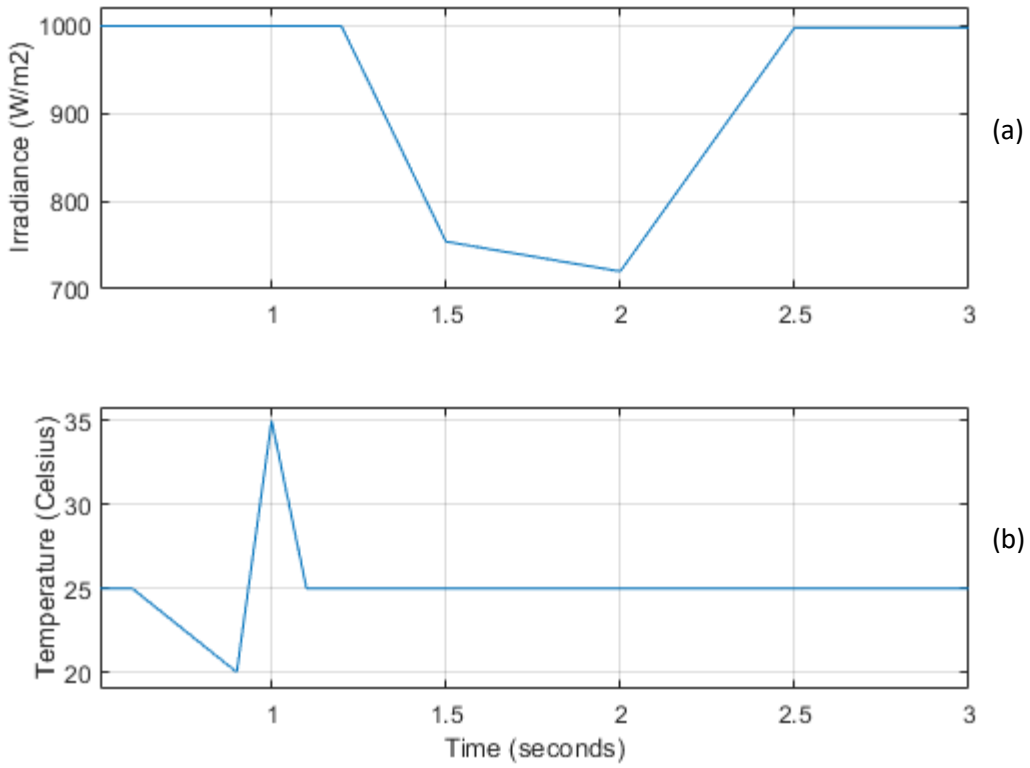

Figure 3.9 - Variable PV System Input Conditions (Irradiance – a, Temperature – b)

Figure 3.10 shows how the power generated by the PV panels (yellows) is distributed across the battery (blue) and Load (orange). The chart shows that when temperature and irradiance drops, the output PV power also falls, at this point to supplement the home load the battery will also begin to discharge. The stability of the system is shown by the straight orange line which indicates that the system is responding efficiently to variable input conditions.

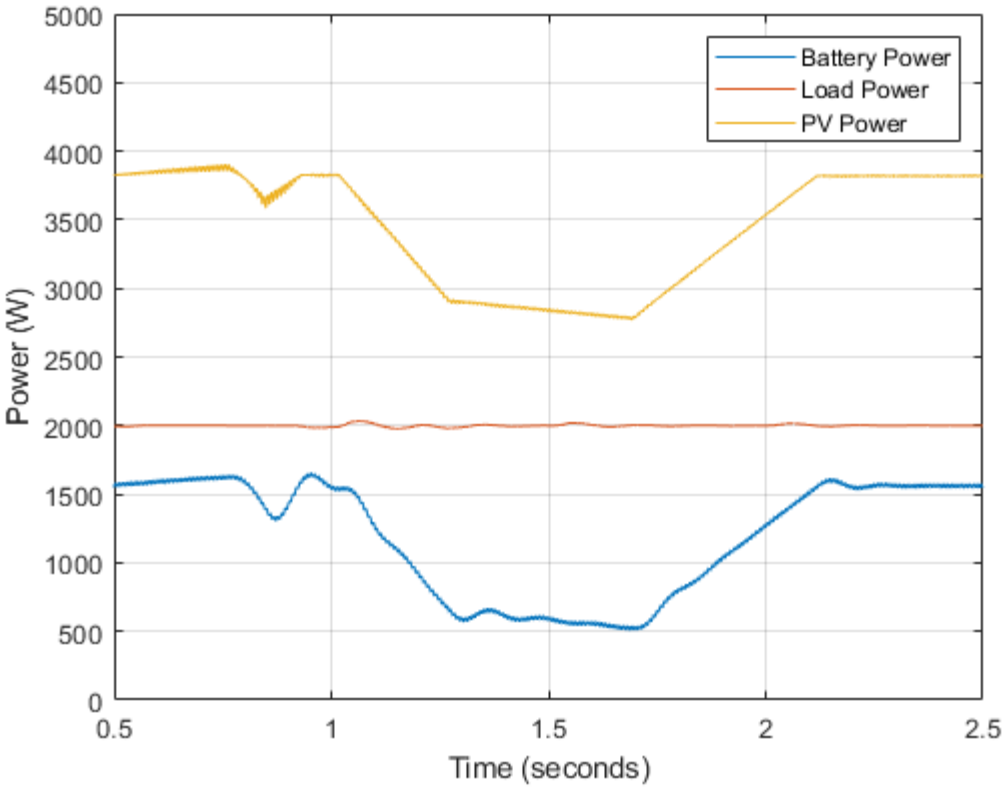

Figure. 3.10. Load Power (orange), Battery Power (blue) and PV Power (Yellow)

3.4 SPSAPVEMS Investigation into Performance under Variable Temperature and Irradiance Conclusions

The stable straight orange line for Load power in Figure 3.9 concludes that despite the variable input conditions, firstly, the change in temperature and then the change in irradiance which impacts the generated power from the PV array, as part of the wider EMS system the battery is able to charge and discharge to supply the load with the power required. The circuit is able to do this is efficiently and the power is both stable and of high quality due to the design of the bidirectional battery charging and switched capacitor inverter circuit.

3.5 Chapter Summary

Chapter 6 details how the proposed Single Phase Standalone Photovoltaic Energy Management System (SPSAPVEMS) is able to respond to variable input conditions. The variable input conditions have simulated, with the data from MATLAB Simulink presented and discussed. The analysis focused on how the battery, DC link and load power was able to respond when the temperature and irradiance input conditions were varied to mimic the conditions that a residential PV energy management system would be exposed to in practice. The overall objective of ensuring load power serving the home load remained constant despite the variable conditions has been achieved.

4 An Interleaved Bidirectional DC-DC Battery Charging Circuit Subsystem for a Single-Phase Standalone PV EMS

4.1 SPSAPVEMS Battery Charging Subsystem

As concluded in the literature review, there is an abundance of published literature that focuses specifically on MPPT for PV EMS applications, however, whilst there is a lot of research and published literature on DC-DC battery charging, there is less of an abundance of DC-DC battery charging for PV EMS applications. For a Single Phase Standalone Photovoltaic Energy Management System (SPSAPVEMS) it is important that power is available when there is no irradiance from the sun (e.g. at night) to feed a load at all times of the day. It is therefore important to have a high functioning, highly efficient battery charger that is able to charge the battery when the load is not demanding the generated PV power and discharge the battery when the PV array is not generating enough power to supply the home load.

The approach for this study disregards pre-configured systems that are modelled on known datasets as this will ensure that the system is adaptable for many different applications without the need for redesign or complex pre-configurations. This DC-DC battery charger has been designed and simulated on MATLAB Simulink to provide a stable bi-directional DC load balance for the inverter supply, the objective of this circuit is to rapidly and efficiently respond to variable input conditions and load demands. The proposed approach and method is theorised in detail with the simulated data analysed and discussed.

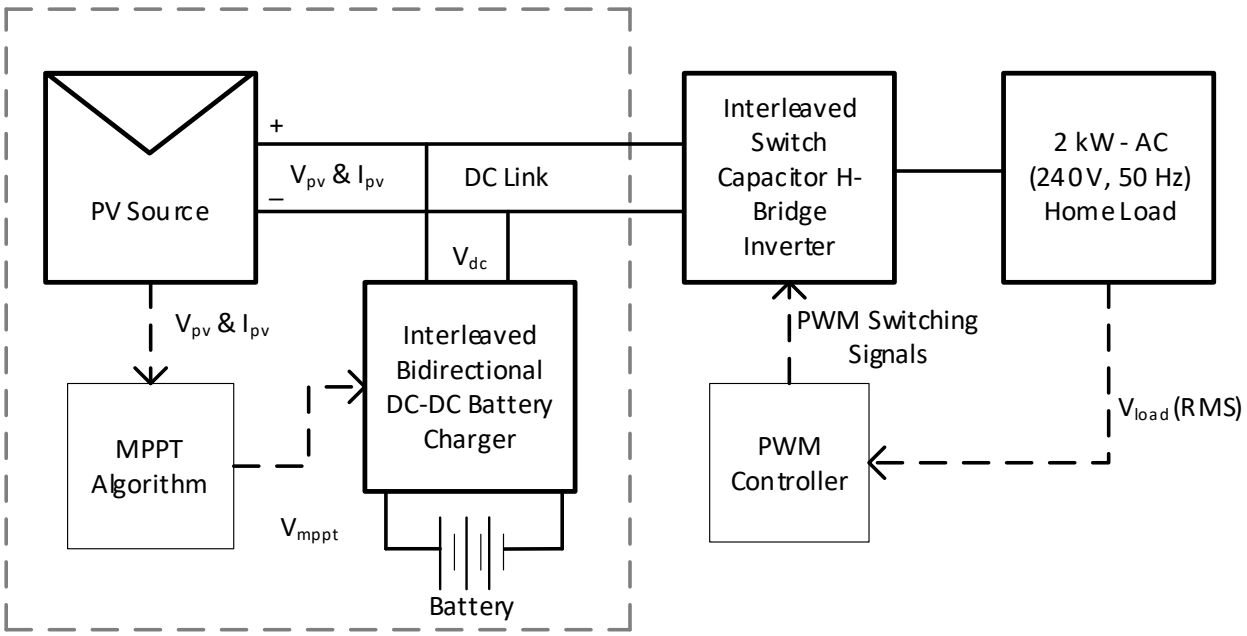

Figure 4.1 – Chapter 4 Sub-systems of PV EMS

Figure 4.2 is the circuit design & control strategy designed for the battery charger subsystem; Figure 4.2 (a) shows how the IGBT switches are controlled via pulses to the gate of each IGBT. The principle of this control circuit is to compare the voltage at the MPPT with V_{pv} and to pass that through a PI controller. A PI controller is used in control circuits and are part of a feedback loop where the basic principle is to calculate the error of a signal and apply a correction. The comparison is done on a process variable and a set point. V_{pv} is the setpoint and the voltage at the MPPT is the process variable. The error is classed as the difference between V_{pv} and the MPPT output is corrected using the PI controller and fed-back through the circuit and combined with a reference charge current controller to derive the gate signals that switch IGBT pairs ON/OFF.

To ensure the battery does not over-charge or over-discharge the controller shown in Figure 4.2 (b). has been included. This does not allow the circuit to operate in the Buck if the battery charge reaches 100% and it prevents the circuit from operating in the Boost direction if the battery charge reaches 25%.

In Figure 4.2 (c), to control the second pair of IGBTs (G3, G4) and therefore the current flow through L6, the gate pulses generated from G1 and G2 are phase shifted by 180 degrees. There are 4 states that this circuit can be split across two modes: Charging (Buck) or Discharging (Boost). The filter capacitor C6 is tuned to minimize current ripples.

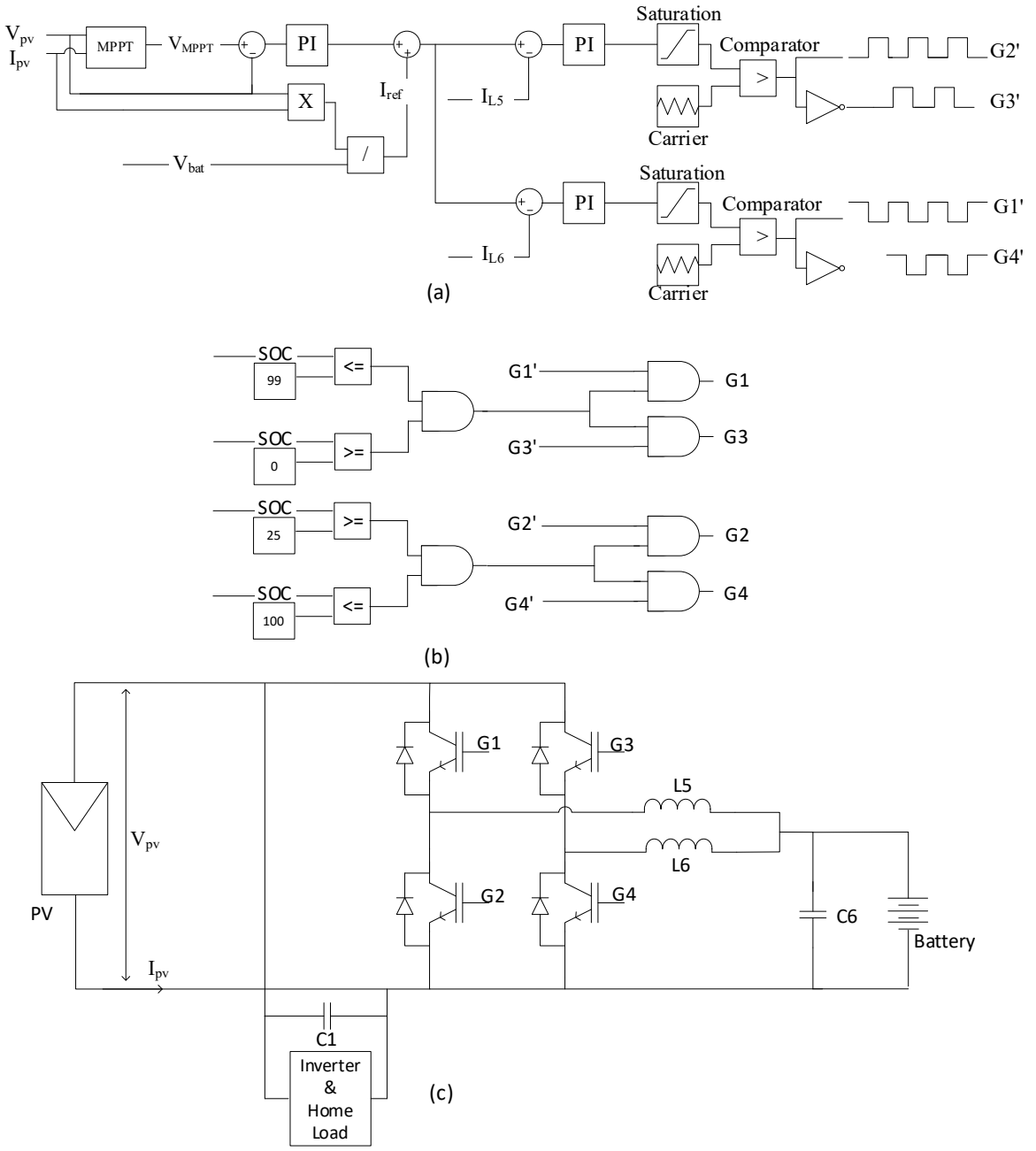

Figure 4.2 - P&O MPPT Algorithm and Current Control Strategy for SPSAPVEMS Battery Charging Sub System (b). State of Charge Controller (c). DC/DC Battery Charging Circuit for SPSAPVEMS

4.1.1 Photovoltaic Source Configuration and Parameters

From Figure 4.2 it can be seen that in order to simulate a SPSAPVEMS, a PV source must also be configured and its behaviour under varying conditions be understood as part of the investigation of the performance of the proposes SPSAPVEMS.

Figure 4.3 and Figure 4.4 show how the I-V & P-V characteristics change for varying irradiance and temperature conditions. When considering the irradiance, the higher the irradiance the higher the peaks of the curves, which means the MPP is much larger with higher irradiance figures. For temperature, the higher the temperature the lower the peaks of the curves which means the MPP is considerably lower with higher temperatures. It is worth noting that the peaks of these curves do not exponentially rise, meaning that the relationship between MPP and temperatures is not linear and that there will be a low temperature after which MPP will start to fall.

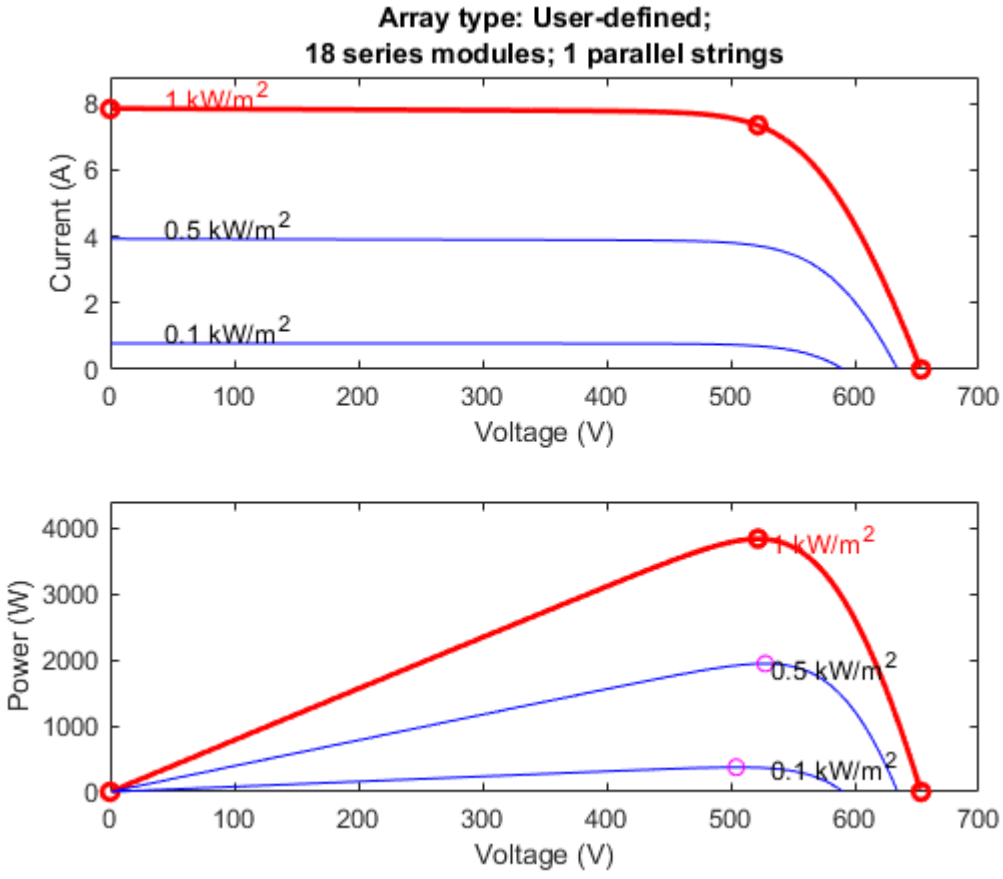

Figure 4.3 - I-V Characteristic & P-V Characteristic for Varying Irradiance

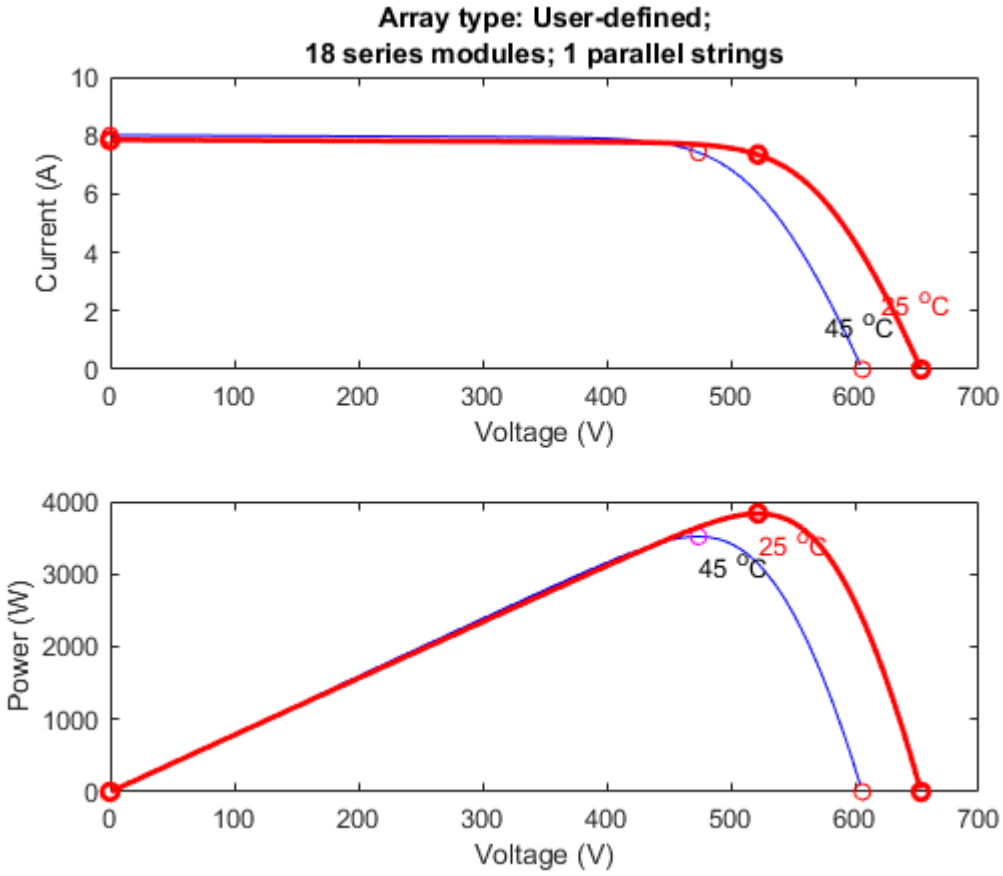

Figure 4.4 - I-V Characteristic & P-V Characteristic for Varying Temperature

Table 4.1 - PV Circuit Parameters – Single Panel

Parameter	Value (Single Panel)	Value (Array)
Module	1Soltech 1STH-215-P	N/A
Max Power (W)	213.15W	4,092.48W
Open Circuit Voltage V_{OC}	29V	522V
Cells per panel (N_{cell})	60	60

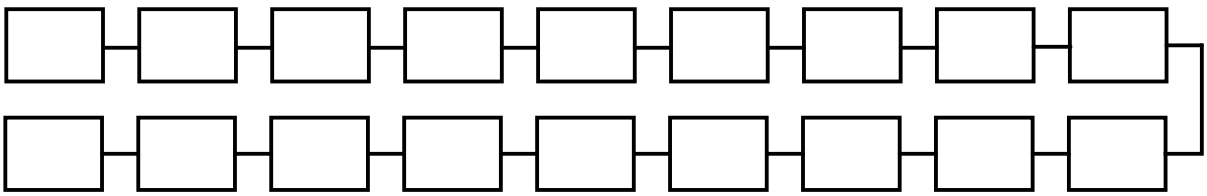

Figure 4.5 – Multiple Panel Configuration

Table 4.1 - PV Circuit ParametersTable 4.1 details the value of the parameters of a single PV cell used in the energy management system for this study. Figure 4.5 shows the configuration of the multiple panels used; this allows for the maximum expected output voltage calculation for the PV array (V_{pv}) to be shown in equation (4.1) :

$$V_{pv} = N_s * V_{oc}\ , \tag{4.1}$$

Using (4.1) the maximum voltage output of the PV cell can be calculated as 29 * 18 which is 522V.

4.2 SPSAPVEMS Battery Charging Subsystem – Circuit & Control Strategy Design

The principle of this control circuit is to compare the MPPT output with Vpv and to pass that through a proportional integral (PI) controller. A PI controller is used in control circuits as a feedback loop mechanism as shown in Figure 4.6 below. The basic principle is to calculate the error of a signal and apply a correction. The comparison is done on a process variable and a set point. For this system, Vpv is the setpoint and the MPPT output is the process variable. The error, classed as the difference between Vpv and the MPPT output, is corrected using the PI controller and fed back through the circuit using gate signals to drive the ON/OFF state of the IGBT pair in the circuit.

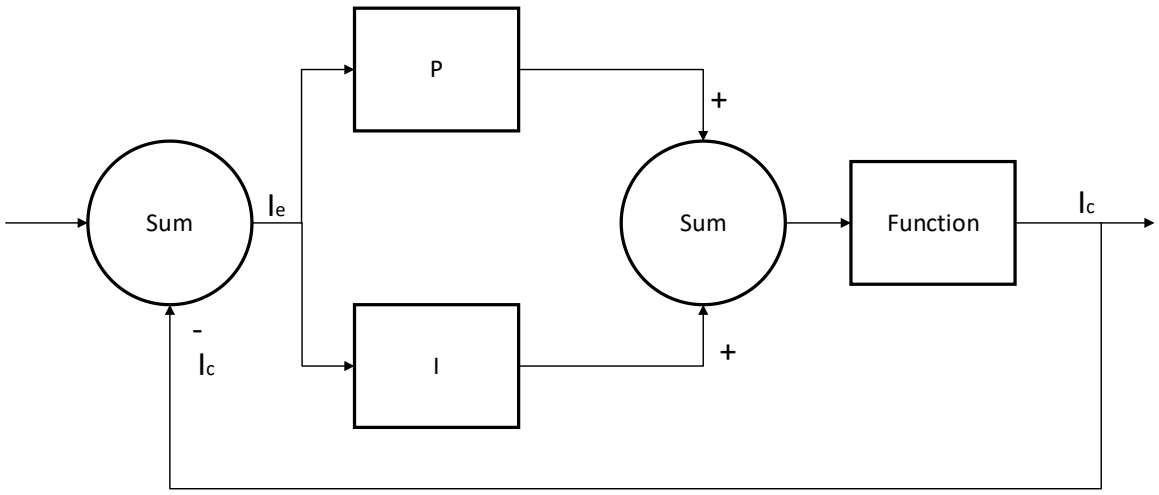

Figure 4.6 - Basic Flowchart for a PID Controller

$$\begin{aligned} Set\ Point &= Iref\ (t), \\ Measured\ Point &= Ic\ (t), \\ Error = Ie\ (t) &= Iref(t) - Ic\ (t) \end{aligned} \tag{4.2}$$

The “P” in PI is proportional to the error. It is directly proportional based on the gain value, denoted as Kp below. The “I” in PI takes the error and integrates it over a set time. The integral term will reduce all residual error.

For P, I & D the following calculations are executed (4.4):

$$P = K_p * Ie(t), \tag{4.3}$$

$$I = K_i * \int_0^t Ie(\tau) * d(\tau), \tag{4.4}$$

This means that the overall output for the PI controller and Laplace transfer function (4.6) is:

$$u(t) = K_p * I\, e(t) + K_i * \int_0^t Ie(\tau) * d(\tau), \tag{4.5}$$

$$L(s) = K_p + \frac{K_i}{s} * S \tag{4.6}$$

The output of this PID controller is passed through a saturation block with an upper limit of 0.9 and a lower limit of 0.1, which is then compared to a repeating signal that moves from 0 to 1 to 0 with a frequency of 20 KHz. The output of this feeds the gate of the bottom IGBT of the IGBT pair (shown in Figure 4.2(a)) used for the battery charging circuit. Using a simple NOT gate, the inverse pulse feeds the gate of the top IGBT of the IGBT pair (shown in Figure 4.2(a)).

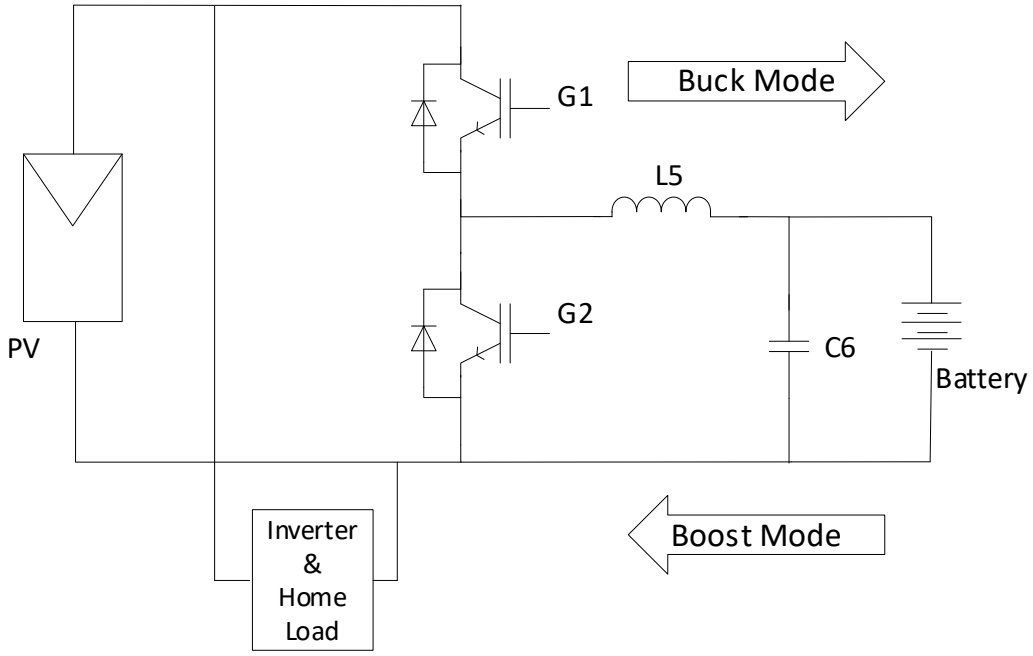

Figure 4.7 - Bidirectional Buck Boost DC/DC Converter Topology

This topology operates in Boost (Battery discharging Mode) or Buck (Battery charging Mode) and the basic explanation for modes of this circuits are as follows:

Boost Mode: G2 gate pulse is high, and the IGBT is switched on. During this mode G1 can exist in one of two states:

- State 1: G2 high and G1 low and this shows the DC/DC converter in a short circuit state. The inductor L5 is charged by the battery voltage.
- State 2: G2 low and G1 low and this shows the DC/DC converter in an open circuit state. The inductor voltage operates in series with the DC link voltage, and this means that C6 charges therefore output voltage is boosted up.

Buck Mode: G1 gate pulse is high and the IGBT is switched on and during this mode G2 can exist in one of two states:

- State 1: G1 high and G2 is low, and this means the battery will be charging from capacitor C6 and inductor L5.
- State 2: G1 low and G2 is low, and this means the inductor will be discharged across the freewheeling diode and the voltage across the battery will step down.

The paper takes the principle explained above (as shown in Figure 4.7) and interleaves it with a second pair of IGBT switches and inductor. The resulting battery charging circuit is shown in Figure 4.2 (c) above.

Figure 4.8. details the P&O algorithm used to track the maximum power point. This algorithm uses the measured I_{pv} and V_{pv} from the PV panel as inputs. The current and voltage are then multiplied to calculate power. The controller in the P&O method makes small adjustments to the voltage and takes current and voltage measurements to give the power. When the power increases the controller adjusts further until an increase in power is no longer detected. The output of the MPPT algorithm is similar to the V_{pv} graph but it is squarer and more stepped. This method and its nature can result in large oscillations for the output power. The efficiency of this method can be improved by ensuring the predictive steps used to take the measurements are refined and accurate. The P&O is the most used method for MPPT as it is easy to implement within an energy management system. The output of this algorithm is compared with V_{pv}; this passes through the PI controller and then added to the calculated reference charge current. This then feeds the rest of the current control strategy for this system. In Figure 4.8, V(k) and I(k) are the measured voltage and current used to derive power (by multiplying), V_{ref} is the reference voltage (the calculated reference voltage) and ΔV is the change in voltage.

The MPPT method chosen for the investigation, simulation and analysis of this energy management system is the P&O method. The flowchart displayed in Figure 4.8. shows the computational steps taken to track the maximum power point. The step change set in this simulation is +/- 6V for step 3 of the switching stage shown in Figure 4.8.

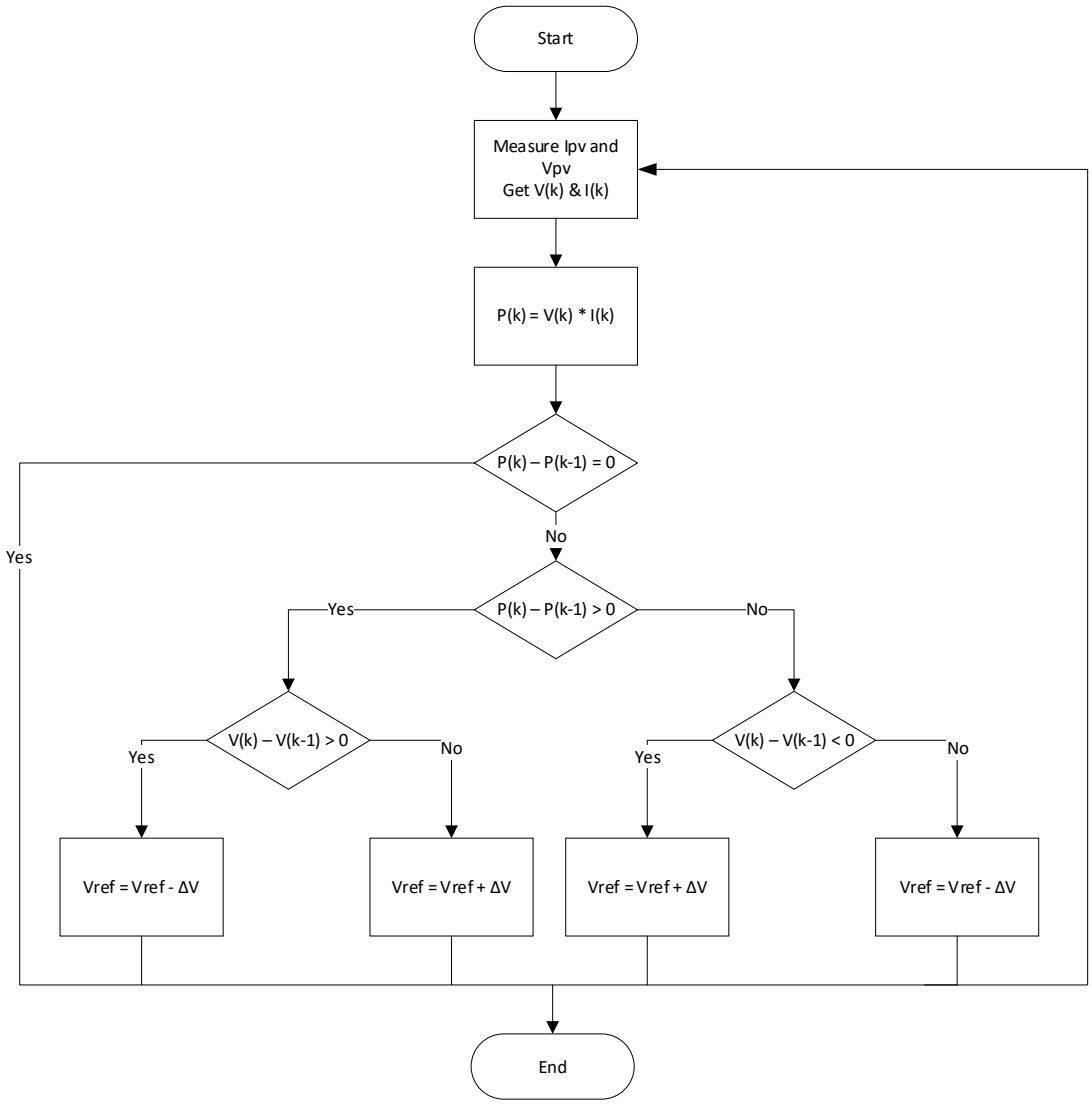

Figure 4.8 - P&O MPPT Algorithm Flowchart

From Figure 4.2 (c) the circuit is in charging State A – G1 and G3 are high (or on). The current flows from the PV panel and is halved to pass through the two interleaving stages where it is stored in the two inductors. In charging State B – G1 and G3 are low (or off) this allows the current to flow through the diodes at G2 and G4 which allows energy stored in L5 and L6 to charge the battery.

In discharging State C – G2 and G4 are high (or on) this allows the current to flow from the battery to charge the L5 and L6 inductors. The current is now flowing in the opposite direction (Boost) to State A and State B (Buck) above demonstrating the bidirectional capability of the circuit to charge and discharge. Finally, discharging State D – G2 and G4 are low (or off) this allows the current to flow from the inductors to the DC link through the diodes at G1 and at G3.

The values of the components used in the bidirectional battery charger circuit are selected using the following equations. These equations give the critical value ranges for the capacitor C6 and inductors L5=L6.

Charging mode DC/DC Conversion V_{out}:

$$V_{out} = V_{in} * D \tag{4.7}$$

Discharging Mode DC/DC Conversion V_{out}

$$V_{out} = V_{in} * \frac{1}{1-D}, \tag{4.8}$$

Discharging Mode DC/DC Conversion Duty Cycle,

$$D = \frac{t_{on}}{T_s}, D = \frac{f_s}{t_{on}}, \tag{4.9}$$

$$T_s = t_{on} + t_{off} = \frac{1}{f_s} \tag{4.10}$$

Discharging Mode DC/DC Conversion State 1 Inductor Current,

$$L\frac{\Delta I_{L1}}{t_{on}} = V_{in} - 0, \tag{4.11}$$

$$\frac{\Delta I_{L1}}{t_{on}} = \frac{V_{in}}{L}, \tag{4.12}$$

$$\Delta I_{L1} = \frac{V_{in}}{L} DT_s, \tag{4.13}$$

Discharging Mode DC/DC Conversion State 2 Inductor Current,

$$L\frac{\Delta I_{L2}}{t_{off}} = V_{in} - V_{out}, \tag{4.14}$$

$$\frac{\Delta I_{L2}}{t_{off}} = \frac{V_{in} - V_{out}}{L}, \tag{4.15}$$

$$\Delta I_{L2} = \frac{V_{in} - V_{out}}{L} (1-D)T_s, \tag{4.16}$$

Charging Mode DC/DC Conversion State 3 Inductor Current,

$$L\frac{\Delta I_{L1}}{t_{on}} = V_{in} - V_{out}, \tag{4.17}$$

$$\frac{\Delta I_{L1}}{t_{on}} = \frac{V_{in} - V_{out}}{L}, \tag{4.18}$$

$$\Delta I_{L1} = \frac{V_{in} - V_{out}}{L}\ DT_s, \tag{4.19}$$

Charging Mode DC/DC Conversion State 4 Inductor Current,

$$L\frac{\Delta I_{L2}}{t_{off}} = 0 - V_{out}, \tag{4.20}$$

$$\frac{\Delta I_{L2}}{t_{off}} = \frac{-V_{out}}{L}, \tag{4.21}$$

$$\Delta I_{L2} = \frac{-V_{out}}{L}\ (1-D)T_s, \tag{4.22}$$

DC/DC Conversion Inductor Calculations,

$$\Delta I_{L1} + \Delta I_{L2} = 0\ , \tag{4.23}$$

$$I_{L-Peak} = I_{L-average} + \frac{1}{2}\Delta I_L\ , \tag{4.24}$$

$$\Delta I_L = 2I_{L-average} = 2I_{out} = \frac{2V_{out}}{R} = \frac{2DV_{in}}{R} \tag{4.25}$$

$$Critical\ Inductor\ Value: L_C = \frac{(1-D)R}{2f_s} \tag{4.26}$$

DC/DC Conversion Capacitor Calculations,

$$Critical\ Capacitor\ Value: C_C = \frac{(1-D)}{16Lf_s{}^2} \tag{4.27}$$

Table 4.2. details the PV source parameters used for this simulation. The PV panel used in this simulation has two inputs Irradiance and Temperature. The initial state of charge for the battery used in this energy management system is 24.997% with the battery voltage for the simulation set to 48 Volts. The home load is also set to constant for the purposes of this experiment. The battery parameters shown in Table 4.3 below have been selected from a predetermined list of batteries in the MATLAB/Simulink software package.

Table 4.2 – PV Source Parameters

Parameter	Value
Parallel strings	1
Panels in series	18
Cells per panel	60
Maximum power per panel (W)	213.15
Open circuit voltage per panel (V)	36.3
Short circuit current per panel (A)	7.84
Voltage at maximum power per panel (V)	29
Current at maximum power per panel (A)	7.35

The initial state of charge for the battery used in this EMS is 70% with the battery ageing and temperature derating factors can be incorporated to show the aging and temperature effects however for this simulation they have not been used. The battery voltage for the simulation has been set to 48 Volts however for a practical circuit there would be 3x 12V batteries connected in series as this is more practical, feasible and cheaper in terms of industrial batteries that are fit for purpose.

Table 4.3 - Battery Parameters

Parameter	Value
Type	Lithium-Ion
Nominal Voltage	48 V (3 x 12V)
Initial State of Charge	24.996%
Rated Capacity	330 Ah

The component values for the circuit in Figure 4.7 (c) are shown in Table 4.4 below. In Table 4.5 the control circuit component parameters are also shown.

Table 4.4 - Battery Charging Circuit Component Parameters

Parameter	Value
Inductor – L5 & L6	2.5mH
Capacitor – C6	10μF
IGBT Pair Internal Resistance R_{on}	1mΩ
IGBT Pair Snubber Resistance R_s	0.1MΩ
IGBT Pair Snubber Capacitance C_s	inf F

Table 4.5 - Battery Charging Control Circuit Parameters

Parameter	Value
Repeating Sequence	Time Values – 0, 0.00002, 0.00004 Output Values – 0, 1, 0 & 1, 0, 1
Saturation	Upper 0.9 Lower 0.1

Table 4.6. shows the parameters for the home load that is connected in series with the battery charger circuit in this system.

Table 4.6 - Home Load Parameters

Parameter	Value
Nominal Voltage (V_{rms})	240 V
Nominal Frequency	50 Hz
Active Power	2 KW
Inductive Reactive Power Q_L	100 +var
Capacitive Reactive Power Q_c	0 -var

4.3 Battery Charging Subsystem Investigation Results and Discussion

To validate the performance of the control strategy, the next experiment required collecting the data from the 4 gate pulses and plotting them on the same figure to observe and compare the pulse characteristics. From the simulations carried out, Figure 4.9 is a chart of the 4 gate pulses generated by the combined MPPT and Current Controller circuit. These are the gate pulses used to control the battery charger circuit. The measured output of the gate pulses shows that (a) and (b) are 180 degrees out of phase with (c) and (d) therefore the IGBTs are controlled as interleaved switch pairs.

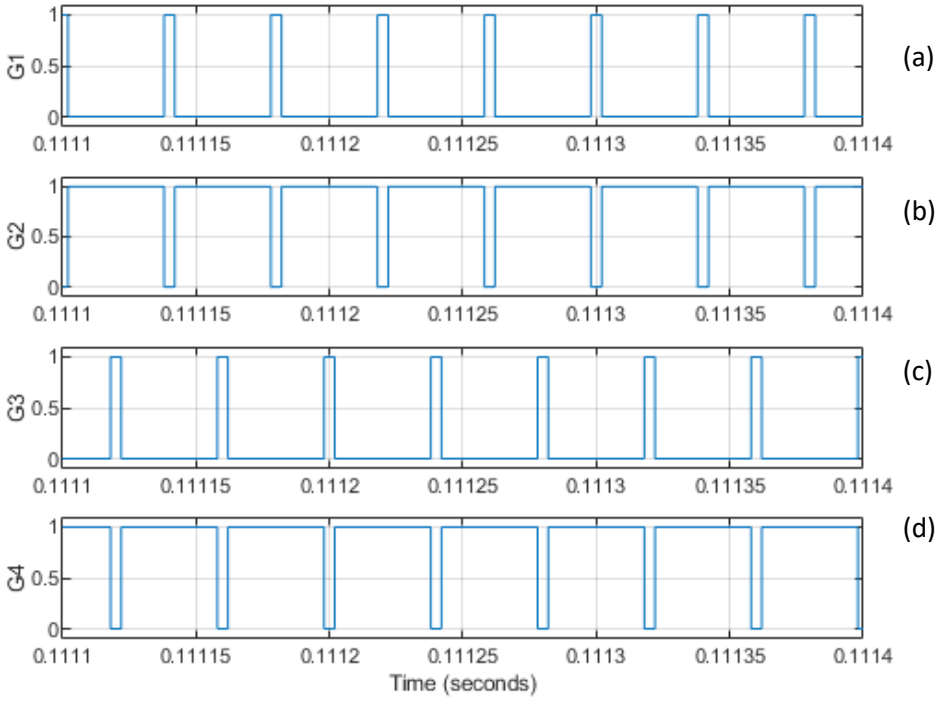

Figure 4.9 – Battery Charging Subsystem Control Strategy Output Gate Signals for Battery Charging Subsystem IGBT Switch Gate Pulses (a) G1 (b) G3 (c) G2 (d) G4

To adequately test the system performance, there is a requirement to vary the input conditions for the PV panel and observe the system's response to changes in these variables. Figure 4.10. shows how these variables are varied for the duration of the simulated timeframe. The inductor currents I_{L5} and I_{L6} are shown in Figure 4.11.

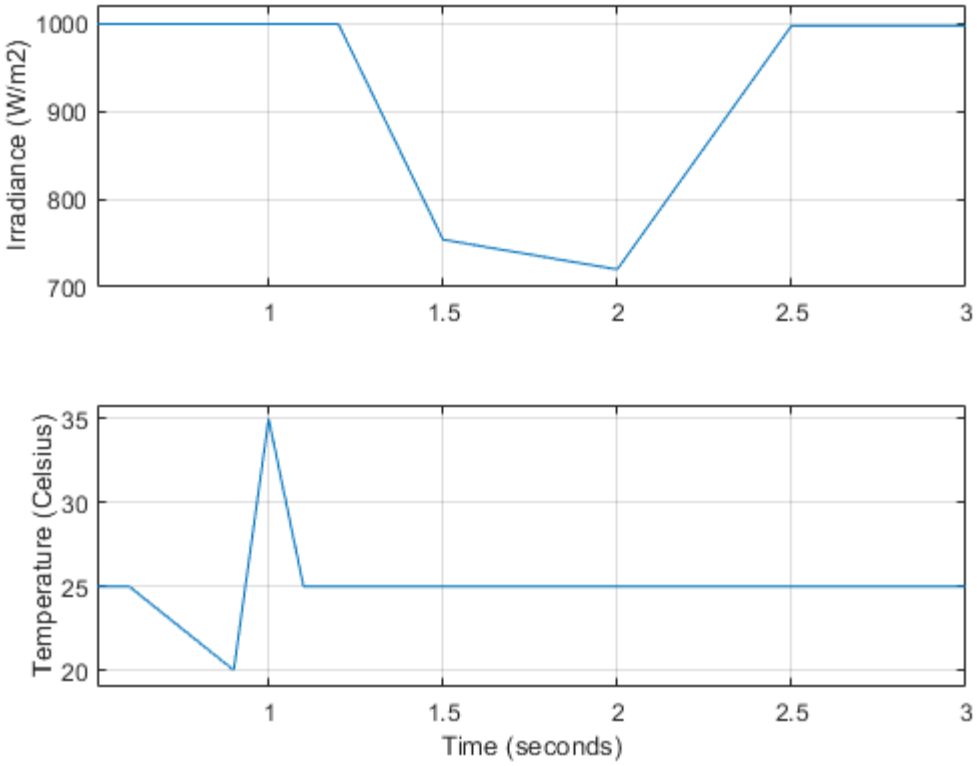

Figure 4.10 - Variable Input Conditions (a) Irradiance (b) Temperature

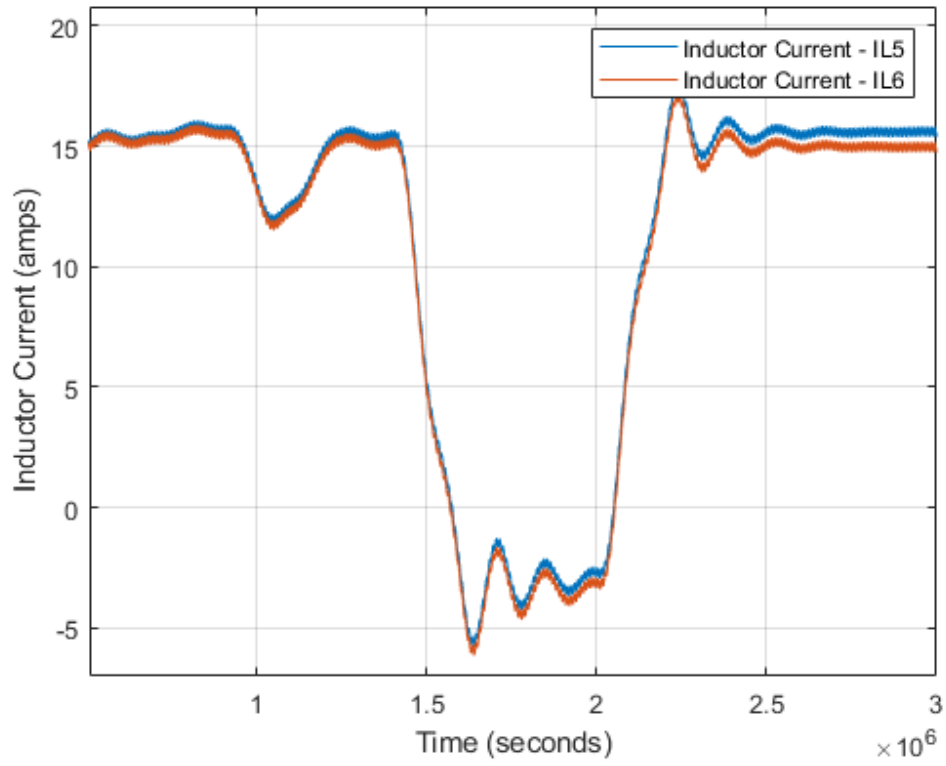

Figure 4.11 – Battery Charger Subsystem Inductor Current (I_{L5}-Orange and I_{L6}-Blue)

The interleaving of the two inductor currents can be observed when comparing the I_{L5} with the charge current (I_{L5}+I_{L6}) as show in Figure 4.12, there is more output ripple of the blue signal compared to the orange signal which validates the interleaving performance, zooming in closer to the inductor current of I_{L5} and the charge current is shown in Figure 4.13.

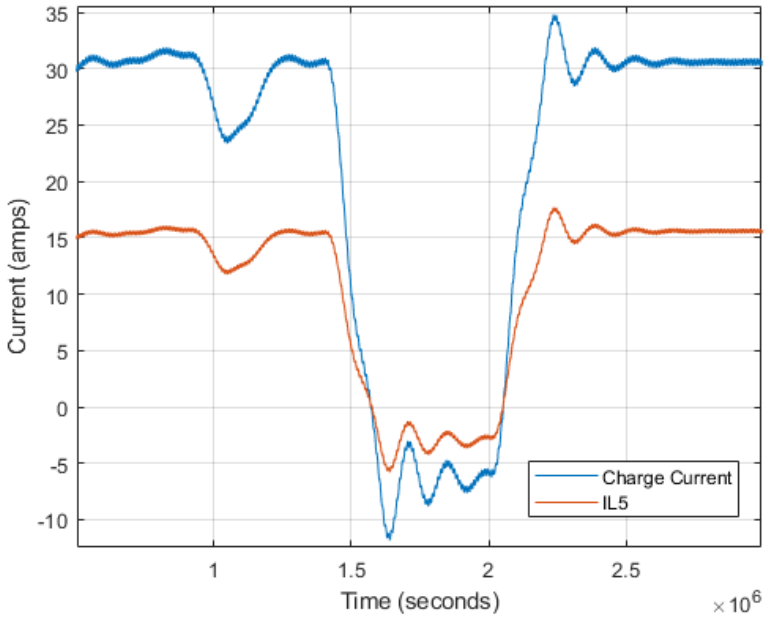

Figure 4.12 - Battery Charger Subsystem Inductor Current & Charge Current (I_{L5}-Orange and Charge Current (I_{L5} + I_{L6}) -Blue)

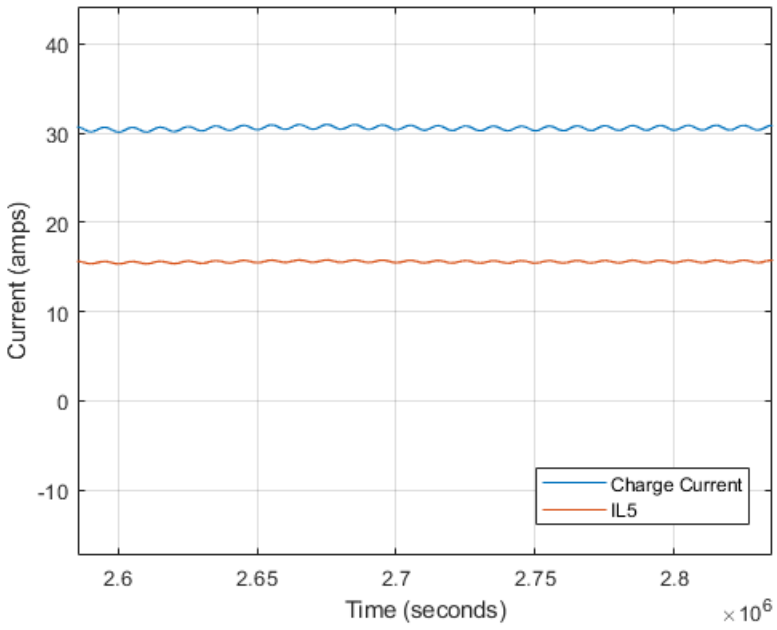

Figure 4.13 - Battery Charger Subsystem Inductor Current & Charge Current Zoomed (I_{L5}-Orange and Charge Current (I_{L5} + I_{L6}) -Blue)

Figure 4.14. shows the state of charge of the battery for the duration of the simulation experiment. The objective of observing this characteristic is to verify that the battery can be charged and discharged to meet the requirements of the energy management system.

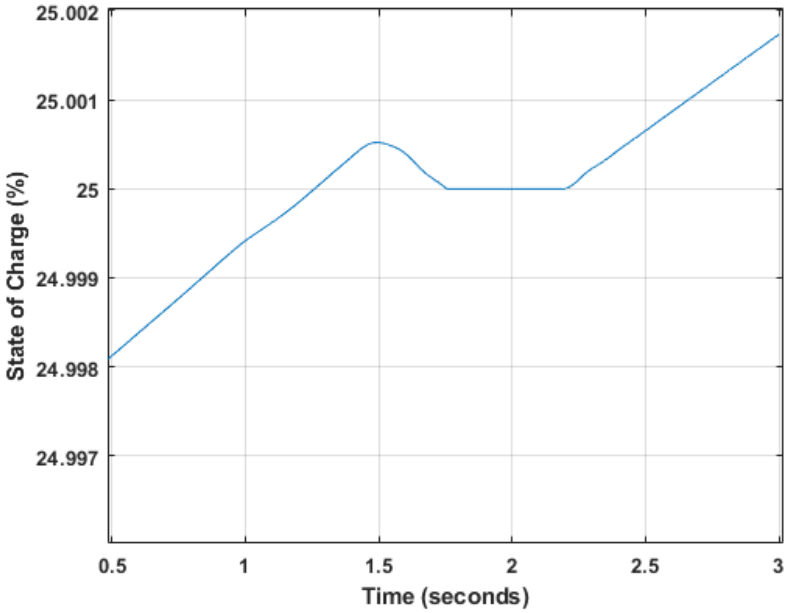

Figure 4.14 - Battery State of Charge – Percentage

The investigation focuses on the battery charger therefore the performance of the battery current and voltage should also be observed. Figure 4.15. shows how the battery current (blue) and voltage (red) perform for the duration of the simulation, particularly when the input conditions are varied.

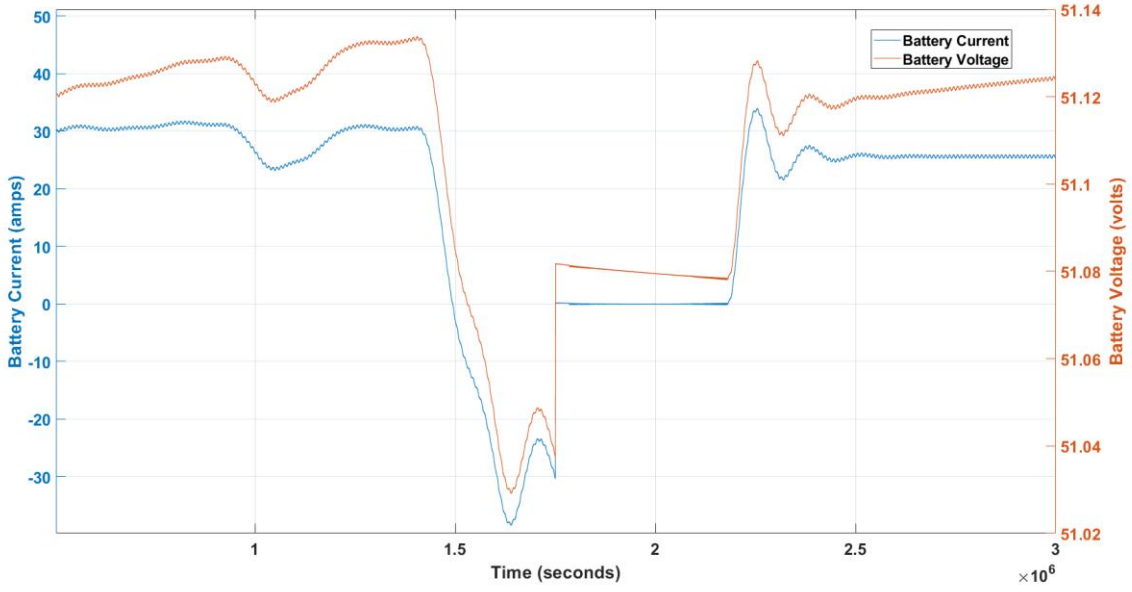

Figure 4.15 - Battery Current (Blue) and Battery Voltage (Red)

To further validate the performance of the circuit, Figure 4.16 can also be observed as it shows how the PV power and battery power change as the input conditions vary. It is important that the battery power supplements the 2kW home load when the PV power drops below the required threshold. The balance of the power can be observed in Figure 4.16. As this chapter focuses specifically on the battery charger, the scope for the load power has not been included in Figure 4.16 but it is included and discussed in chapter 3 the variation between PV power and Battery power is shown in the scope for load power.

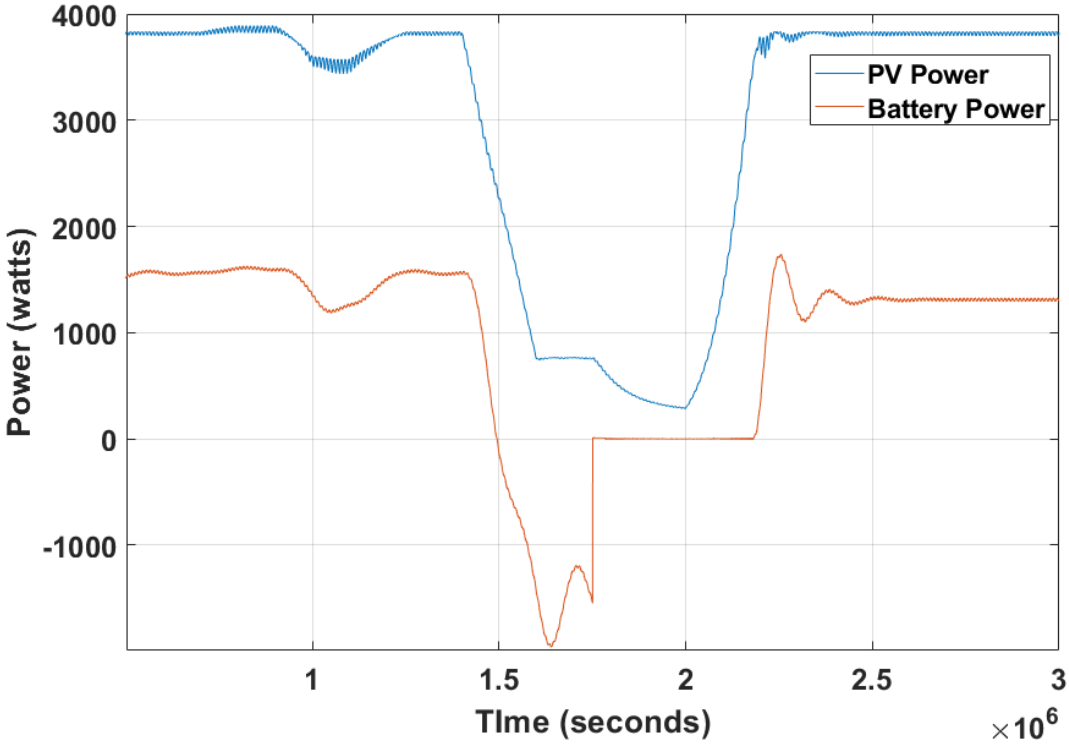

Figure 4.16 - System Power Output (Battery – Red, PV – Blue)

The result of this experiment is displayed in Figure 4.17 which shows a comparison of the DC Link voltage for three types of battery chargers. The strategy utilized in this global system is the current controlled interleaved strategy, which is shown in blue, while the red line in Figure 4.17 shows the DC Link voltage for a voltage controlled interleaved strategy, and the yellow in Figure 4.17 shows the DC Link voltage for a voltage-controlled strategy without an interleaved stage.

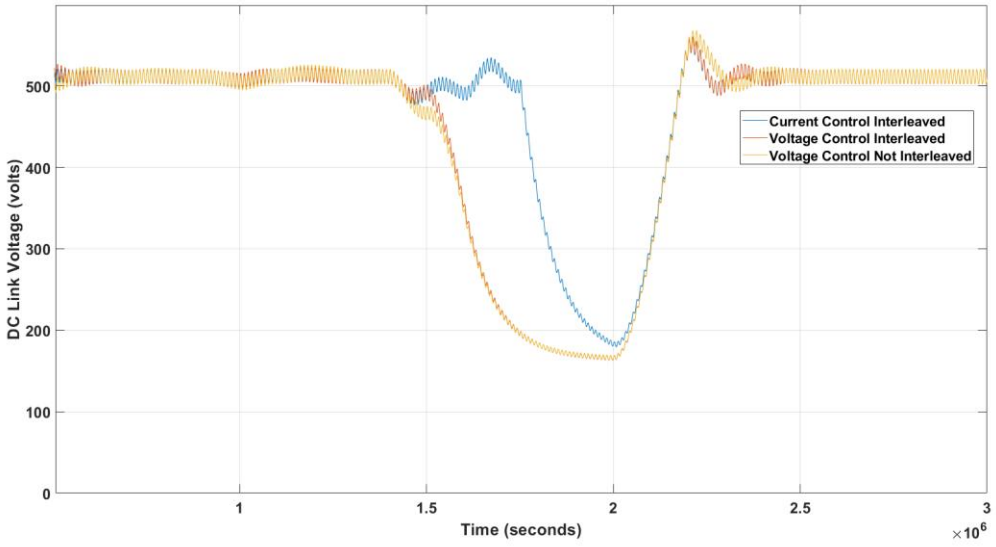

Figure 4.17 - DC Link Voltage – Interleaved Circuit with Current Control Strategy (Blue), Interleaved Circuit with Voltage Control Strategy (Red), Non-Interleaved Circuit with Voltage Control Strategy (Yellow).

The pulses shown in Figure 4.9 confirms that the control strategy successfully interleaves the gates of the two switch pairs. As can be observed from Figure 4.10, the temperature decreases from 25°C to 20°C at 0.65 seconds to 0.80 seconds before moving up from 20°C at 0.9 seconds to 40°C by 1 second. The irradiance stays at 1000 W/m2 until 1.4 seconds where it drops to 200 W/m2 by 1.6 seconds, at 2 seconds it increased from 200 W/m2 to 1000 W/m2 by 2.2 seconds before remaining at 1000 W/m2 until 3 seconds.

For the control circuit to work as theorized above, the response of the circuit to a change in input voltage should be observed when plotting the inductor current. The inductor current is shown in Figure 4.11 and from visual inspection it can be concluded that the inductor current curve tracks with the V_{pv} and voltage at MPPT which shows that the intended function of the combined MPPT and current controller works as designed. The battery does not discharge further than 25% to prolong the battery lifecycle and improve/protect long-term battery performance.

The performance of the battery for the duration of the simulation is important data to gather and analyse. Figure 4.14 shows the state of charge of the battery. The initial state of charge of the battery has been set to 24.997% as this will allow a demonstration of the state of charge controller to be observed within the duration of the 3 second data gathering in MATLAB/Simulink. Figure 4.14 shows that the battery is charging until the point at which the irradiance falls and when this happens, the battery is required to supplement the 2kW home load as the PV panel is no longer producing the required power. The battery begins to discharge at 1.5 seconds to support the 2kW home load. However, at the

point where the battery reaches 25% charge the state of charge controller circuit prevents the battery charger circuit from discharging the battery (to keep in the nominal range and prolong battery life). In this case, for a standalone system the home load would experience an outage/dip in power.

Looking at Figure 4.15, firstly, the scale of the voltage axis is very small by comparison to the scale of the current axis. The change in temperature can be observed via the small decrease and increase of both the battery current and voltage from 0.9 to 1.2 seconds. This change is not significant to cause the battery to stop charging or begin discharging. The state of charge in Figure 4.14. shows the curve to be less steep during the same period, which would indicate a reduction in the rate of charge. This shows that the circuit is performing as designed.

When the irradiance falls, it can clearly be observed that the battery is discharging, indicated by the negative current values shown in Figure 4.15. The point at which the battery circuit stops discharging and charging is when the battery reaches 25%, this is indicated by 0 amps of current flow in either direction. When the irradiance increases and the PV panel begins to generate power, the battery begins to charge once more which is again indicated by the positive current values. There are some steady state oscillations that are observed in both the battery current and voltage and therefore power.

Another way to evaluate the circuit performance is to observe the power for both the PV panel and the battery, this is shown on Figure 4.16. The envisaged pattern of behaviour is that the battery power should mimic the PV power curve, this would confirm that the battery charging circuit is performing in harmony with the PV panel to supply the home load. The point at which this synchrony is not visible is where the battery reaches the 25% discharge threshold. The overall performance of the global system can be validated to operate as required when observing Figure 4.16.

Due to the combination of the integrated interleaved battery charger and interleaved switched capacitor H-bridge inverter the global system is unique by comparison to other published methods. To validate the significance of the proposed control strategy as part of the global system an experiment was done where the control of the battery charger within the global system varied. As can be observed from Figure 4.17 the response of the proposed system is much faster than the voltage-controlled circuits, the system is also first to reach steady state at approximately 0.4 seconds compared with 0.55-0.60 seconds for the voltage-controlled circuits. The proposed system also provides a more stable DC Link voltage to the DC-AC Inverter for a longer period when the PV Output power begins to fall. This is shown from 0-0.5 where more oscillations are observed from the voltage-controlled strategies in Figure 4.17. Also, from 1.5 to 2 seconds on Figure 4.17. the DC Link voltage of the pro-posed system is shown to only begin to drop at the point at which the battery reached the 25% discharge threshold. The same behaviour was not observed for the two volt-age-controlled strategies which saw the DC Link voltage drop at the point at which the irradiance dropped.

4.4 Proposed Battery Charging Subsystem Conclusion

The circuit has been designed to reduce the number of conversion stages compared with conventional approaches in published literatures. The MPPT typically controls a boost converter connected in parallel to the battery charger that is controlled a voltage controller. Removing the boost converter increases the speed of the response, reduces the number of components required and improves efficiency by reducing the number of conversions and therefore conversion losses. This modified control strategy that combines P&O MPPT with a current controller to drive the IGBTs used in the circuit configuration is successful in providing the required performance. The results of the study showed that the gate pulses for the four IGBTs align with expected gate pulses for IGBT switch pairs in an interleaved circuit. The current flowing through the inductors shows similar characteristics to the PV output curve which shows the circuit can adapt to detected increases and decreases in PV output.

The circuits response to variable environmental conditions was observed to test this circuit further. The results gathered showed that circuit's response to irradiance changes align with expectations of an energy management system such that the battery can supplement the home load when the PV output reduces below the required threshold.

The interleaved bidirectional battery charger presented in this study shows the desired response characteristics to variable irradiance that is typically expected for a PV energy management system. As observed from the inductor currents, the results of this study conclude that the combined MPPT and current controller performs as theorized. The response of the circuit is fast with a low current ripple. The proposed approach differs from published literature due to the reduced components and the single stage of DC-DC conversion (as opposed to the boost converter in parallel). The study could be developed further by gathering practical data to validate the simulations.

4.5 Chapter Summary

This chapter utilised a simple P&O MPPT method to drive a current controlled a bi-directional interleaved DC-DC battery charger as part of the SPSAPVEMS. The method has been theorised and then simulated using MATLAB Simulink, the data gathered from the simulation has been presented and discussed, different methods of control for this circuit were tested and discussed. A balance of complexity/performance has been proposed to optimise the performance of this sub-system.

5 A Switched Capacitor Based DC-AC Inverter Controlled by RMS Feedback and Phase Shifted SPWM for a PV EMS.

5.1 SPSAPVEMS Inverter Subsystem

The proposed system utilizes a conventional P&O MPPT that drives the switches in the bidirectional DC/DC interleaved battery charger. The battery charger is connected to the DC link that supply the dc voltage to the interleaved switched capacitor inverter in parallel. The inverter is controlled via phase shifted unipolar sinusoidal PWM with an RMS output voltage feedback loop to control the output voltage. The advantage of this system is that the system considers the combination of all the circuit elements compared with the literature described above that do not also contain a battery charging stage. The harmonic performance and efficiency of the proposed system is shown to be an improvement on existing method.

Figure. 5.1 shows the block diagram and system configuration of the standalone system. The system includes a PV array that is connected to the single-stage switch capacitor based single-phase inverter using the DC link. The DC link voltage is controlled by battery charging circuit using P&O MPPT algorithm to capture the maximum power from PV array for given solar conditions. The interleaved battery charging circuit controlled by a standard P&O MPPT method in parallel with a two-stage interleaved switched capacitor circuit [87], with a DC/AC H-bridge inverter and filter across the nominal home load. Fundamentally, when the PV array is generating power, provided there is no load demand, the bidirectional interleaved DC/DC battery charger allows the battery to be charged. When there is load demand, the battery discharges to supply the home load when the PV array is not generating the required power.

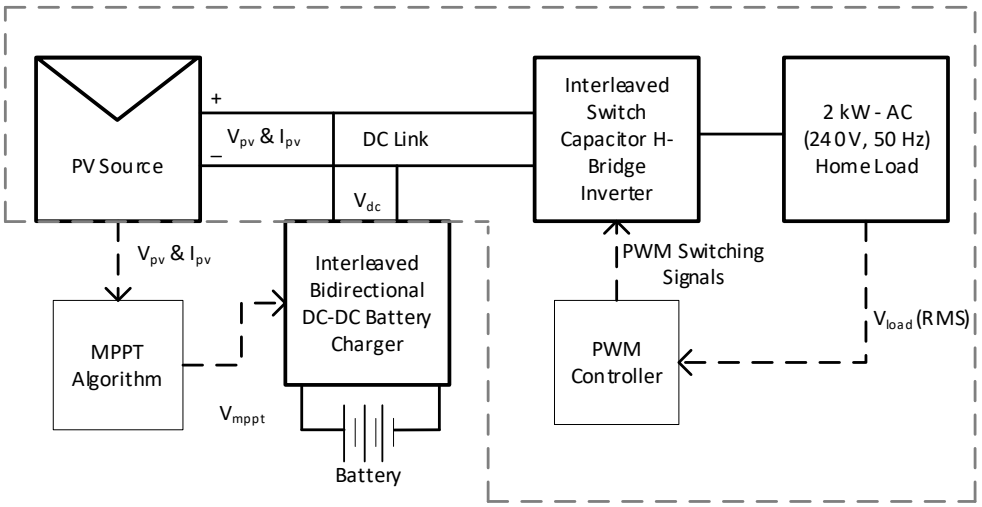

Figure 5.1 – Chapter 5 Sub-systems of PV EMS

5.2 SPSAPVEMS Inverter Subsystem – Circuit & Control Strategy Design

When analysing Figure 5.2 - DC/AC H Bridge Inverter Circuit the various elements that make up the inversion subsystem of this energy management system can be seen. The DC link capacitor C1 can be seen with a current measurement block placed in series and a voltage measurement block placed in parallel. This then feeds in directly to H bridge, which can be seen as the two pairs of IGBT switches connected via a home load, a LPF has also been added. A measurement block for current and voltage has also been placed across the home load so that the output of the system can be monitored. The values for all the components used in the management system can be found in Table 5.1 – Inverter Circuit Parameters.

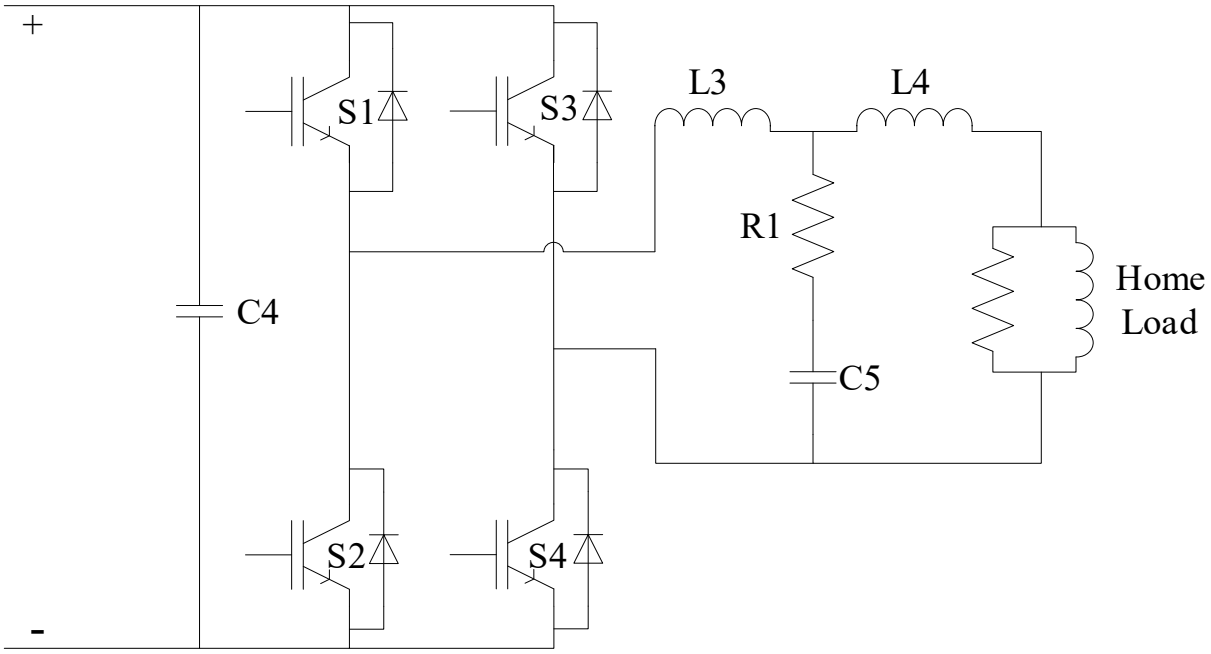

Figure 5.2 - DC/AC H Bridge Inverter Circuit

Table 5.1 – Inverter Circuit Parameters

Parameter	Value
DC Link Capacitor (C4)	1 nF initial value of 520V
IGBT s1, s2, s3 & s4	Internal Resistance R_{on} 1 mΩ Snubber Resistance R_s 100 KΩ Snubber Capacitance C_s inf F
L3	15 mH
L4	15 mH
C5	1 µF

The sinusoidal PWM circuit as described above is shown in Figure 5.5 - (a) Control Configuration for Stage A Switch Capacitor Circuit - Simulink (b) Control Configuration for Stage B H-Bridge Inverter – Simulink, this shows the reference sine wave compared with a triangular carrier signal. The values for both signals can be shown in Table 5.2 – Inverter Control Circuit Parameters. The two pairs of IGBT switches have gate pulses that are totally opposite, this can be seen from the circuit diagram as S2 & S4 are fed from the same path whereas S1 & S3 are fed from a NOT gate.

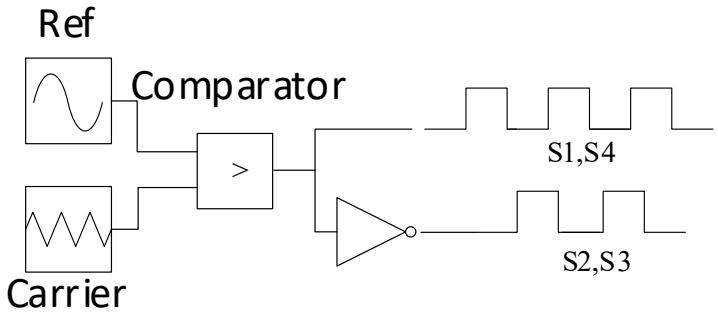

Figure 5.3 - Control Circuit for H Bridge Inverter

Table 5.2 – Inverter Control Circuit Parameters

Parameter	Value
Reference Signal Amplitude	339 V
Reference Signal Frequency	50 Hz
Reference Signal Phase	0 rad
Carrier Signal Amplitude	520 V
Carrier Signal Frequency	20 KHz
Carrier Signal Output Values	520, 0, -520, 0, 520

Figure 5.4 shows the interleaved switched capacitor and H-bridge inverter circuit including phase shifted unipolar sinusoidal PWM. The method used to control the interleaved switched capacitor is called phase shifted unipolar sinusoidal PWM. When analysing Figure 5.4, the various elements that make up the inverter subsystem of this energy management system can be seen. From left to right, the DC link capacitor C_1 feeds the input of the interleaved switched capacitor circuit. This then feeds in directly to H bridge, which can be seen as the two pairs of IGBT switches connected via a home load, a low pass filter (LPF) has also been added. The values for all the components used in the management system can be found in Table 5.3.

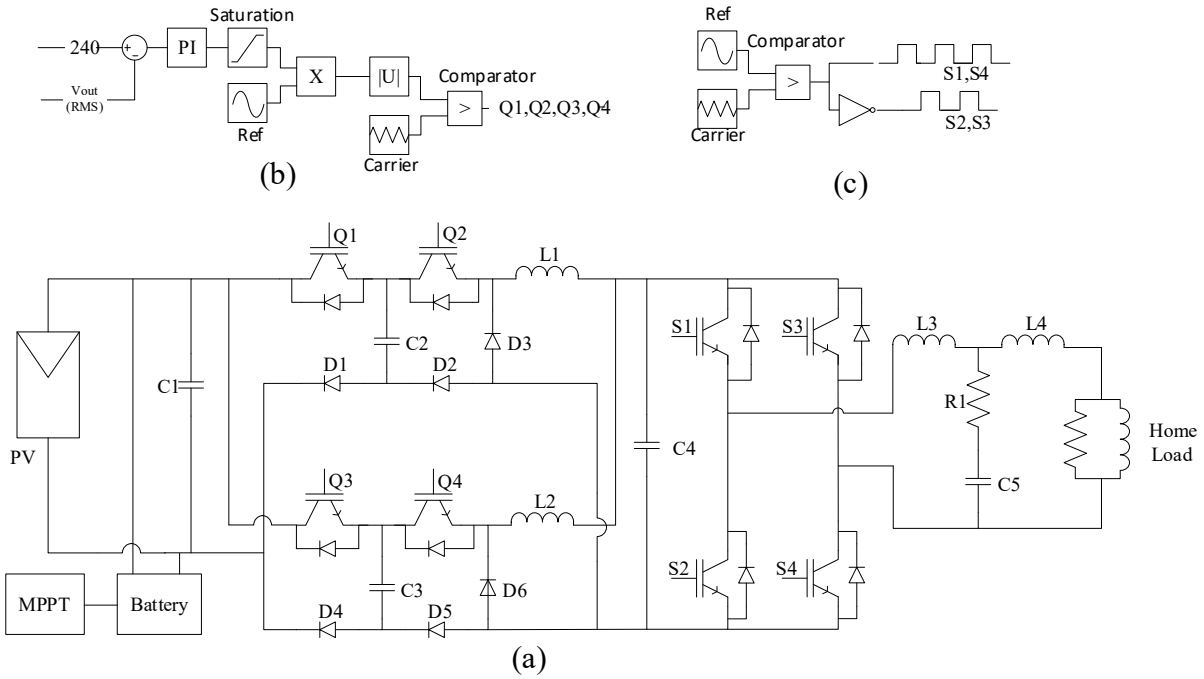

Figure 5.4 . (a) Interleaved switched capacitor and H-bridge inverter circuit, (b) Phase shifted unipolar sinusoidal PWM control for switched capacitor circuit (c) Sinusoidal PWM control for H-bridge inverter circuit

Table 5.3 – Inverter Control Circuit Parameters

Parameter	**Value**
Reference Signal Amplitude	339 V
DC Link Capacitor (C_1)	1000uF
Switched Capacitor (C_2 and C_3)	10uF
Filter Capacitor (C_4)	1nF
Load Filter Capacitor (C_5)	10uF
Filter Inductors (L_1 and L_2)	1.1 mH
Load Filter Inductors (L_3 and L_4)	10 mH
Load Filter Resistance (R_1)	1 Ω
Irradiance	1000 W/m2
Temperature	25°C
PV Array	18 modules per string 60 cells per module

The key parameters in relation to the interleaved switched capacitor circuit are capacitors C_1 and C_4 and inductors L_1 and L_2 are derived by equations (1) - (3) from the study described in [87]. A process to derive the value of the switched capacitors C_2 and C_3 is outlined in [112]. These equations

are used to calculate some of the capacitor values used in the circuit configuration where MPPT is used to modulate the amplitude of the reference signal used in the PWM.

$$C_1 = \frac{P}{4 * (2 * \pi * f_d) * V_{PV} * \Delta v_{PV}} \qquad \mathrm{C_1 = \frac{P}{4*(2*\pi*f_d)*V_{PV}*\Delta v_{PV}}} \tag{5.1}$$

$$C_4 = \frac{(L * {I^2}_{P_L})}{4 * V_o * \Delta v_o} \qquad \mathrm{C_F = \frac{(L*{I^2}_{P_L})}{4*V_o*\Delta v_o}} \tag{5.2}$$

$$L_{1,2} < \frac{(U * {V_{PV}}^2 * T_s)}{4 * P_{PV}} \tag{5.3}$$

Where,

P = the output power of the PV array,

V_{PV} = the output voltage of the PV array

P_{PV} = the output power of the PV array

T_s = the period for the carrier wave

L = the switched capacitor circuit inductance

I^2_P = the peak current flow through the inductor

V_O = the output load voltage

f_d = load frequency (50Hz)

U = modulated reference signal (RMS feedback)

The home load shown in Figure 5.4 shows a section of the inverter circuit where the home load is positioned. This home load is positioned across the output for the inverter circuit. The values shown in Table 5.4 give the nominal values of a home load and allow this simulation to accurately represent a standard home load. A power of 2KW was assigned to the home load which allowed the power regulation between the home load and the battery circuit to be observed.

For similar systems described in literature, the reference signals are modulated using MPPT however, considering the inclusion of a bi-directional DC/DC battery charging circuit, a novel approach to modulating the sinusoidal reference signal is proposed. The pulses are modulated using a closed loop

feedback system where the output RMS voltage is compared to the desired reference output voltage. This method allows for voltage control of the overall DC/AC inverter, this control enables the load voltage to reach steady state at RMS value of 240 V.

As shown in Figure 5.5 (a), the switched capacitor circuit is controlled using a series of phase shifted unipolar sinusoidal PWM generators that drive the gates of the IGBTs Q1, Q2, Q3 and Q4 and each of the pulses are equally phase shifted.

A standard switched capacitor stage would utilize two IGBTs and therefore gate pulses would only be required for Q1 and Q2. As the circuit interleaves two switched capacitor stages, there is a requirement for four gate pulses, in this case, at each stage of the circuit operation where one of the IGBTs is "on". Figure 5.5 (b) shows the control circuit for the H-Bridge inverter. The configuration shown is called sinusoidal PWM. The circuit shows the reference sine wave compared with a triangular carrier signal.

The values for both the carrier and reference signals are shown below in Table 5.5. From the circuit shown in Figure 5.4. There are two pairs of IGBT switches S1 & S4 and S1 & S3 the gate pulses for each pair are opposite as shown by the NOT gate in Figure 5.5 (b). The H-bridge therefore has two operating stages, namely 1.) Clockwise configuration S1 & S4 = 1 with S2 & S3 = 0 therefore current flows S1 – Load – S4 and 2.) Anti-clockwise configuration S1 & S4 = 0 with S2 & S3 = 0, therefore current flows S2 – Load – S3.

Table 5.4 – Home Load Parameters

Parameter	**Value**
Reference Signal Amplitude	339 V
Nominal Output Voltage (V_{rms})	240 V
Nominal Frequency	50 Hz
Active Power	2 KW
Inductive Reactive Power QL	100 +var
Capacitive Reactive Power Qc	0 -var

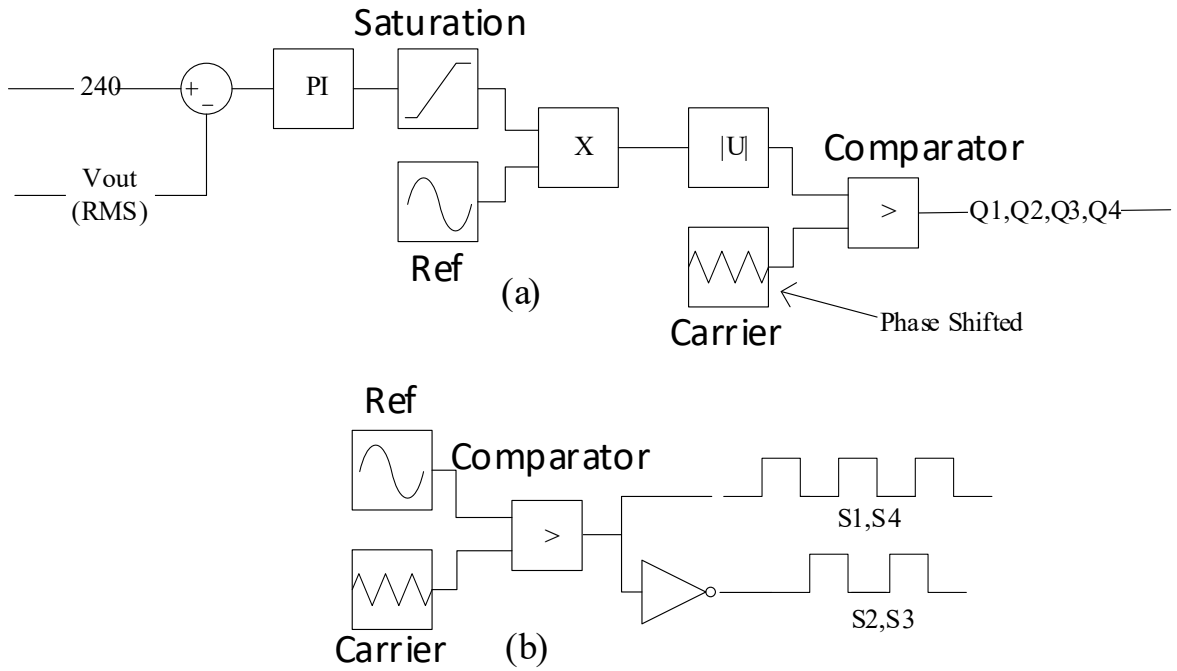

Figure 5.5 - (a) Control Configuration for Stage A Switch Capacitor Circuit - Simulink (b) Control Configuration for Stage B H-Bridge Inverter – Simulink

Table 5.5 – Inverter Control Circuit Parameters

Parameter	**Value**	
Parameter	Stage A Values	Stage B Values
Reference Signal Amplitude (Output Voltage)	|(1 * (240-VO) * PI) | Modulating ensures waveforms are in the positive domain.	1
Reference Signal Frequency	50 Hz	50 Hz
Reference Signal Phase	0 rad	0 rad
Carrier Signal Amplitude	0 and 1	0
Carrier Signal Frequency	5 kHz	0
Carrier Signal Output Values	Q1 [0 1 1 1 1] Q2 [1 0 1 1 1] Q3 [1 1 1 1 0] Q4 [1 1 1 0 1]	0

The pulse generation is shown visually in Figure 5.6 and are a representation of the gate pulses. The chart is not to scale. The rectified sinusoidal reference signal shows the control methodology to be unipolar and sinusoidal as described. To shift the phases of the four gate pulses required to drive the

IGBTs in the switched capacitor stage, signals Q1+ Q3 and Q2 + Q4 can be considered as pairs which a phase shift to enable the interleaving principal. In this control strategy, the repeating sequence block in Simulink has been adapted such that the relevant carrier signal pairs (shown as (a) in Figure 5.6) are out of phase by Ts:

- Q1 repeating signal output values: [0 1 1 1 1]
- Q3 repeating signal output values: [1 1 1 1 0]
- Q2 repeating signal output values: [1 0 1 1 1]
- Q4 repeating signal output values: [1 1 1 0 1]

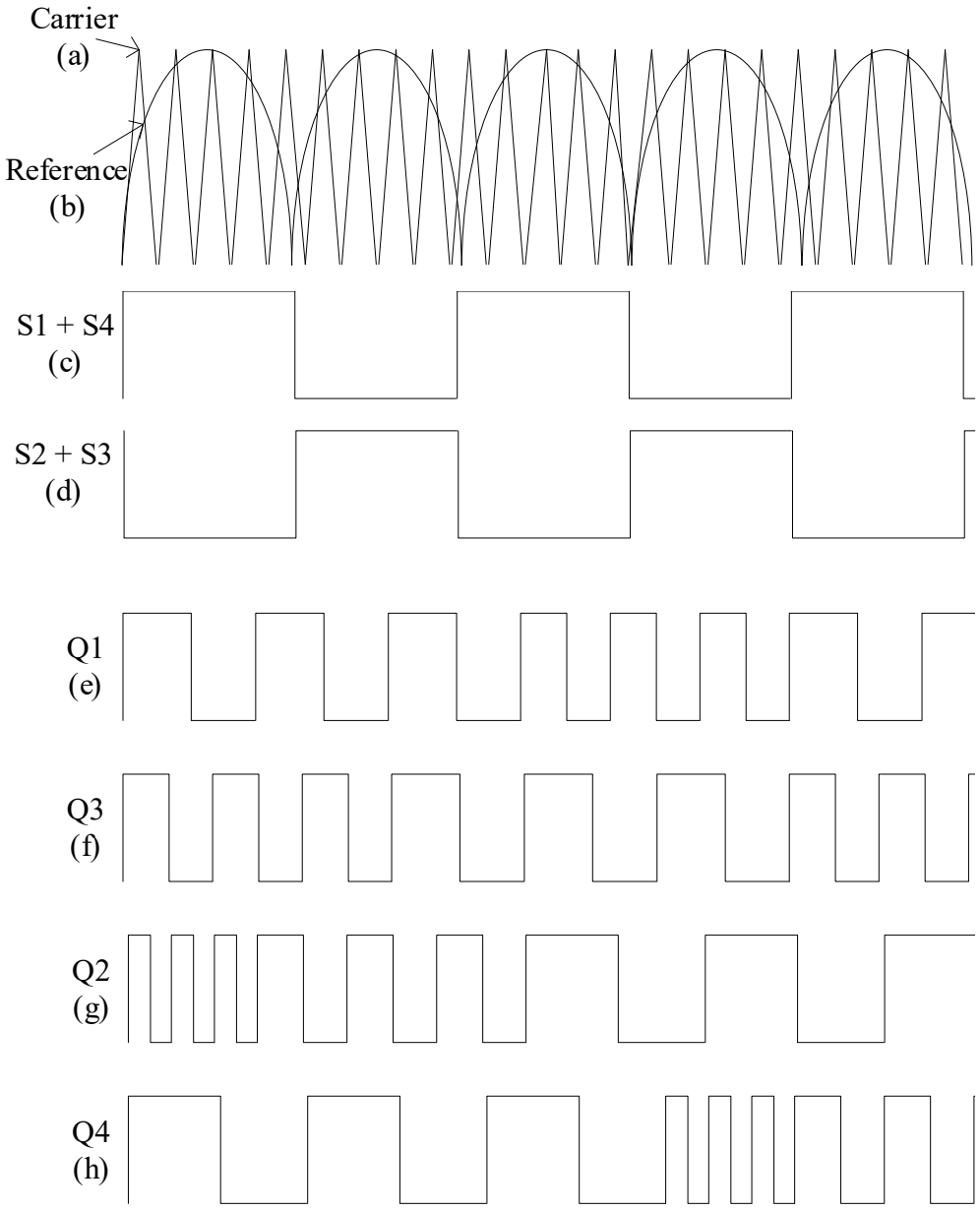

Figure 5.6 (a) The PWM carrier signal, (b) The modulated RMS feedback reference signal, (c) The gate pulses for S1 & S4, (d) The gate pulses S2 & S3, (e) Q1 gate pulse, (f) Q3 gate pulse, (g) Q2 gate pulse and (h) Q4 gate pulse

Using this methodology, the control circuit can provide the two interleaved pairs of phase-shifted gate pulses required to drive the switched capacitor circuit. From observing Figure 5.7, the inductor current waveform, is generated when capacitors C2 and C3 are charged and discharged synchronously.

- State A: Q1 is triggered, and the current can then flow through Q1 and D1 which charges C2 from the PV array and C1,
- State B: Q2 is triggered, and the current can then flow through Q2 and D2 which discharges C2 to the H-bridge (and consequently the home load) via L1,
- State C: Compared to the Q1 trigger, after a delay of Ts (hence phase shifted PWM) Q3 is triggered and current can then flow through Q3 and D4 which charges C3 from the PV array and C1,
- State D: Compared to the Q2 trigger, after a delay of Ts (hence phase shifted PWM) Q4 is triggered, and the current can then flow through Q4 and D5 which discharges C3 to the H-bridge (and consequently the home load) via L2.

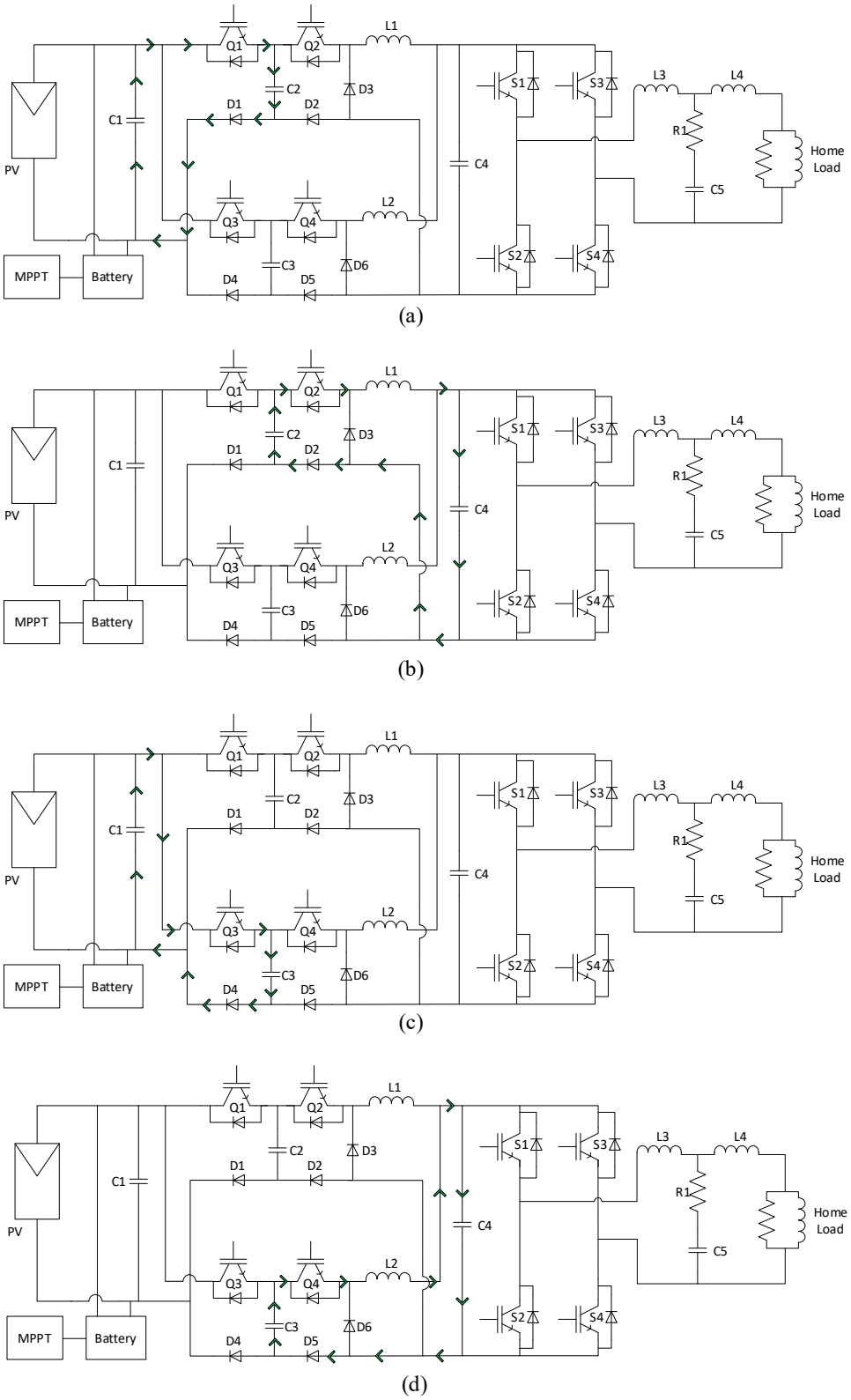

Figure 5.7 - Proposed Inverter Current Flow (a) State A – C2 Charge (b) State B – C2 Discharge (c) State C – C3 Charge (d) State D – C3 Discharge

5.3 Inverter Subsystem Investigation Results and Discussion

This section presents the results of this study. The charts are taken from a simulation on MATLAB using the Simulink package. The circuit parameters are outlined in Table 5.3 and Table 5.4 for the H bridge control circuit , with Table 5.5 showing the circuit parameters. The output of the PV cell is shown in Figure 5.8. As can be seen from the chart, the circuit reaches its steady stage within 5.5 seconds. The output of the PV array charges the battery (controlled by MPPT to extract the maximum power from the PV array) and is connected in parallel to the inverter circuit.

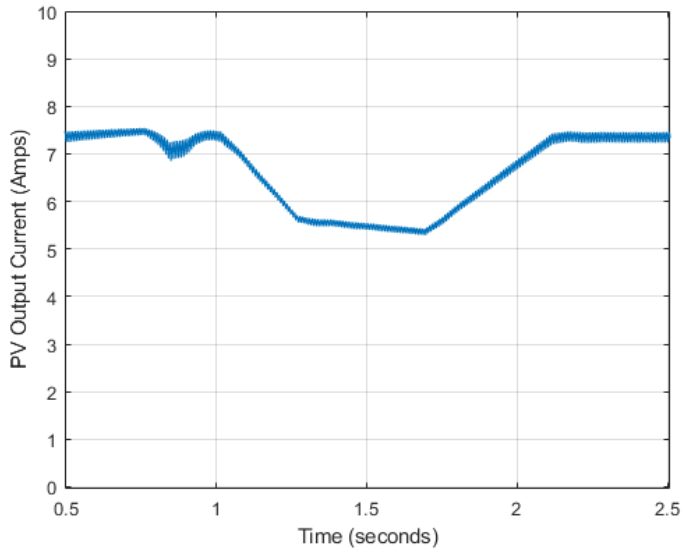

Figure 5.8 - (a) PV Output current and (b) PV Output Voltage

The waveforms shown in Figure 5.9 (a) are the current across both inductors, the interleaving of the waveforms for L1 and L2 can be observed when the waveform is examined further, this is shown

in Figure 5.9 (b) as the waveforms appear out of phase. From observing Figure 5.5, the current shown in Figure 5.9 is generated when capacitors C2 and C3 are charged and discharged synchronously.

- Q1 is triggered and the current can then flow through Q1 and D1 which charges C2 from the PV array and C1,
- Q2 is triggered and the current can then flow through Q2 and D2 which discharges C2 to the H-bridge (and consequently the home load) via L1,
- Compared to the Q1 trigger, after a delay of Ts (hence phase shifted PWM) Q3 is triggered and current can then flow through Q3 and D4 which charges C3 from the PV array and C1,
- Compared to the Q2 trigger, after a delay of Ts (hence phase shifted PWM) Q4 is triggered, and the current can then flow through Q4 and D5 which discharges C3 to the H-bridge (and consequently the home load) via L2.

Based on the control of the switch pair (Q1 + Q2) described above, the switched capacitors charge and discharge therefore the current observed through the inductors L1 alternates from 0-12A. The same observation can be made for the other switch pair (Q3 + Q4) when observing the L2 current waveform, however as the arrangement is interleaved, the L2 current is out of phase with the L1 current waveform.

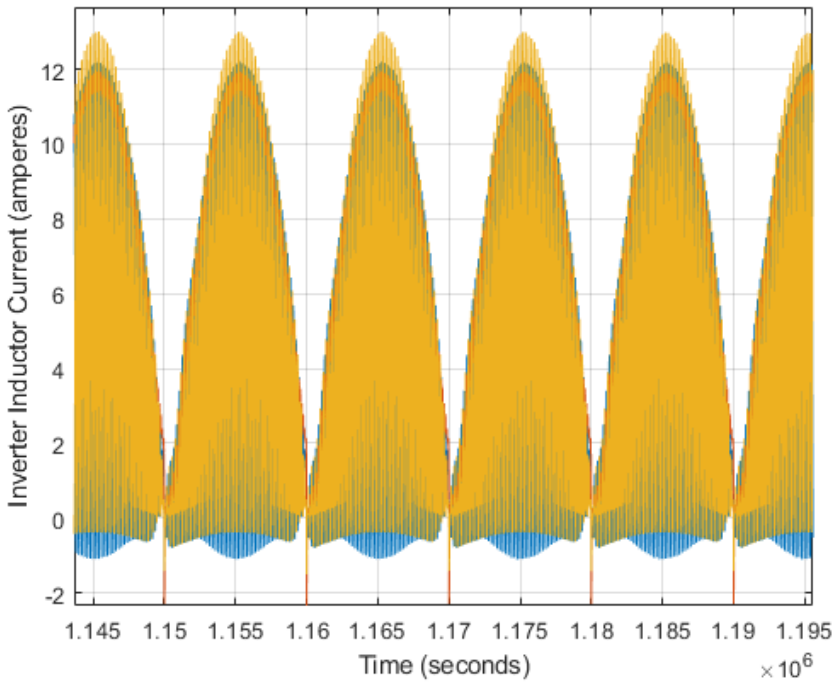

(a)

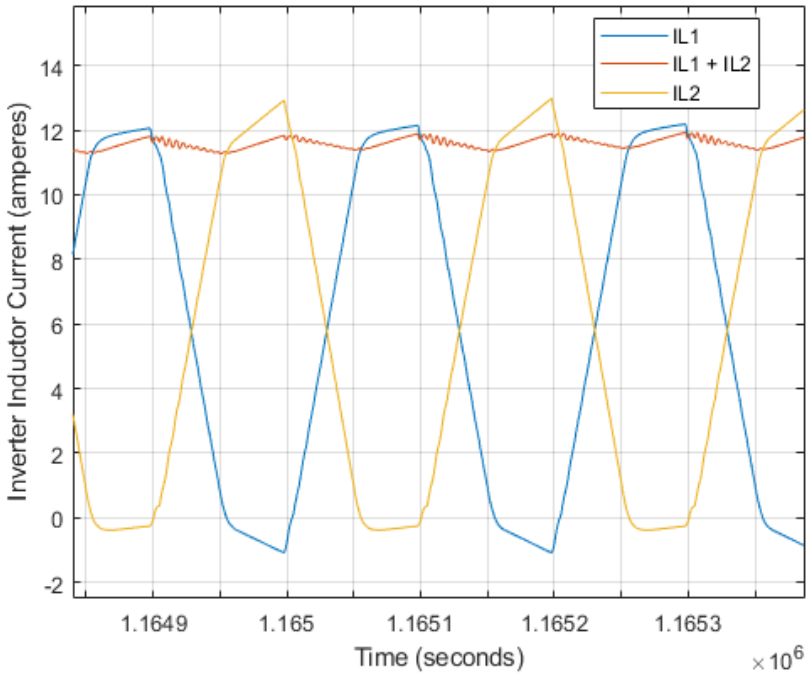

(b)

Figure 5.9 (a) Inverter Subsystem Inductor Currents (Blue – I_{L1} and Orange – I_{L2}) and (b) Inverter Subsystem Inductor Currents Zoomed (Blue I_{L1} and Orange – I_{L2})

The output of the switched capacitor circuit is shown in Figure 5.9 (a) shows current from 0A to 12A (as designed), as can be seen from Fig. 7. Below, the H-bridge inverts this current to -12A to 12A. The overall objective of the system is to produce a sinusoidal AC output waveform at 240V with a frequency of 50Hz to support a home load. Evidence of this system's overall output load is shown in Figure 5.10. and Figure 5.11. for current and voltage respectively, these waveforms are sinusoidal as required. As expected, the output of the system shows a very small output ripple. Figure 5.12. is a combined chart of the output current and voltage.

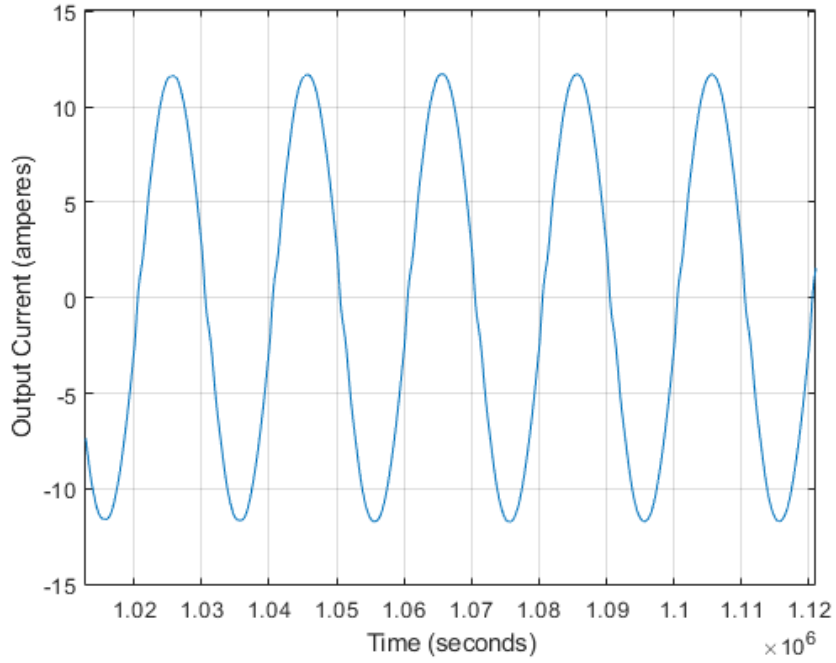

Figure 5.10 - Inverter Output Current

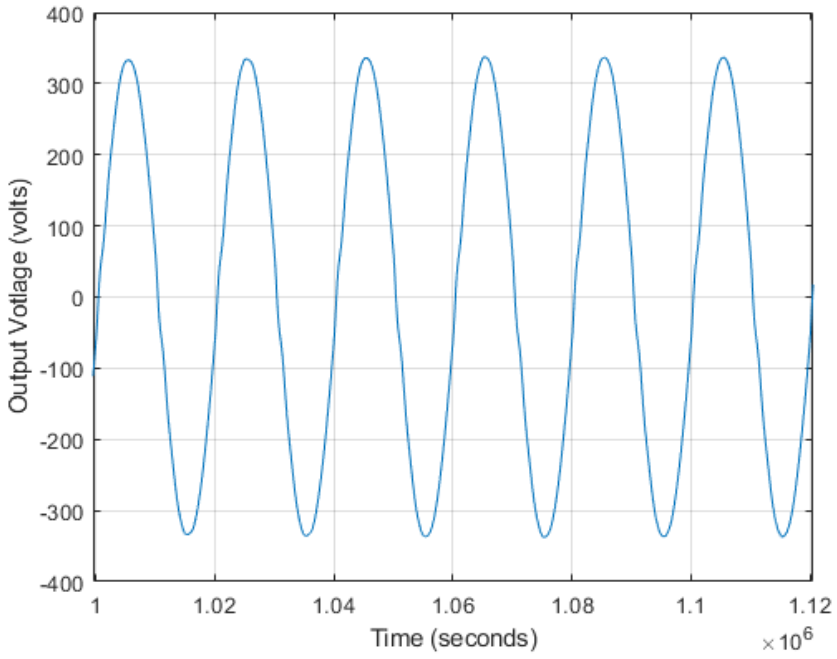

Figure 5.11 Inverter Output Voltage

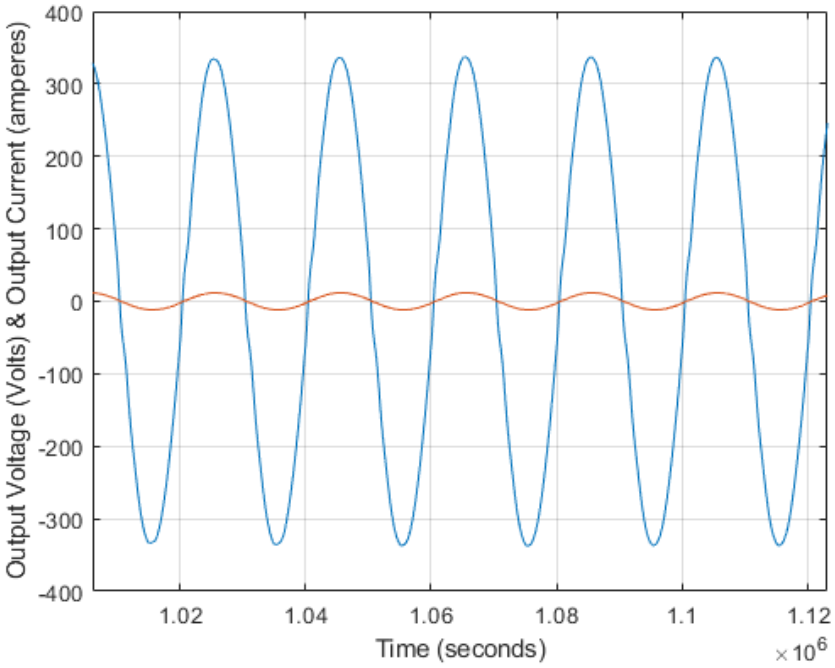

Figure 5.12 Load Voltage (a-orange) and Current (b-blue)

Harmonic analysis was undertaken from Simulink, the results of this analysis (considering a fundamental frequency of 50Hz) show that the THD for this circuit is 1.81%. Table 5.6 summarizes the results of the literature review conducted as part of this study, it shows comparisons with other types of inverters including SPUC, Interleaved and Multilevel. As can be concluded from the table, this adapted approach is able to utilize a novel approach combined with other elements of a PV system to produce a lower THD and reduces the quantity of capacitors, diodes and switches compared with other novel and conventional approaches.

Table 5.6 – PV Inverter Comparison

Parameter	Inverter Type	Output Voltage (THD)	Components	Control
S-Packed U Cell (SPUC) **[82]**	Multilevel Inverter	27.58%	Input Sources x1 Switches x5 Capacitors x2	PWM
5-level Multilevel Inverter **[102]**	Multilevel Inverter	14.20%	Input Sources x1 Switches x5 Capacitors x2 Diodes x4	PWM
9-level inverter **[86]**	Cascaded H Bridge	Symmetrical – 4.49% Asymmetrical - 17.53%	Input Sources x4 Switches x16	Phase Disposition PWM
Interleaved Inverter **[87]**	Switched Capacitor H Bridge	3.92%	Input Sources x1 Switches x8 Capacitors x4 Diodes x9	Phase Shift Sinusoidal PWM
7-level Multilevel Inverter **[105]**	Multilevel Inverter	10.99%	Input Source x1 Switches x8 Diodes x7 Capacitors x5	Selective Harmonic Elimination PWM
21-level Multilevel Inverter **[106]**	Multilevel Inverter	3.49%	Input Source x3 Switches x10 Diodes x10 Capacitors x2	PWM
This study	Switched Capacitor H Bridge	1.81%	Input Sources x1 Switches x8 Capacitors x5 Diodes x6	Unipolar Phase Shift Sinusoidal PWM modulated with an RMS feedback loop

5.4 Proposed Inverter Subsystem Conclusion

All RLC values within the circuit have been tuned such that the lowest THD can be achieved and therefore the best harmonic performance of the circuit can be observed. The simulation ran from 10 seconds and the harmonic analysis of the output was carried out after the circuit reached steady state. The objective of the system is to improve the harmonic performance of the circuit compared with other literature. As a guideline, for a residential home load according to the guidelines in IEEE 519 [15] standard there is a harmonic limit of 5% for AC voltages within the home.

Considering other literature, a standard H bridge has limitations such as high switching losses, harmonics performance, high voltage stress and the system is usually less reactive to multiple voltage levels. Using a capacitor compensator and LC filters helps to improve harmonic performance and interleaving the inverter helps to reduce the output ripple. Multilevel inverters utilize many components however they are simple by nature. The 7- and 21- level multilevel inverters show the desired smooth sinusoidal input required for a home load.

The THD for this proposed study improves on all the recorded values extracted from the literature review. The number of components used in this study is equal to or less that the studies that have THD values under 5%. PWM is the most popular control methodology used across the studied literature; this aligns with the PWM approach used in this study. The RMS feedback loop helps to control the inverter input voltage and ensures that the output voltage remains at a constant 240V to meet the requirements of a home load.

The presented circuit shows an interleaved switched capacitor inverter circuit controlled by a modified method of unipolar phase shifted sinusoidal PWM that uses an RMS feedback loop due to the MPPT circuit controlling a battery charger. The outcome of this study concludes that all the elements required for a stand-alone residential home load can be combined to produce a high-performance PV energy management system. The interleaved inverter can reduce the output ripple which also has a positive impact on the THD without an excessive number of components. The system can react to varied irradiance and temperature conditions.

5.5 Chapter Summary

Chapter 5 summarised the investigation into an inverter subsystem as part of a Single Phase Standalone Photovoltaic Energy Management System (SPSAPVEMS). The inverter proposed has been theorised and simulated, with the data from MATLAB Simulink presented and discussed. The control strategy proposed has been modified and drives a switched capacitor interleaved inverter. The analysis focused on comparing component count for simplicity purposes with harmonic performance to ensure the quality of the load power is within acceptable tolerances to serve a home load.

6 Conclusions and Future Research

The key finding from analysing the existing literature shows that a hybrid model which involves a combination of two different MPPT elements are the most effective and give a balance of performance when considering efficiency, response time and stability. Novel approaches give a faster response and improved efficiency however they do not always give the most stable response, however, they can involve pre-configuration of the system to a known or expected dataset. Whilst in an ideal situation this is an ideal approach, in practical systems there is always data that are outliers and in the case of standalone PV systems weather will always change and therefore irradiance and temperature will also be changing frequently. Given that a standalone PV system will utilise a battery there is less of a requirement for a rapid response time, more so the quality of the power and the system's ability to adapt to variable conditions. Compared with some other inverters investigated during the literature review, to improve further, the MPPT element of this circuit could be improved as the system currently utilizes a conventional P&O MPPT, exploring & comparing existing MPPT methods and how they perform within this circuit is an area of future research and development for this circuit.

There has been substantial research done on MPPT methodologies for PV energy management systems, to develop the existing research further, the proposed hybrid/modified MPPT methodologies should be practically tested and compared. This research should focus particularly on the perceived benefits of complex, highly technical solutions that could be complicated to integrate and implement in practical scenarios vs the actual ability of the system to reasonably respond to variable environmental conditions better than the traditional MPPT methods.

Some published literature explores the use of different battery technology or super capacitors. The purpose of this study is to provide an off-grid solution that can be widely adopted across multiple different scenarios and applications. A perceived development of this study would be the exploration of newer battery/super capacitor technologies.

The system has been designed to reduce the number of conversion stages compared with conventional approaches in published literatures. The MPPT typically controls a boost converter connected in parallel to the battery charger that is controlled a voltage controller. Removing the boost converter increases the speed of the response, reduces the number of components required and improves efficiency by reducing the number of conversions and therefore conversion losses. This modified control strategy that combines P&O MPPT with a current controller to drive the IGBTs used in the circuit configuration is successful in providing the required performance. The interleaved bidirectional battery charger presented in this study shows the desired response characteristics to variable irradiance that is typically expected for a PV energy management system. The response of the circuit is fast with

a low current ripple. The proposed approach differs from published literature due to the reduced components and the single stage of DC-DC conversion (as opposed to the boost converter in parallel).

The presented circuit shows an interleaved switched capacitor inverter circuit controlled by a modified method of unipolar phase shifted sinusoidal PWM that uses an RMS feedback loop due to the MPPT circuit controlling a battery charger. The outcome of this study concludes that all the elements required for a stand-alone residential home load can be combined to produce a high-performance PV energy management system. The interleaved inverter can reduce the output ripple which also has a positive impact on the THD without an excessive number of components. The circuits response to variable environmental conditions was observed to test this circuit further. The results gathered showed that circuit's response to irradiance changes align with expectations of an energy management system such that the battery can supplement the home load when the PV output reduces below the required threshold.

Overall, the aim of this study was to propose a single phase standalone photovoltaic energy management system (SPSAPVEMS) that is capable of serving residential off-grid applications without the need for pre-configuration "plug-and-play", able to react to variable input conditions by providing stable load power, low-cost from optimised component counts as well as providing control circuits that do not use expensive embedded controllers, reduced response time by omitting the traditional boost DC-DC conversion stage, good quality and efficient response time through lower harmonic performance, it can be concluded that the aims of this study have been met.

There are some ways this study could be improved or developed further, this would firstly look to validate the simulated data and theoretical approach by gathering practical data either on a sub-system by sub-system basis or by looking at the overall system in its entirety. Additionally, a novel/modified approach based on existing literature is used for most of the PV EMS subsystems except for MPPT, a further investigation into a simplified hybrid MPPT algorithm that does not require an embedded controller but can improve the MPPT performance can be explored to further improve the overall system performance. To develop this work further, both the load and the input conditions could be varied to see how the system performs when the load demand is variable. However, due to the nature of the bidirectional DC-DC converter it is likely that this system is capable of providing stable load power for these variable conditions in addition.

7 Appendices

A. **MATLAB Simulink Model**

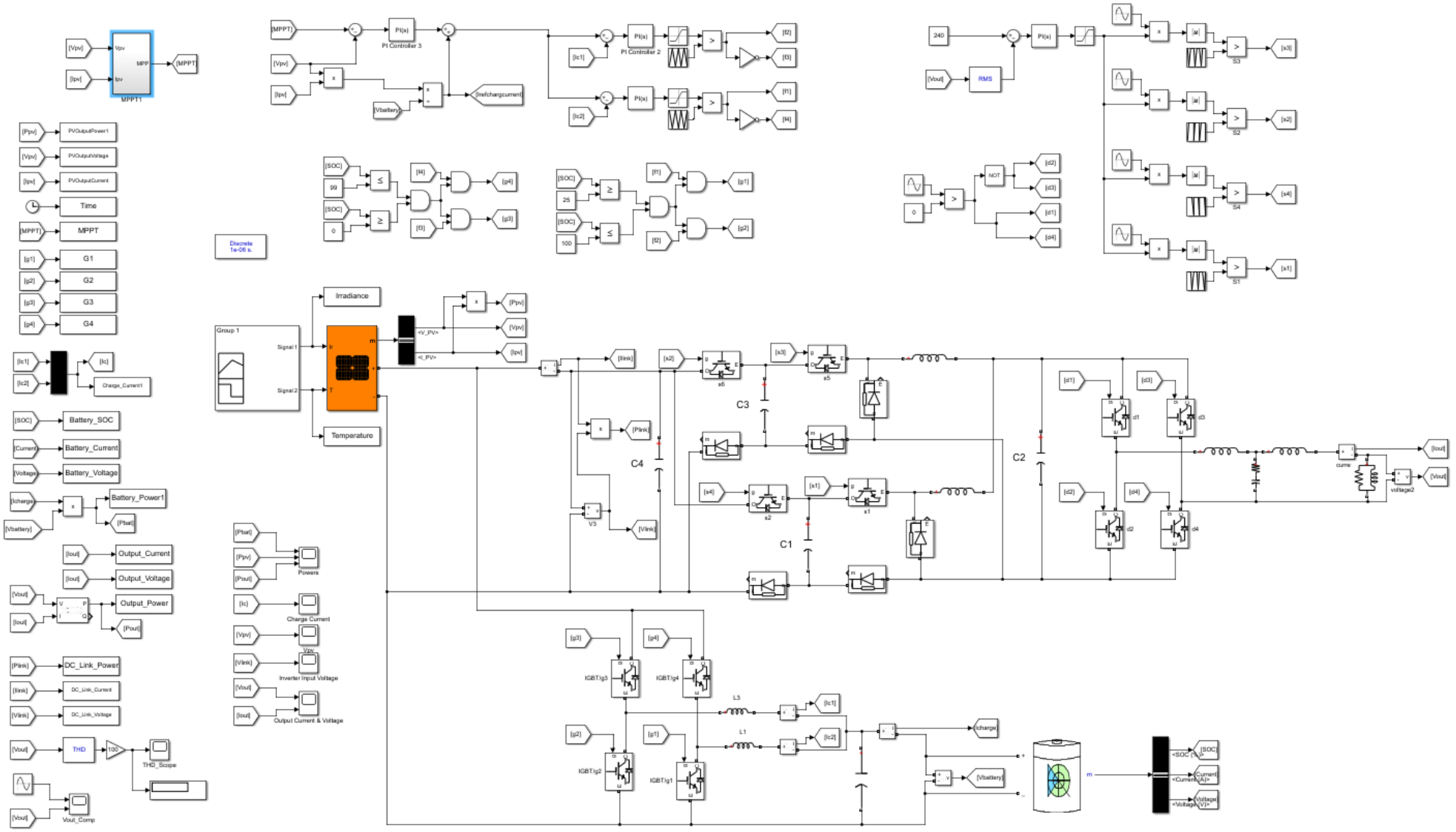

8 Glossary

AC	Alternating Current
AI	Artificial Intelligence
BS	British Standard
CCC	Climate Change Committee
CdTe	Cadmium Telluride
CIGS	Copper Indium Gallium Selenide
DC	Direct Current
EMS	Energy Management System
FOCC	Fractional Order Current Control
FOVC	Fractional Order Voltage Control
GWO	Grey Wolf Optimisation
HOSM	High Order Switching Mode
IAS	Industry Applications Society
IEA	International Energy Agency
IEC	International Engineering Committee
IEEE	Institute of Electrical and Electronic Engineering
IGBT	Insulated Gate Bipolar Transistors
INC	Incremental Conductance
LDR	Light Dependant Resistor
Li-Ion	Lithium Ion
LPF	Low Pass Filter
MPP	Maximum Power Point
MPPT	Maximum Power Point Tracking
NOT	Logic NOT gate
PHEV	Plugin Hybrid Electric Vehicle

P&O	Perturb and Observation
PID	Proportional Integral Derivative
PV	Photovoltaic
PWM	Pulse Width Modulation
RMS	Root Mean Square
SM	Switching Mode
SMC	Switching Mode Controller
SPSAPVEMS	Single Phase Standalone Photovoltaic Energy Management System
SPWM	Sinusoidal Pulse Width Modulation
THD	Total Harmonic Distortion
UK	United Kingdom
VSI	Voltage Source Inverter

9 Units

A (I)	Ampere (Amp) - Current
Ah	Amphours
EJ	Exajoule
GW	Gigawatt
F	Farad (Capacitor)
H	Henry (Inductor)
Hz	Hertz
J	Joule
kHz	Kilohertz
kW	Kilowatts
kWh	Kilowatt hour
k Ω	KiloOhm
mH	milihenry
S	Seconds
TW	Terawatts
TWh	Terawatt hour
V	Volts
Var	Power
W/m2	Watt per Square Meter
°C	Degrees Celsius
µF	Micro-Farad
µΩ	Micro-Ohm
Ω	Ohm (resistance)

10 Bibliography

[1] Climate Change Committee, “Sector Summary Building,” December 2020. [Online]. Available: https://www.theccc.org.uk/wp-content/uploads/2020/12/Sector-summary-Buildings.pdf.

[2] Climate Change Committee, “Accelerated Electrification and the GB Electricty System,” May 2019. [Online]. Available: https://www.google.com/url?sa=t&source=web&rct=j&opi=89978449&url=https://www.theccc.org.uk/wp-content/uploads/2019/05/CCC-Accelerated-Electrification-Vivid-Economics-Imperial.pdf. [Accessed December 2024].

[3] B. Gallizzi, “UK renewable energy statistics 2024,” December 2023. [Online]. Available: https://www.uswitch.com/gas-electricity/studies/renewable-statistics/. [Accessed December 2024].

[4] B. Johnson, “Gov UK,” September 2022. [Online]. Available: https://www.gov.uk/government/publications/british-energy-security-strategy/british-energy-security-strategy. [Accessed January 2024].

[5] P. Bojek, “Renewable Energy System - Solar PV,” IEA, 03 02 2025. [Online]. Available: https://www.iea.org/energy-system/renewables/solar-pv. [Accessed 23 02 2025].

[6] B. S. Institute, *BS 7671,* London: British Standard Institute, 2018.

[7] H. C. Yang, J. Yahaya and A. Ponniran, “The Study of MPPT Algorithm for Solar Battery Charging System,” *Malaysian Journal of Science and Advanced Technology,* vol. 109, no. 121, 2022.

[8] Cambridge English Dictionary, *Cambridge English Dictionary - Photon,* Cambridge: Cambridge University Press, 2025.

[9] J. Donev, “Energy Education,” University of Calgary, 2024. [Online]. Available: https://energyeducation.ca/encyclopedia/Photovoltaic_cell . [Accessed October 2024].

[10] S. N. Laboratories, “Single DIode Equivalent Circuit Models,” Sandia National Laboratories, 03 2025. [Online]. Available: https://pvpmc.sandia.gov/modeling-guide/2-dc-module-iv/single-diode-equivalent-circuit-models/. [Accessed 03 2025].

[11] R. N. P. H. Podder A, “MPPT methods for solar PV systems: a critical review based on tracking nature,” *IET Renewable Power Generation,* vol. 13, no. 10, pp. 1615-1632, 2019.

[12] MathWorks, “MPPT Algorithm,” The MathWorks Inc., 1995-2025. [Online]. Available: https://uk.mathworks.com/discovery/mppt-algorithm. [Accessed September 2024].

[13] CHARGETEK, “Battery charger basics,” Chargetek Inc, 2015. [Online]. [Accessed January 2023].

[14] D. N. N. S. B. V. Jadhav S, “Bidirectional DC-DC converter in Solar PV System for Battery Charging Application,” *International Conference on Smart City and Emerging Technology (ICSCET),* 2018.

[15] IEEE, “IEEE Standard for Harmonic Control in Electric Power Systems,” *IEEE Std 519-2022 (Revision of IEEE Std 591-2014),* pp. 1-31, 2022.

[16] A. Banik, B. Bairwa and N. Mamatha, “A Literature Review on PV Inverter Topologies,” River Publishers, Bangalore, 2021.

[17] Electronics Tutorials, “Passive Low Pass Filter,” ASPENCORE, 2021. [Online]. Available: https://www.electronics-tutorials.ws/filter/filter_2.html. [Accessed December 2024].

[18] A. Allouhi, S. Rehman, M. Buker and Z. Said, “Up-to-date literature review on Solar PV systems: Technology progress, market status and R&D,” *Journal of Cleaner Production,* vol. 362, 2022.

[19] Y. Amara, R. Boukenoui, R. Bradai, H. Salhi and IEEE Editors, “. Design and Control of Two-Stage Standalone Photovoltaic Generation System,” in *ICCEE*, Eloued, Algeria, 2018.

[20] N. Debnath and C. Chakraborty, “Synthesis of Three-Port Converter from existing dc-dc converters for PV based dc stand-alone system,” *IEEE International Conference on Power Electronics, Smart Grid and Renewable Energy (PESGRE2020),* pp. 1-6, 2020.

[21] S. Deshmukh, R. Thorat and I. Korachagaon, “Modelling and Analysis of PV Standalone System with Energy Management Scheme,” in *CONECCT*, Bangalore, India, 2020.

[22] S. Das, M. R. Haque and M. Razzak, “Development of One-kilowatt Capacity Single Phase Pure Sine Wave Off-grid PV Inverter,” *IEEE Region 10 Symposium,* pp. 747-777, 2020.

[23] K. Bharathi, S. Sakthi and M. Sasikumar, “Power Optimization of Embedded Controller PV Powered Stand-Alone System for Rural Electrification,” in *Fifth International Conference on Science Technology Engineering and Mathematics (ICONSTEM)*, Chennai, India, 2019.

[24] B. Postovoit, D. Susoeff, D. Daghbas, J. Holt, C. Pomona and H. Le, “A Solar-Based Stand-Alone Family House for Energy Independence and Efficiency,” in *IEEE Conference on Technologies for Sustainability (SusTech)*, Santa Ana, California, 2020.

[25] S. Ruttala, S. Nayak, A. Chakraborti and P. Kasari, “Decoupled Control of Asymmetrical Multilevel VSI for Standalone PV Application,” in *IEEE International Conference on Power Electronics, Drives and Energy Systems (PEDES)*, Jaipur, India, 2020.

[26] J. Hivziefendic and L. Vuic, “Application of the Voltage Control Technique and MPPT of Stand-alone PV System with Storage,” *Advances in Electrical and Computer Engineering,* vol. 22, no. 1, pp. 21-30, 2022.

[27] M. Alghassab, “Performance Enhancement of Stand-Alone Photovoltaic Systems with household loads,” in *2nd International Conference on Computer Applications & Information Security (ICCAIS)*, Riyadh, Saudi Arabia, 2019.

[28] A. Betti, M. Ebrahim and M. Mustafa Hassan , “Modeling and Control of Stand-alone PV System Based on Fractional-Order PID Controller,” in *Twentieth International Middle East Power Systems Conference (MEPCON)*, Cairo, Egypt, 2018.

[29] R. Gupta and A. Singh, “Integrated Battery Management Configurations for Standalone Solar PV fed CHBMLI,” in *IEEE International Conference on Power Electronics, Drives and Energy Systems (PEDES)*, Jaipur, India, 2020.

[30] S. Mane, F. Kazi, H. Jonghale and N. Seth, “Controller Design and Analysis of Standalone PV System for DC Microgrid Applications with Combined MPPT and DPC Strategy,” in *2018 International Conference on Computing, Power and Communication Technologies (GUCON)*, Greater Noida, India, 2018.

[31] Z. Dalala and O. Saadeh, “A New Robust Control Strategy for Multistage PV Battery Chargers,” in *2018 9th IEEE International Symposium on Power Electronics for Distributed Generation Systems (PEDG)*, Charlotte, NC, 2018.

[32] N. Bodele and P. Kulkarni, “A multi-input hybrid converter for small off-grid solar photo-voltaic system,” in *2020 IEEE First International Conference on Smart Technologies for Power, Energy and Control (STPEC)*, Nagpur, India, 2020.

[33] M. Eid, S. Abdelwahab, H. Ibrahim and A. Alaboudy, “Improving the Resiliency of a PV Standalone System Under Variable Solar Radiation and Load Profile,” in *2018 Twentieth International Middle East Power Systems Conference (MEPCON)*, Cairo, Egypt, 2018.

[34] A. Garg, D. Mathur, H. Tanwar and S. Joshi, “Comparative Analysis of Maximum Power Point Algorithms for Solar PV Applications,” in *2020 21st National Power Systems Conference (NPSC)*, Gandhinagar, India, 2020.

[35] A. Ali, K. Almutairi, S. Padmanaban, V. Tirth, S. Algarni and K. Irshad, “Investigation of MPPT Techniques Under Uniform and Non-Uniform Solar Irradiation Condition - A Retrospection,” *IEEE Access,* pp. 127368-127392, 2020.

[36] Z. Salah, S. Krim, M. Hajjaji, B. Alshammari, K. Alqunun and A. Alzamil, “A New Efficient Cuckoo Search MPPT Algorithm Based on a Super-Twisting Sliding Mode Controller for Partially Shaded Standalone Photovoltaic Systems,” *Sustainability,* vol. 15, no. 12, 2023.

[37] D. Behera, B. Reddy and S. Senthilkumar, “A Robust Power Control Scheme for a Dual-Input Single-Output converter with a Standalone Solar PV System,” in *2018 IEEE International Conference on Power Electronics, Drives and Energy Systems (PEDES)*, Chennai, India, 2018.

[38] P. Behera, B. Dash, R. Sahoo, P. Ray, R. Padhi and A. Achary, “Design and performance analysis of ZVS interleaved boost converter in standalone PV system,” in *2018 Technologies for Smart-City Energy Security and Power (ICSESP)*, Bhubaneswar, India, 2018.

[39] E. Sarika, J. Jacob, S. Sulthan and S. Paul, “Standalone PV System with Modified VSS P&O MPPT Controller Suitable for Partial Shading Conditions,” in *2021 7th International Conference on Electrical Energy Systems (ICEES)*, Chennai, India, 2021.

[40] H. Ali, R. Vilanova and J. Pelez-Restrepo, “Perturb & Observe based Adaptive Sliding Mode MPPT Control of Solar Photovoltaic System,” in *2020 IEEE International Conference on Environment and Electrical Engineering and 2020 IEEE Industrial and Commercial Power Systems Europe (EEEIC / I&CPS Europe)*, Madrid, Spain, 2020.

[41] N. Swaminathan, N. Lakshminarasamma and Y. Cao, “A Fixed Zone Perturb and Observe MPPT Technique for A Standalone Distributed PV System,” *IEEE Journal of Emerging and Selected Topics in Power Electronics,* vol. 10, no. 1, pp. 361-374, 2022.

[42] D. Agarwhal, D. Dash, S. Dalai, I. Anand and S. Subramaniam, “A power flow controller for a Standalone solar PV system employing a three port Luo converter,” in *2018 20th National Power Systems Conference (NPSC)*, Tiruchirappalli, India, 2018.

[43] K. Huang, T. Qian and W. Tang, “Solar energy tracking based on extremum seeking control method,” in *2020 IEEE Sustainable Power and Energy Conference (iSPEC)*, Chengdu, China, 2020.

[44] S. Karthika, M. Asok, M. Mohan, R. Hima, J. Das and C. Varghese, “An Enhanced P and O Algorithm for Maximum Power Point Tracking,” in *2020 International Conference on Futuristic Technologies in Control Systems & Renewable Energy (ICFCR)*, Malappuram, India, 2020.

[45] I. Rougab, A. Cheknane and N. Abouchabana, “Study and simulation of MPPT techniques to control a stand-alone photovoltaic system under varying irradiance,” *Romanian Journal of Information Technology and Automatic Control,* vol. 31, no. 4, pp. 109-221, 2021.

[46] I. Anya, C. Saha, H. Ahmed, S. Rajbhandari, M. Huda and A. Mumtaz, “Experimental evaluation of adaptive maximum power point tracking for a standalone photovoltaic system,” *Energy Systems,* vol. 13, pp. 835-853, 2022.

[47] N. Manuel and N. Inanc, “Sliding Mode Control-Based MPPT and Output Voltage Regulation of a Standalone PV System,” *Power Electronics and Drives,* vol. 7, no. 42, pp. 159-173, 2022.

[48] P. Atri, P. Modi and N. Gujar, “Design and Development of Solar Charge Controller by Implementing two different MPPT Algorithm,” in *2021 International Conference on Advances in Electrical, Computing, Communication and Sustainable Technologies (ICAECT)*, Bilai, India, 2021.

[49] X. Liu, Q. Teng, K. Xing and X. Ma, “Adaptive Exponential Convergence Law Based Sliding Mode Control for Photovoltaic Maximum Power Tracking Control,” in *2022 3rd International Conference on Advanced Electrical and Energy Systems (AEES)*, Lanzhou, China, 2022.

[50] S. Chtita, S. Motahhir and A. Ghzizal, “A New Design and Embedded Implementation of a Low-Cost Maximum Power Point Tracking Charge Controller for Stand-Alone Photovoltaic Systems,” *Energy Technology,* vol. 12, no. 4, 2024.

[51] S. Agrawal, L. Umanand and S. Basappa, “A novel converter using MPPT algorithm and acceleration factor for standalone PV system,” *Electrical Engineering,* vol. 105, pp. 3681-3702, 2023.

[52] A. Adawi, G. Bouattour, M. Ibbini and O. Kanoun, “Single,Double and Quadruple Maximum Power Point Trackers for a Stand-Alone Photovoltaic System,” in *2020 17th International Multi-Conference on Systems, Signals & Devices (SSD)*, Monastir, Tunisia, 2020.

[53] I. Al-Wesabi, F. Zhijian, H. Farh, I. Dagal, A. Al-Shamma'a, A. Al-Shaalan and Y. Kai, “Hybrid SSA-PSO based intelligent direct sliding-mode control for extracting maximum photovoltaic output power and regulating the DC-bus voltage,” *International Journal of Hydrogen Energy,* vol. 51, no. Part C, pp. 348-370, 2024.

[54] Y. Chaibi, M. Salhi and A. El-jouni, “Sliding Mode Controllers for Standalone PV Systems: Modeling and Approach of Control,” *International Journal of Photoenergy,* vol. 2019, pp. 1-12, 2019.

[55] N. AbdRahim, A. Amir, A. Amir, H. Che and A. ElKhateb, “Hill climbing maximum power point tracking on four stage switch capacitor based boost converter,” in *5th IET International Conference on Clean Energy and Technology (CEAT2018)*, Kuala Lumpar, Malaysia, 2018.

[56] H. Ikaouassen, K. Moutaki, A. Raddaoui and M. Rezkallah, “Modified Predictive Model Control based MPPT for Standalone PV in Distribution System,” in *018 6th International Renewable and Sustainable Energy Conference (IRSEC)*, Rabat, Morocco, 2018.

[57] U. Chauhan, A. Rani, V. Singh and B. Kumar, “A Modified Incremental Conductance Maximum Power Point Technique for Standalone PV System,” in *2020 7th International Conference on Signal Processing and Integrated Networks (SPIN)*, Noida, India, 2020.

[58] R. Faranda and K. Akkala, “Reduction Power Point Tracking for Standalone PV Systems: Preliminary Studies,” in *2020 International Symposium on Power Electronics, Electrical Drives, Automation and Motion (SPEEDAM)*, Sorrento, Italy, 2020.

[59] A. Ba, C. Ehssein, A. Benkaddour and E. Hassan, “Optimization of a Standalone PV System with a New Proposed MPPT Method,” in *2020 11th International Renewable Energy Congress (IREC)*, Hammamet, Tunisia, 2020.

[60] A. Rehman, L. Khan, F. Khan and W. Karam, “GRNN Based Higher Order Sliding Mode MPPT Control Paradigms for Standalone PV system,” in *2019 15th International Conference on Emerging Technologies (ICET)*, Peshawar, Pakistan, 2019.

[61] A. Sharma and N. Kumar, “Lyapunov Stability Theory based Non Linear Controller Design for a Standalone PV System,” in *2020 IEEE International Conference for Innovation in Technology (INOCON)*, Bangluru, India, 2020.

[62] K. Panda, A. Anand, P. Bana and G. Panda, “Novel PWM Control with Modified PSO-MPPT Algorithm for Reduced Switch MLI Based Standalone PV System,” *International Journal of Emerging Electric Power Systems,* vol. 19, no. 2, 2018.

[63] S. Obukhov, A. Ibrahim, Z. Diab, S. Al-Sumaiti and R. Aboelsaud, “Optimal Performance of Dynamic Particle Swarm Optimization Based Maximum Power Trackers for Stand-Alone PV System Under Partial Shading Conditions,” *IEEE Access,* vol. 8, pp. 20770-20785, 2020.

[64] V. Balaji and A. Fathima, “Enhancing the Maximum Power Extraction in Partially Shaded PV Arrays using Hybrid Salp Swarm Perturb and Observe Algorithm,” *International Journal of Renewable Energy Research-IJRER,* vol. 10, no. 2, 2020.

[65] A. Taissala, D. Goron, N. Nisso, D. Kidmo, P. Ekam, F. Mbakop and N. Djongyang, “An Optimized Synergetic Nonlinear Controller (OSNC) based maximum power point tracking for a standalone photovoltaic system using a boost converter,” *Energy Reports,* vol. 8, no. 9, 2022.

[66] K. Chao, Y. Lai and W. Chang, “Development of a Stand-Alone Photovoltaic System Considering Shaded Effect for Energy Storage and Release,” *Electronics,* vol. 8, no. 5, 2019.

[67] N. Elbehairy, R. Swief, A. Abdin and T. Abdelsalam, “Maximum Power Point Tracking For a Stand Alone PV System Under Shading Conditions Using Flower Pollination Algorithm,” in *2019 21st International Middle East Power Systems Conference (MEPCON)*, Cairo, Egypt, 2019.

[68] P. Behera, S. Das and M. Pattnaik, “Performance Comparison Between Bipolar and Unipolar Switching Scheme for a Single-Phase Inverter Based Stand-alone Photovoltaic System,” in *2019 IEEE 16th India Council International Conference (INDICON)*, Rajkot, India, 2018.

[69] K. Wibowo, I. Apripriharta, G. Fadlika, J. Horng, S. Wibawanto and F. Saputra, “A New MPPT based on Queen Honey Bee Migration (QHBM) in Stand-alone Photovoltai,” in *2019 IEEE International Conference on Automatic Control and Intelligent Systems (I2CACIS)*, Selangor, Malaysia, 2019.

[70] O. Saadeh, S. Tamimi and F. Amoura, “A Hybrid Battery / Ultracapacitor Energy Storage Solution for PV Systems,” in *2020 6th IEEE International Energy Conference (ENERGYCon)*, Gammarth, Tunisia, 2020.

[71] S. Mohammadsalehian, F. Sedaghati, R. Eskandari, H. Shayeghi and E. Asi, “A Modified Double Input Z-source DC-DC Converter for Standalone PV/Battery System Application,” in *2020 11th Power Electronics, Drive Systems, and Technologies Conference (PEDSTC)*, Tehran, Iran, 2020.

[72] S. Battula, A. Panda and M. Garg, “Stand-alone PV connected system with energy storage with flexible operation,” *Electrical Engineering,* vol. 106, pp. 2893-2907, 2023.

[73] D. Bhule, S. Jain and S. Ghosh, “Control Strategy for Photovoltaic-Battery Based Standalone System,” in *2020 IEEE First International Conference on Smart Technologies for Power, Energy and Control (STPEC)*, Nagpur, India, 2020.

[74] S. Bhattacharyya and S. Samanta, “DC Link Voltage Control based Power Management Scheme for Standalone PV Systems,” in *2018 IEEE International Conference on Power Electronics, Drives and Energy Systems (PEDES)*, Chennai, India, 2018.

[75] R. Bhagiya and R. Patel, “PWM based Double loop PI Control of a Bidirectional DC-DC Converter in a Standalone PV/Battery DC Power System,” in *2019 IEEE 16th India Council International Conference (INDICON)*, Rakjot. India, 2019.

[76] R. Mahmud, M. Hossain and H. Pota, “Robust Nonlinear Controller Design for Islanded Photovoltaic System with Battery Energy Storage,” in *2020 IEEE International Conference on Power Electronics, Smart Grid and Renewable Energy (PESGRE2020)*, Cochin, India, 2020.

[77] K. Pathak, S. Trivedi and M. Ayalani, “Operation and Control of Non-isolated Interleaved Bidirectional DC-DC Converter integrated with Solar PV system,” in *2019 IEEE*

International Conference on Innovations in Communication, Computing and Instrumentation (ICCI), Chennai, India, 2019.

[78] I. Anand, S. Senthilkumar, D. Biswas and M. Kaliamoorthy, "Dynamic Power Management System Employing a Single-Stage Power Converter for Standalone Solar PV Applications," *IEEE Transactions on Power Electronics,* vol. 33, no. 12, pp. 10352-10362, 2018.

[79] C. Nalamati and R. Gupta, "Isolated bidirectional battery converter control for standalone solar PV applications," in *2018 IEEMA Engineer Infinite Conference (eTechNxT)*, New Delhi, India, 2018.

[80] Y. Sato, M. Uno and H. Nagata, "Nonisolated Multiport Converters Based on Integration of PWM Converter and Phase-Shift-Switched Capacitor Converter," *EEE Transactions on Power Electronics,* vol. 35, no. 1, pp. 455-470, 2020.

[81] M. Uno, R. Igarashi and Y. Sato, "Switched Capacitor-Based PWM- and Phase Shift-Controlled Multiport Converter With Differential Power Processing Capability for Standalone Photovoltaic Systems Under Partial Shading," *IEEE Journal of Emerging and Selected Topics in Power Electronics,* vol. 9, no. 5, pp. 6019-6032, 2021.

[82] H. El Ouardi, A. El Gadari, Y. Ounejjar, K. Al-Haddad and S. Alibou, "A Standalone Photovoltaic System Based on The SPUC5 Inverter," in *2020 IEEE 29th International Symposium on Industrial Electronics (ISIE)*, Delft, Netherlands, 2020.

[83] M. Uno and K. Sugiyama, "Switched Capacitor Converter Based Multiport Converter Integrating Bidirectional PWM and Series-Resonant Converters for Standalone Photovoltaic Systems," *IEEE Transactions on Power Electronics,* vol. 34, no. 2, pp. 1394-1406, 2019.

[84] J. Roy, G. Seo and A. Singh, "Highly Reliable Multi-Port Smart Inverter Modules for PV-Based Energy Systems," in *46th IEEE Photovoltaic Specialists Conference, PVSC 2019*, Chicago, Illinois, 2019.

[85] C. Boonmee and Y. Kumsuwan, "Single-Phase Cascaded Inverter to Reduce Common Mode Current in Standalone PV System Using A Modified Phase-shifted Carrier-Based PWM," in *2018 15th International Conference on Electrical Engineering/Electronics, Computer, Telecommunications and Information Technology (ECTI-CON)*, Chiang Rai, Thailand, 2018.

[86] N. Yadav and D. Sambariya, ""Analysis and Integration of Nine Level Cascaded H-Bridge Multilevel Inverter Configuration in a Photovoltaic System," in *2018 9th International*

Conference on Computing, Communication and Networking Technologies (ICCCNT), Bengaluru, India, 2018.

[87] K. Ankit, P. Karthikeyan Shanmugam, R. Bhosale and F. Shahnia, "An Interleaved Switched-Capacitor based PV-fed Standalone Single-Stage Single-phase Inverter using Minimum Number of Controlled Switches," in *2019 9th International Conference on Power and Energy Systems (ICPES)*, Perth, Australia, 2019.

[88] S. Behera, M. Behera, H. Majhi and F. Akram, "Study of PWM Control Techniques for Single Phase Inverter with Variable DC Input," in *2018 Second International Conference on Intelligent Computing and Control Systems (ICICCS)*, Madurai, India, 2018.

[89] Y. Singh, B. Singh and S. Mishra, "Control of Multiple PV Integrated Parallel Inverters for Microgrid Applications," in *2020 International Conference on Power, Instrumentation, Control and Computing (PICC)*, Thrissur, India, 2020.

[90] N. S, D. Debnath and C. Chakraborty, "Synthesis of Three-Port Converter from existing dc-dc converters for PV based dc stand-alone system," in *2020 IEEE International Conference on Power Electronics, Smart Grid and Renewable Energy (PESGRE2020)*, Cochin, India, 2020.

[91] W. Chen, S. Farooqui, H. Liu, S. Lai and P. Lin, "Novel MPPT algorithm based on honey bees foraging characteristics for solar power generation systems.," *Undergraduate Program of Vehicle and Energy Engineering,* vol. 10, no. 6, 2024.

[92] A. Bhandari, S. Bose, P. Dwivedi and S. Pandey, "Standalone PV Based BESS Using Bidirectional DC-DC SEPIC/ZETA Converter," in *2022 2nd International Conference on Intelligent Technologies (CONIT)*, Hubli, India, 2022.

[93] T. Rout, M. Maharana, A. Chowdhury and S. Samal, "A Comparative study of Stand-alone Photo-Voltaic System with Battery storage system and Battery Supercapacitor storage system," in *2018 4th International Conference on Electrical Energy Systems (ICEES)*, Chennai, India, 2018.

[94] D. Behera, I. Anand, I. Reddy and S. Senthilkumar, "A Novel Control Scheme for a Standalone Solar PV System Employing a Multiport DC-DC Converter," in *2018 9th International Conference on Computing, Communication and Networking Technologies (ICCCNT)*, Bengaluru, India, 2018.

[95] D. Bhule, S. Jain and S. Ghosh, “Power Management Control Strategy for PV-Battery Standalone System,” in *2020 IEEE 9th Power India International Conference (PIICON)*, Sonepat, India, 2020.

[96] S. Nagarjun, D. Debnath and C. Chakraborty, “Buck-Boost Buck CCM-DCM Converter for PV Based DC Standalone System,” in *2018 IEEE International Conference on Power Electronics, Drives and Energy Systems (PEDES)*, Chennai, India, 2018.

[97] A. Iqbal, S. Gore and P. Maroti, “Single Phase Multilevel Inverter for Standalone PV system Application,” in *IECON 2020 The 46th Annual Conference of the IEEE Industrial Electronics Society*, Singapore, 2020.

[98] M. Akhil, C. Nirmal Mukundan, M. Rajesh and P. Jayaprakash, “A Novel Single Stage Standalone Five Level MLI Topology Scheme Having Battery as Energy Storage Element for Rural Deployment,” in *2019 2nd International Conference on Intelligent Computing, Instrumentation and Control Technologies (ICICICT)*, Kannur, India, 2019.

[99] J. Missula, “Single-phase Five-level Boost Inverter for Stand-alone PV Applications.,” in *IECON 2020 The 46th Annual Conference of the IEEE Industrial Electronics Society*, Singapore, 2020.

[100] M. Farhadi-Kangarlu and M. Marangalu, “A Single DC-Source Five-Level Inverter Applied in Stand-Alone Photovoltaic Systems Considering MPPT Capability.,” in *2019 10th International Power Electronics, Drive Systems and Technologies Conference (PEDSTC)*, Shiraz, Iran, 2019.

[101] K. Benamrane, T. Abdelkrim, B. Benlahbib, N. Bouarroudj, A. Borni and A. Lakhdari, “. Realization of Photovoltaic Conversion Cascade Based Single-Phase Five-Level H Bridge Inverter for Stand-Alone application in South Algeria.,” in *2023 14th International Renewable Energy Congress (IREC)*, Sousse, Tunisia, 2023.

[102] P. Kumar, D. Thanki, M. Kour and H. Singh, “Single Phase Five Level Inverter for Solar-PV Applications,” in *2018 International Conference on Intelligent Circuits and Systems (ICICS)*, Phagwara, India, 2018.

[103] S. Aute and S. Naveed, “Simulation and Analysis of Multilevel Inverter Based Solar PV System,” in *2019 3rd International Conference on Computing Methodologies and Communication (ICCMC)*, Erode, India, 2019.

[104] M. Hamidi, D. Ishak, M. Zainuri, C. Ooi and T. Tarmizi, "Asymmetrical Multi-level DC-link Inverter for PV Energy System with Perturb and Observe Based Voltage Regulator and Capacitor Compensator," *Journal of Modern Power Systems and Clean Energy,* vol. 9, no. 1, pp. 199-209, 2021.

[105] P. Sen, "Novel Multilevel Inverter Based Standalone PV System Using Reduced Number of Components," in *2020 International Conference on Renewable Energy Integration into Smart Grids: A Multidisciplinary Approach to Technology Modelling and Simulation (ICREISG)*, Bhubaneswar, India, 2020.

[106] S. Khasim, D. Padmanaban, J. Holm-Nielsen and M. Mitolo, "A Novel Asymmetrical 21-Level Inverter for Solar PV Energy System with Reduced Switch Count," *IEEE Access,* vol. 9, pp. 11761-11775, 2021.

[107] L. Pratomo and C. Tjokro, "Hardware Implementation of an Asymmetrical 11-Level Inverter with Automatic Boost Charge Control in PV Applications," in *2019 International Seminar on Application for Technology of Information and Communication (iSemantic)*, Semarang, Indonesia, 2019.

[108] S. Kumar and J. Kumar, "A Modified Single Phase Nine Level Multilevel Topology for Standalone Solar System," in *2019 Global Conference for Advancement in Technology (GCAT)*, Bangalore, India, 2019.

[109] M. Bhukya, V. Kota and S. Depuru, "A Simple, Efficient, and Novel Standalone Photovoltaic Inverter Configuration with Reduced Harmonic Distortion," *IEEE Access,* vol. 7, pp. 43831-43845, 2019.

[110] K. Rout, K. Srinivas and S. Mishra, "System using Synchronous Boost Converter and Reduced Switch Five Level Inverter," in *2018 International Conference on Recent Innovations in Electrical, Electronics & Communication Engineering (ICRIEECE)*, Bhubaneswar, India, 2018.

[111] A. Latif, L. Khan and S. Ahmad, "Nonlinear Backstepping Based Control of Single-Phase Inverter in a Standalone Photovoltaic System," in *2021 International Bhurban Conference on Applied Sciences and Technologies (IBCAST)*, Islamabad, Pakistan, 2021.

[112] S. Jain and V. Agarwal, "A Single-Stage Grid Connected Inverter Topology for Solar PV Systems with Maximum Power Point Tracking," *IEEE Transactions on Power Electronics,* vol. 22, no. 5, pp. 1928-1940, 2007.

[113] V. Agarwal, “Sinusoidal Pulse Width Moderation,” Encyclopedia of Electrical and Electronic Power Engineering, Elsevier, 2023.